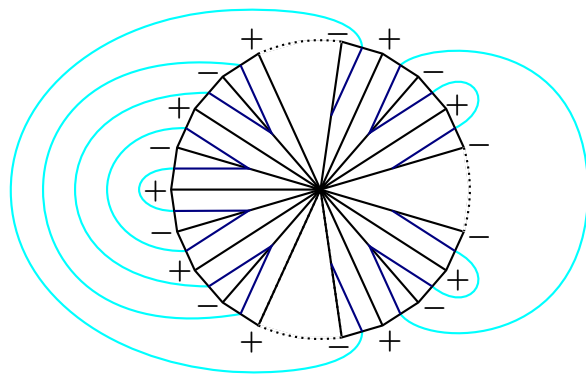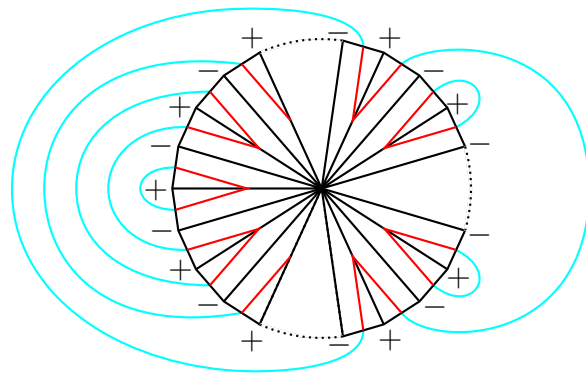# REALIZATION PROBLEMS FOR POINT CONFIGURATIONS AND POLYHEDRAL SURFACES

DAGMAR TIMMRECK

Realization Problems for Point Configurations and Polyhedral Surfaces

vorgelegt von
Dipl.-Math. Dagmar Timmreck
aus Berlin

Beim Fachbereich Mathematik und Informatik
der Freien Universität Berlin
zur Erlangung des akademischen Grades

Doktor der Naturwissenschaften
– Dr. rer. nat. –

eingereichte Dissertation

Acknowledgements

Many people helped me in various ways during these past years of the preparation of this thesis.

Thank you for your support!

I would like to thank Günter Ziegler for giving me the opportunity to do research in his workgroup first at the Technische and then at the Freie Universität. He always had an open door for me whenever I needed mathematical or other advice.

The people of the Discrete Geometry Group were always a mathematically and otherwise inspiring crowd and made my time there not only successful but also enjoyable. In particular I want to thank Bernd Gonska, Katharina Jochemko, Carsten Lange, Elke Pose, Thilo Rörig and Raman Sanyal.

Special thanks go to Lars Schewe for providing me with his source code and support to adjust it to my needs.

Finally I would like to thank my family and most of all my beloved husband Martin for his love, support and patience during all the ups and downs in the preparation of this thesis.

INTRODUCTION

Realization problems are a recurrent theme in Discrete Geometry.

The generic realization problem can be phrased as follows:

Is there an object living in Euclidean space $\mathbb{R}^d$ that satisfies some given conditions?

The most straightforward way to give a solution of such a problem is the construction of an object with the desired properties.

For non-realizability the straightforward approach is complete enumeration of all possible objects and showing for each one of them that it doesn't meet the conditions given. In theory this often is possible because the discrete setting reduces to a finite number of combinatorial possibilities. However, the number of possibilities typically grows exponentially with the size of the object and thus makes this approach intractable very quickly.

Therefore indirect methods and conceptual arguments are pursued. One method is to expose an "obstruction" to realizability, i.e. a property all realizable instances have and that contradicts the given conditions. Another approach is to exhibit "impossible substructures."

Chapter 1 takes place in the Euclidean plane $\mathbb{R}^2$. We are given a finite point set $\mathcal{P}$ and look at subsets $\mathcal{S}$ of non–parallel segments between points of $\mathcal{P}$.

Is there a subset $\mathcal{S}$ of $\#\mathcal{P}$ segments between points of $\mathcal{P}$ that are non–avoiding (a stronger version of non–parallel) and primitive (only the endpoints lie in $\mathcal{P}$) at the same time?

We present two algorithms that solve the problem for each condition separately. One is essentially the algorithm given by Pach, Pinchasi and Sharir in their paper [30]. The other one uses ideas from Ungar's proof of the slope problem (see [37]). Then we turn our attention to the Jamison–Hill catalogue of slope–critical examples which have the minimal possible number of non–parallel segments. Among these we find three examples where the two conditions listed above cannot be met simultaneously. In the other examples of the catalogue we give complete systems of non–avoiding primitive segments.

In Chapter 2 we construct a family of special deformed d-cubes. To this end we streamline an approach of Ziegler [40] and Rörig [31]. For every dimension $d \geq 4$ we get a cube C_d that has an increasing Hamiltonian path with respect to the last coordinate x_d. At the same time C_d contains the quadrilateral surface F_d on 2^d vertices constructed by McMullen, Schulz and Wills [26] in

its 2-skeleton in such a way that F_d survives the projection to the last three coordinates.

The starting point for Chapter 3 is Stratified Morse Theory (SMT) as developed by Goresky and MacPherson [18]. For polyhedral complexes in $\mathbb{R}^d$ and especially for polyhedral surfaces in $\mathbb{R}^3$ the Morse data can be obtained in a purely combinatorial way once a vertex ordering is fixed. Afterwards we go beyond pure SMT for surfaces and do a more detailed analysis of possible forms of critical points.

In Chapter 4 we follow the approach of Novik [29] that exploits the classical obstruction theory for piecewise linear embeddability to find "obstruction systems" for geometric realizability.

We associate with any simplicial complex K and any integer m a system of linear equations and inequalities. If K has a simplicial embedding in $\mathbb{R}^m$ then the system has an integer solution. This extends the work of Novik by using not only intersection but also linking numbers.

This chapter has appeared in the proceedings of the Oberwolfach Seminar "Discrete Differential Geometry" held in May–June 2004 [7].

Contents

Non-Avoiding Primitive Segments in the Plane

1.1 The Problem

The starting point for this chapter is the following theorem, which settled a conjecture by Scott from 1970 [34].

Theorem 1.1 (Ungar 1982 [37])**.** *Let $\mathcal{P}$ be a set of $N = 2n$ or $N = 2n + 1$ points in the plane, not all on a line. Then the lines determined by points in $\mathcal{P}$ assume at least $2n$ different directions.*

For $N = 3$ the points form the vertices of a triangle, so they even determine 3 directions, one more than required. For $N \geq 4$ the bound is sharp, as the family of bipencils shows (see Figure 1.1).
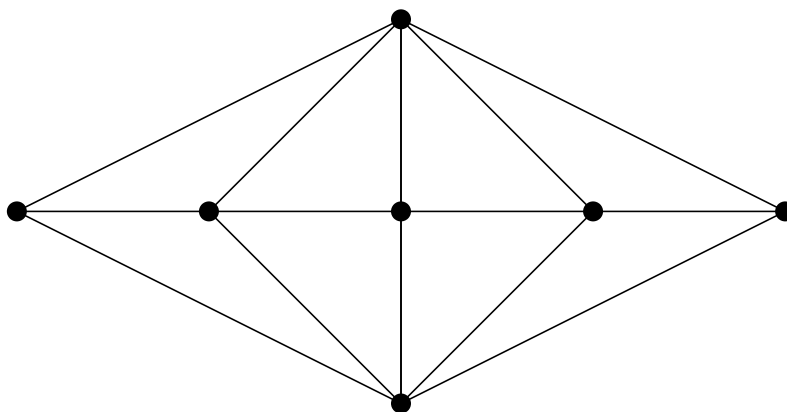
Figure 1.1: A bipencil with 7 points determines 6 directions

A configuration of $N = 2n + 1$ points that determines only $2n$ directions is called *slope–critical*. In particular slope–critical configurations contain an odd number of points. There are three infinite families of slope–critical configurations known, one of which includes the family of bipencils mentioned

above as a special case. These families and 97 slope–critical configurations not in these families were catalogued by Jamison and Hill in 1983 [20]. We thank Marc Fitch, who made this catalogue available for us in MATHE-MATHICA format [12].

Ungar's proof of Theorem 1.1 uses the combinatorial model of "allowable sequences" developed by Goodman and Pollack [17]. One can represent the $2n$ directions of Ungar's theorem by $2n$ segments that connect two points of $\mathcal{P}$. In this context there are two properties of line segments in the plane we investigate further.

Definition 1.2 (primitive, avoiding)**.**

1. A line segment s is *primitive* with respect to the set $\mathcal{P}$ if s connects two points of $\mathcal{P}$ and these are the only points of s contained in $\mathcal{P}$.
2. Two segments belonging to distinct lines are *avoiding* if these lines are parallel or meet outside the segments. Otherwise they are called *non-avoiding*.

(a) primitive   (b) not primitive

(c) avoiding
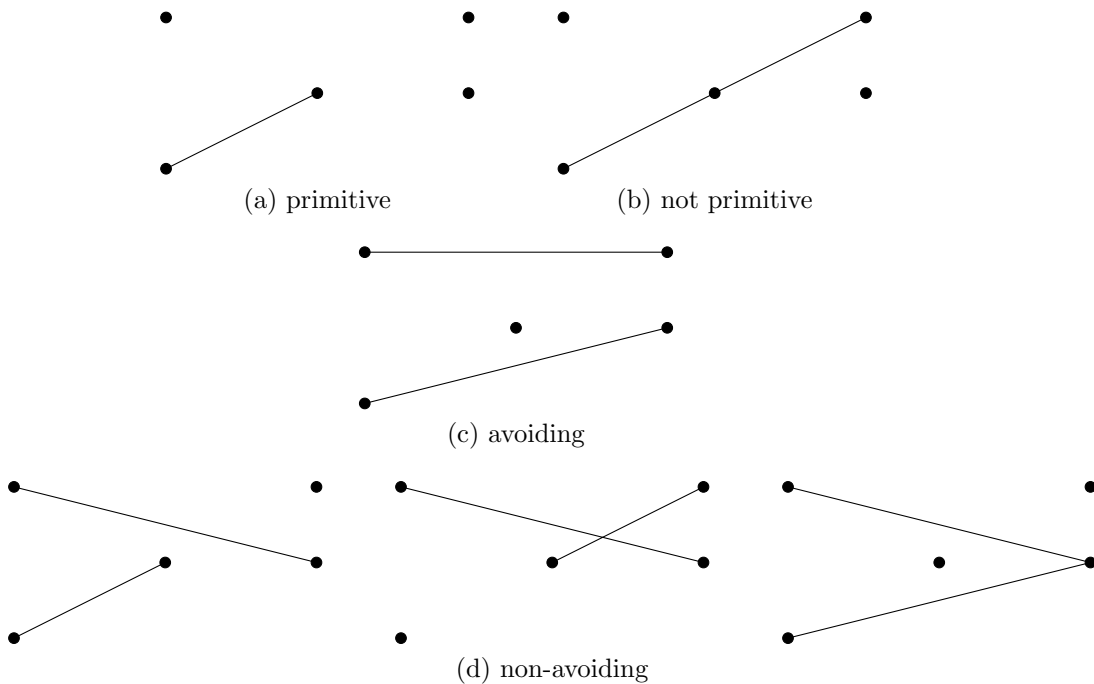
(d) non-avoiding

Figure 1.2: Properties of line segments

We observe that two segments are avoiding iff they form the opposite edges of a convex quadrilateral and that they are non-avoiding iff one intersects the line determined by the other.

The $2n$ directions guaranteed by Ungar's Theorem can obviously be represented by $2n$ segments that are *primitive* with respect to $\mathcal{P}$.

In 2003 Pach, Pinchasi and Sharir proved the following strengthening of Ungar's Theorem.

Theorem 1.3 (Pach, Pinchasi, Sharir, [30])**.** *Let $\mathcal{P}$ be a set of $N = 2n$ or $N = 2n + 1 \geq 4$ points in the plane not all on a line. Then there are $2n$ non-avoiding segments whose endpoints lie in $\mathcal{P}$.*

Their proof is algorithmic and uses primal as well as dual methods.

Since the segments guaranteed by Ungar's theorem can be chosen to be primitive and according to Pach, Pinchasi and Sharir they can also be chosen non-avoiding it seems natural to ask for both conditions to be satisfied simultaneously.

Conjecture 1.4 (Ziegler [39])**.** *Let $\mathcal{P}$ be a set of $N = 2n$ or $N = 2n + 1$, $n \geq 2$, points in the plane not all on a line. Then there are $2n$ non-avoiding primitive segments whose endpoints lie in $\mathcal{P}$.*

1.2   Outline

In Section 1.3 we present an algorithm that works entirely in the primal plane and finds the same set of segments as the algorithm of Pach, Pinchasi and Sharir. We call this algorithm PPS Algorithm. We prove correctness of the PPS algorithm and thus have a proof of Theorem 1.3 that uses only primal methods. The segments found by this algorithm are not primitive in general and cannot always be chosen primitive by shortening them without losing the non-avoiding property.

In Section 1.4 we survey Ungar's classical proof of Theorem 1.1. We present an algorithm that is inspired by this proof and works only in the geometric setting. Its correctness is proved by going back to the allowable sequences.

The segments found by this algorithm are avoiding (i.e. not non–avoiding) in general, as a small example shows.

Section 1.5 we turn our attention to *complete* systems of non–avoiding primitive segments in slope–critical configurations. Where a system $\mathcal{S}$ of segments between points of $\mathcal{P}$ is called *complete*, if every direction defined by $\mathcal{P}$ is represented by a segment in $\mathcal{S}$. We describe the methods used to search complete systems of non-avoiding primitive segments in the examples of the

Jamison–Hill catalogue and present complete systems of non-avoiding primitive segments for all but three of the known slope–critical point configurations.
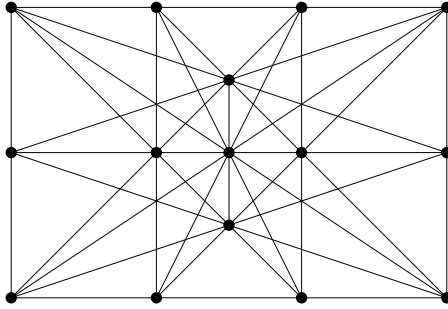
Figure 1.3: Counterexample to Conjecture 1.4 with 15 points

In Section 1.6 we present the main result of this chapter: Conjecture 1.4 does not hold. There are three slope–critical counterexamples with $2n + 1 = 15$, $2n + 1 = 17$ and $2n + 1 = 23$ points respectively where the $2n$ segments guaranteed by Ungar's proof cannot be chosen both primitive and non-avoiding. For the smallest example we will present a verification of this fact by hand.

Theorem 1.5 (Main Result). *The slope–critical configuration number $\mathbb{Z}\_15\_4D$ in the Jamison–Hill catalogue (see Figure 1.3) consists of $2n + 1 = 15$ points and does not admit $2n = 14$ non-avoiding primitive segments.*

1.3   The PPS Algorithm in the primal plane

In this section we present the PPS algorithm. It works with an even number of points. If $\mathcal{P}$ contains $2n + 1$ points we may delete any point and apply the algorithm to the remaining $2n$ points to get the $2n$ segments required in this case.

For this algorithm as well as for the Ungar algorithm we need the following basic notions of planar geometry.

Definition 1.6. Any oriented line ℓ is the boundary of two closed halfplanes, the left halfplane $\overline{\ell}^{+}$ and the right halfplane $\overline{\ell}^{-}$. When the boundary is dropped we get the open halfplanes $\ell^{+} = \overline{\ell}^{+} \setminus \ell$ and $\ell^{-} = \overline{\ell}^{-} \setminus \ell$. We say that a point $p \in \mathbb{R}^2$ lies *strictly to the left* of ℓ if $p \in \ell^{+}$. Similarly $p \in \mathbb{R}^2$ lies *strictly to the right* of ℓ if $p \in \ell^{-}$.

For sets $\mathcal{P}$ and $\widetilde{\mathcal{P}}$ with disjoint convex hulls there are two *common inner tangents*, i.e. oriented lines ℓ such that $\mathcal{P} \subset \overline{\ell}^{+}$, $\widetilde{\mathcal{P}} \subset \overline{\ell}^{-}$, $\widetilde{\mathcal{P}} \cap \ell \neq \emptyset$ and $\mathcal{P} \cap \ell \neq \emptyset$.

The algorithm consists of two phases.

1.3.1 PPS Algorithm Phase 1

In Phase 1 we partition the given set $\mathcal{P}$ into sets $\mathcal{Q}_i^{\pm}$, $i = 1, \ldots, k$ that are contained in lines ℓ_i and of cardinalities $\#\mathcal{Q}_i^{\pm} =: d_i$ with $\sum d_i = n$.

Algorithm 1.7 (PPS Phase 1).
Input: A point set $\mathcal{P} \subset \mathbb{R}^2$ with $\#\mathcal{P} = 2n$ and an extremal point p_0 of $\mathcal{P}$.
Output:
  - lines $\ell_0, \ldots, \ell_k$,
  - segments $s_0, \ldots, s_k$ on $\ell_0, \ldots, \ell_k$,
  - sets $\mathcal{P}_i^{+}, \mathcal{P}_i^{-}, \mathcal{Q}_i^{+}, \mathcal{Q}_i^{-}$ for $0 \leq i \leq k$ and
  - numbers $d_0, \ldots, d_k$

with the properties asserted by Lemma 1.10.

split $\mathcal{P}$ into two sets $\mathcal{P}_0^{+}$ and $\mathcal{P}_0^{-}$ with disjoint convex hulls both of size n such that a common inner tangent ℓ_0 oriented from $\mathcal{P}_0^{+}$ to $\mathcal{P}_0^{-}$ runs through $p_0 \in \mathcal{P}_0^{-}$. W.l.o.g. $\mathcal{P}_0^{-}$ lies to the right of ℓ_0. (see Figure 1.4)
$d_0 := \min\{\#\mathcal{P}_0^{-} \cap \ell_0, \#\mathcal{P}_0^{+} \cap \ell_0\}$.
let $\mathcal{Q}_0^{-}$ contain the first d_0 points of $\mathcal{P}_0^{+} \cap \ell_0$ and $\mathcal{Q}_0^{+}$ contain the last d_0 points of $\mathcal{P}_0^{-} \cap \ell_0$ along ℓ_0.
$\mathcal{P}_1^{-} := \mathcal{P}_0^{-}$ and $\mathcal{P}_1^{+} := \mathcal{P}_0^{+}$.
$i := 1$.
while $\mathcal{P}_i^{-} \cup \mathcal{P}_i^{+}$ is not contained in a line, **do**
  construct the common inner tangent ℓ_i oriented from $\mathcal{P}_i^{-}$ to $\mathcal{P}_i^{+}$ such that $\mathcal{P}_i^{-}$ lies to the right and $\mathcal{P}_i^{+}$ lies to the left of ℓ_i.
  let s_i be the shortest segment on ℓ_i that has one endpoint in $\mathcal{P}_i^{+}$ and the other endpoint in $\mathcal{P}_i^{-}$
  $d_i := \min\{\#\mathcal{P}_i^{-} \cap \ell_i, \#\mathcal{P}_i^{+} \cap \ell_i\}$.
  let $\mathcal{Q}_i^{-}$ contain the first d_i points of $\mathcal{P}_i^{-} \cap \ell_i$ and $\mathcal{Q}_i^{+}$ contain the last d_i points of $\mathcal{P}_i^{+} \cap \ell_i$ along ℓ_i.
  $\mathcal{P}_{i+1}^{-} := \mathcal{P}_i^{-} \setminus \mathcal{Q}_i^{-}$ and $\mathcal{P}_{i+1}^{+} := \mathcal{P}_i^{+} \setminus \mathcal{Q}_i^{+}$.
  $i := i + 1$.
let k be the index when the **while** loop terminates.
let ℓ_k be the line that contains $\mathcal{P}_k^{-} \cup \mathcal{P}_k^{+}$.
$d_k := \#\mathcal{P}_k^{-}$.

$$\mathcal{Q}_k^- := \mathcal{P}_k^- \text{ and } \mathcal{Q}_k^+ := \mathcal{P}_k^+.$$

Remark 1.8. *For the lines $\ell_1, \ldots, \ell_k$ we chose the orientation from $\mathcal{P}_0^-$ to $\mathcal{P}_0^+$ and for ℓ_0 the opposite orientation in order to have $\mathcal{P}_i^-$ to the right of ℓ_i for every $i = 0, \ldots, k$. Also $\mathcal{Q}_i^-$ is chosen to contain the first points of $\mathcal{P}_i^+ \cup \mathcal{P}_i^-$ along ℓ_i and $\mathcal{Q}_i^+$ to contain the last ones. These choices lead to a smoother reasoning in the following proofs.*
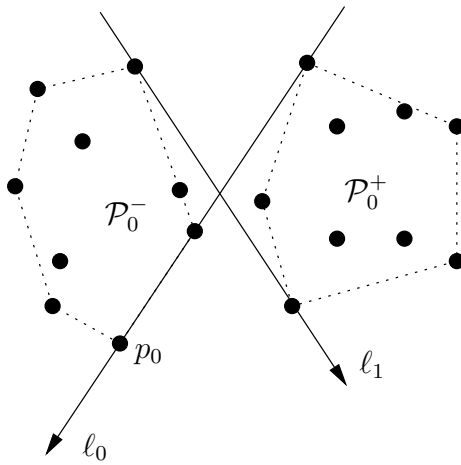

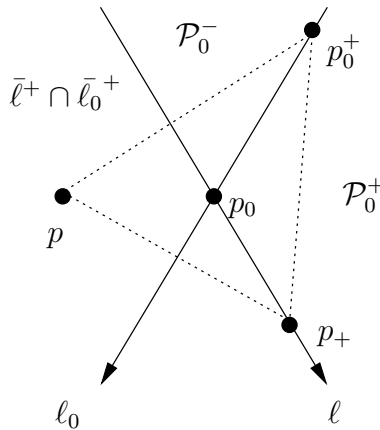Figure 1.4: Preparation step of Algorithm 1.7

Figure 1.5: Illustration for Lemma 1.9

Lemma 1.9. *Let $\mathcal{P} \subset \mathbb{R}^2$ be a point set with $\#\mathcal{P} = 2n$ and p_0 an extremal point of $\mathcal{P}$. Let $\mathcal{P}_0^+$ and $\mathcal{P}_0^-$ be subsets of $\mathcal{P}$ with disjoint convex hulls both of*

size n such that a common inner tangent ℓ_0 oriented from $\mathcal{P}_0^+$ to $\mathcal{P}_0^-$ runs through $p_0 \in \mathcal{P}_0^-$. W.l.o.g. $\mathcal{P}_0^-$ lies to the right of ℓ_0.
Then $\mathcal{P}_0^-$ lies (not neccessarily strictly) to the left of every line $\ell = p_0 p_+$ with $p_+ \in \mathcal{P}_0^+$.

Proof. Write $\ell_0 = \overline{p_0^+ p_0}$ with $p_0^+ \in \mathcal{P}_0^+$. Let $p \in \bar{\ell}^+ \cap \bar{\ell_0}^+$ with $p \neq p_0$. Then p_0 lies inside the triangle $\triangle p p_+ p_0^+$. (see Figure 1.5) As p_0 is extremal for $\mathcal{P}$ we have $p \notin \mathcal{P}$. $\qquad\square$

Lemma 1.10 (Guarantees for PPS Phase 1)**.** *The sets constructed by Algorithm 1.7 have the following properties for all $i = 0, \ldots, k$:*

1. $\#\mathcal{P}_i^+ = \#\mathcal{P}_i^-$,
2. $\mathcal{P}_0^- \supset \mathcal{P}_1^- \supset \ldots \supset \mathcal{P}_k^-$, and $\mathcal{P}_0^+ \supset \mathcal{P}_1^+ \supset \ldots \supset \mathcal{P}_k^+$,
3. $\mathcal{P}_i^- \subset \bar{\ell}_i^-$ and $\mathcal{P}_i^+ \subset \bar{\ell}_i^+$,
4. $\mathcal{Q}_0^- \subset \mathcal{P}_0^+ \cap \ell_0$, $\mathcal{Q}_0^+ \subset \mathcal{P}_0^- \cap \ell_0$,
5. $\mathcal{Q}_i^- \subset \mathcal{P}_i^- \cap \ell_i$, $\mathcal{Q}_i^+ \subset \mathcal{P}_i^+ \cap \ell_i$ for $1 \leq k \leq k-1$,
6. *At least one of the following assertions holds:*
   (a) $\mathcal{Q}_i^- \subset \ell_{i+1}^+$ and $\mathcal{Q}_{i+1}^+ \subset \ell_i^+$
   (b) $\mathcal{Q}_i^+ \subset \ell_{i+1}^-$ and $\mathcal{Q}_{i+1}^- \subset \ell_i^-$,
7. $\#\mathcal{Q}_i^+ = \#\mathcal{Q}_i^- = d_i \geq 1$,
8. $\sum_{i=1}^{k} d_i = n$,
9. $d_0 \geq d_k$.

Proof. The claims 1,2,3,4,5,7 and 8 are obvious by construction.

6. First case $i = 0$.
   By construction we have $\mathcal{Q}_0^- \subset \mathcal{P}_1^+ \subset \bar{\ell}_1^+$, $\mathcal{Q}_0^+ \subset \mathcal{P}_1^- \bar{\ell}_1^-$, $\mathcal{Q}_1^- \subset \bar{\ell}_0^-$ and $\mathcal{Q}_1^+ \subset \bar{\ell}_0^+$. As the point $\ell_1 \cap \ell_0$ lies in at most one of these sets, a) or b) holds.
   Second case $i > 1$.
   Because $\mathcal{Q}_i^-$ lies on ℓ_i before $\mathcal{Q}_i^+$ and ℓ_i runs from ℓ_{i+1}^+ to ℓ_{i+1}^- we have $\mathcal{Q}_i^- \subset \ell_{i+1}^+$ or $\mathcal{Q}_i^+ \subset \ell_{i+1}^-$. By (2) and (3) we also have $\mathcal{Q}_{i+1}^- \subset \mathcal{P}_{i+1}^- \subset \mathcal{P}_i^- \subset \bar{\ell}_i^-$ and similarly $\mathcal{Q}_{i+1}^+ \subset \bar{\ell}_i^+$. Furthermore the sets conv $\mathcal{Q}_i^+$, conv $\mathcal{Q}_i^-$, $\mathcal{Q}_{i+1}^+$ and $\mathcal{Q}_{i+1}^-$ are by construction pairwise disjoint. So $\ell_i \cap \ell_{i+1}$ lies in at most one of them and the claim holds.
9. We show: If supp $\ell_0 \neq$ supp ℓ_k then $\mathcal{Q}_k^- = \{p_0\}$.
   First we show: If $p_0 \in \ell_j$ for $j > 0$ then $\mathcal{P}_j^+ \cup \mathcal{P}_j^-$ is contained in a line, which means $j = k$ and thus $p_0 \in \mathcal{Q}_k^- \subset \ell_k$.
   Let $p_0 \in \ell_j$. The common inner tangent ℓ_j by construction has $\mathcal{P}_j^-$ on the right. But it also is of the form $\overline{p_0 p_+}$ with $p_+ \in \mathcal{P}_j^+$ and thus by

Lemma 1.9 has $\mathcal{P}_j^- \subset \mathcal{P}_0^-$ also on the left. Therefore we get $\mathcal{P}_j^- \subset \ell_j$. Similarly we also get $\mathcal{P}_j^+ \subset \ell_j$. And tus $j = k$.

To complete the proof we observe the following. If $\operatorname{supp} \ell_0 \neq \operatorname{supp} \ell_k$ then $\ell_0 \cap \ell_k = p_0$. Write $\ell_k = \overline{p_- p_+}$ with $p_- \in \mathcal{P}_k^-$ and $p_+ \in \mathcal{P}_k^+$. Then p_- and p_+ lie to the right and the left of ℓ_0 respectively and thus p_0 lies on the segment $\overline{p_- p_+}$. Which implies together with the extremality of p_0 that $p_- = p_0$.

Therefore $\mathcal{Q}_k^- = \{p_0\}$.

$\square$

Lemma 1.11. *Every segment joining a $p_- \in \mathcal{P}_i^-$ and a $p_+ \in \mathcal{P}_i^+$ is non-avoiding with s_i.*

Proof. $\mathcal{P}_i^-$ lies to the right of ℓ_i and $\mathcal{P}_i^+$ lies to the left of ℓ_i. Thus $\overline{p_- p_+}$ intersects ℓ_i. As s_i lies on ℓ_i we have that $\overline{p_- p_+}$ and s_i are non-avoiding. $\square$

1.3.2   PPS Algorithm Phase 2

In Phase 2 we construct $d_i + d_{i+1} - 1$ segments "between" the consecutive pair ℓ_i and ℓ_{i+1} of lines for every $i = 0, \ldots, k-1$.

Lemma 1.12. *Let $\ell, \widetilde{\ell}$ be two lines in the plane. If $q \in \ell \cap \widetilde{\ell}^+$, $\widetilde{q} \in \widetilde{\ell} \cap \ell^+$, $p_+ \in \overline{\ell}^+ \cap \overline{\widetilde{\ell}}^+$ and $p_- \in \overline{\ell}^- \cap \overline{\widetilde{\ell}}^-$. Then the segments $s := \overline{q\widetilde{q}}$ and $\overline{p_+ p_-}$ are non-avoiding. The statement also holds for $q \in \ell \cap \widetilde{\ell}^-$ and $\widetilde{q} \in \widetilde{\ell} \cap \ell^-$.*

Proof. The point p_- lies to the right of the line $q\widetilde{q}$. If p_+ does not lie to the left of $q\widetilde{q}$ it lies inside the triangle $T = \triangle p q \widetilde{q}$. The oriented line $p_- p_+$ crosses ℓ and $\widetilde{\ell}$ to enter T and thus has to leave through the segment $\overline{q_- q_+}$ (see Figure 1.6).

The statement holds for $q \in \ell \cap \widetilde{\ell}^-$ and $\widetilde{q} \in \widetilde{\ell} \cap \ell^-$ by symmetry.

$\square$

Algorithm 1.13 (PPS Phase 2)**.**
Input: Point sets as described by lemma 1.10
Output: Sets $\mathcal{S}_i$ of segments, such that $\#\mathcal{S}_i = d_i + d_{i+1} - 1$ and all segments in $\bigcup_{i=1}^{k}(\mathcal{S}_i \cup \{s_i\})$ are pairwise non-avoiding.

    for $i \in \{0, \ldots, k-1\}$ **do**
       if $\mathcal{Q}_i^- \subset \ell_{i+1}^+$ **and** $\mathcal{Q}_{i+1}^+ \subset \ell_i^+$ **then**
         $\mathcal{Q} := \mathcal{Q}_i^-$ and $\widetilde{\mathcal{Q}} := \mathcal{Q}_{i+1}^+$.

Figure 1.6: The non-trivial case of Lemma 1.12

else
$\mathcal{Q} := \mathcal{Q}_i^+$ and $\widetilde{\mathcal{Q}} := \mathcal{Q}_{i+1}^-$.
sort $\mathcal{Q} = \{q_1, \ldots, q_d\}$ such that q_1 ist nearest to $\ell_i \cap \ell_{i+1}$.
sort $\widetilde{\mathcal{Q}} = \{\widetilde{q}_1, \ldots, \widetilde{q}_{\widetilde{d}}\}$ such that $\widetilde{q}_1$ ist nearest to $\ell_i \cap \ell_{i+1}$.
$\mathcal{S}_i := \{\overline{q_d \widetilde{q}_1}, \ldots, \overline{q_d \widetilde{q}_{\widetilde{d}}}, \ldots, \overline{q_1 \widetilde{q}_{\widetilde{d}}}\}$

Lemma 1.14. *For every $i = 0, \ldots, k-1$ the segments in $\mathcal{S}_i$ constructed by Algorithm 1.13 do not lie on ℓ_i or ℓ_{i+1} and intersect pairwise inside the triangle $\triangle q q_d \widetilde{q}_{\widetilde{d}}$.*

Proof. Because of the choice of $\mathcal{Q}$ and $\widetilde{\mathcal{Q}}$ the intersection point $\ell_i \cap \ell_{i-1}$ does not lie in $\mathcal{Q} \cup \widetilde{\mathcal{Q}}$. So we get the desired property by construction. (See Figure 1.7) $\qquad\square$

Lemma 1.15. *Let $0 \le i < k$. Let $s \in \mathcal{S}_i$ and $p_+ \in \mathcal{P}_{i+1}^+$, $p_- \in \mathcal{P}_{i+1}^-$. Then the segment s and the segment $\overline{p_- p_+}$ are non-avoiding.*

Proof. By construction we have $\mathcal{P}_{i+1}^- \subset \overline{\ell_i}^- \cap \overline{\ell_{i+1}}^-$ and $\mathcal{P}_{i+1}^+ \subset \overline{\ell_i}^+ \cap \overline{\ell_{i+1}}^+$.

We look at the condition of the **if**-clause in Phase 2. If it is satisfied we have $\mathcal{Q}_i^- \subset \ell_{i+1}^+$ and $\mathcal{Q}_{i+1}^+ \subset \ell_{i+1}^+$. So we are in the situation of Lemma 1.12 which completes the proof in this case.

Figure 1.7: Segments between ℓ and $\widetilde{\ell}$

If the condition of the **if**-clause is not satisfied we have by Lemma 1.10(6) that $\mathcal{Q}_i^+ \subset \ell_{i+1}^-$ and $\mathcal{Q}_{i+1}^- \subset \ell_{i+1}^-$. So Lemma 1.12 again completes the proof. $\quad\square$

Theorem 1.16. *The PPS algorithm is correct. In particular:*

1. *It constructs at least $2n$ segments.*
2. *These segments are pairwise non-avoiding.*

Proof.   1. It constructs

$$k + \sum_{i=0}^{k-1}(d_i + d_{i+1} - 1) = d_0 + \sum_{i=1}^{k-1} 2d_i + d_k \geq 2n$$

     segments.

2. Take two segments $t_1 \in \mathcal{S}_i \cup \{s_i\}$ and $t_2 \in \mathcal{S}_j \cup \{s_j\}$ with $i \leq j$. If $i = j$ the segments are non avoiding by Lemma 1.14 or Lemma 1.11. If $i < j$ the segment t_2 has endpoints in $\mathcal{P}_j^- \subset \mathcal{P}_{i+1}^-$ and $\mathcal{P}_j^+ \subset \mathcal{P}_{i+1}^+$. Therefore by Lemma 1.11 or Lemma 1.15 t_1 and t_2 are non-avoiding.

$\hfill\square$

1.3.3   PPS does not find non-avoiding *primitive* segments

In general the non-avoiding segments found by the PPS algorithm are not primitive. But the following example shows that we also cannot always choose primitive segments on the lines found by PPS that are non-avoiding.

Example 1.17. In the following configuration choose $p_0 = 5$. Then we get the initial partition $\mathcal{P}_0^- = \{1, 2, 3, 4, 5\}$ and $\mathcal{P}_0^+ = \{6, 7, 8, 9, 10\}$.
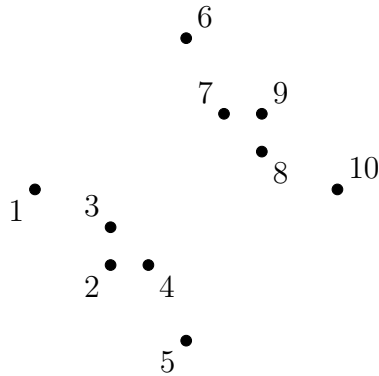
PPS finds the following system of non-avoiding segments.
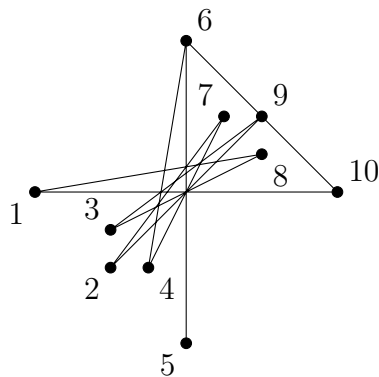
This system cannot be shortened to a system of primitive non-avoiding segments because it contains the configuration

Nevertheless the point configuration itself does admit a system of non-avoiding primitive segments as follows
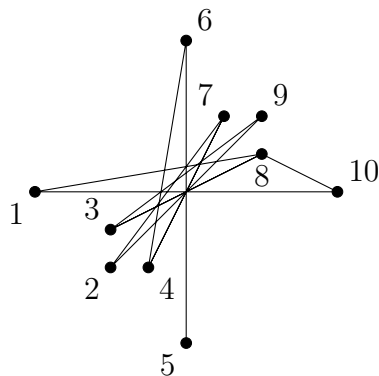
1.4   A Geometric Algorithm following Ungar's proof

In this section we present an algorithm based on Ungar's proof of Scott's conjecture that finds at least $2n$ non-parallel lines defined by $\mathcal{P}$.

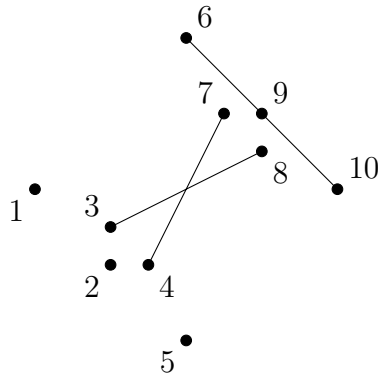#### 1.4.1   Overview of Ungar's proof

For a detailed exposition of Ungar's proof we refer to [6].

Ungar's proof works with an even number of points. If $\mathcal{P}$ contains $2n + 1$ points we may delete any point and apply Ungar's method to the remaining $2n$ points to get the $2n$ directions required in this case.

Given a configuration $\mathcal{P}$ of $2n$ points in the plane, Goodman and Pollack associate with $\mathcal{P}$ a sequence of permutations of $1, \ldots, 2n$ as follows. Choose

a generic line and project $\mathcal{P}$ orthogonally to this line. Number the points of $\mathcal{P}$ by $1, \ldots 2n$ according to the order of the projected points on this line. Make the line rotate clockwise. Then the order of the projected points changes whenever the projection direction passes a direction of one or more lines defined by $\mathcal{P}$. The *allowable sequence* associated with $\mathcal{P}$ is the sequence of permutations of $1, \ldots, 2n$ obtained in this way. (See Figure 1.8.) Every change of permutation in this sequence is called a *move*. Every move reverses one or more disjoint increasing substrings.
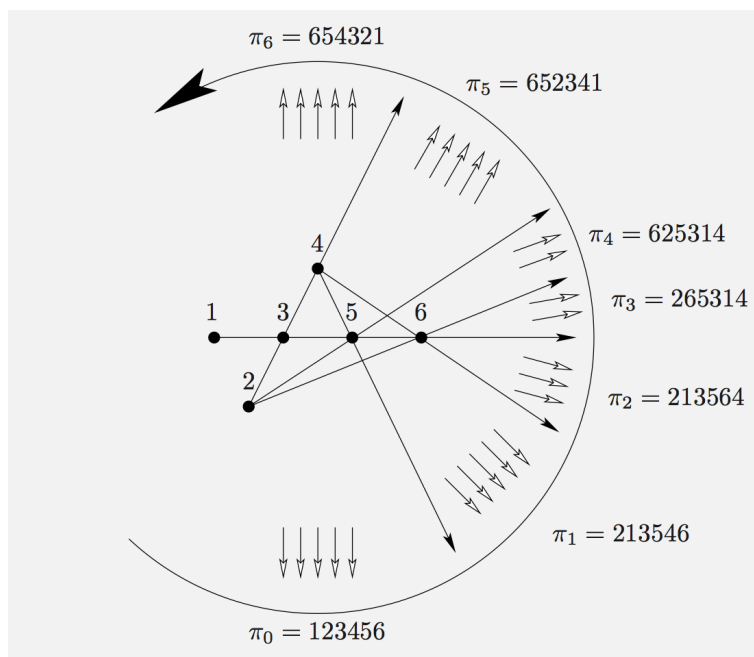
Figure 1.8: Associated allowable sequence for a point set (image from [2], used by permission)

To visualize the key argument of Ungar's proof we separate every permutation into its first half which consists of the first n elements and the second half which consists of the remaining n elements by a *central barrier*.

The backbone of Ungar's proof is formed by those moves that reverse substrings that contain the central barrier. These moves are called *crossing moves*.

Before a crossing move the middle word has to be built up and afterwards it has to be dismantled on either side of the central barrier one letter at a time. On at least one side the letter next to the central barrier is contained in a move which we call *touching move*. On the side of a touching move there are

enough moves to guarantee in total $2n$ moves and thus $2n$ directions defined by $\mathcal{P}$.

We translate Ungar's combinatorial proof into a geometric algorithm by exploiting the following fact:

Lemma 1.18 (Moves and common inner tangents). *Consider a move in the allowable sequence associated with $\mathcal{P}$. Let $k_1, \ldots, k_i, \ldots, k_j, \ldots, k_{2n}$ be the permutation before the move, $k_1, \ldots, k_j, \ldots, k_i, \ldots, k_{2n}$ the permutation afterwards and $k_i, \ldots, k_j$ an increasing substring reverted by the move.*

The substring $k_i, \ldots, k_j$ corresponds to the common inner tangent to the sets $\mathcal{P}^- := \{k_1, \ldots, k_m\}$ and $\mathcal{P}^+ := \{k_{m+1}, \ldots, k_{2n}\}$ with $1 \leq i \leq m < j \leq 2n$ oriented from $\mathcal{P}^+$ to $\mathcal{P}^-$ and with $\mathcal{P}^+$ to the left.

1.4.2   Ungar Algorithm Phase 1

According to Lemma 1.18 the middle word of any crossing move corresponds to a common inner tangent to $\{k_1, \ldots, k_n\}$ and $\{k_{n+1}, \ldots, k_{2n}\}$. Phase 1 of the Ungar algorithm consists of finding all lines which correpond to crossing moves in this way.

Algorithm 1.19 (Ungar Phase 1).
Input: A planar point set $\mathcal{P}$ with $\#\mathcal{P} = 2n$, not all on a line
Output: • lines $\ell_1, \ldots, \ell_k$,
          • sets $\mathcal{P}_i^+, \mathcal{P}_i^-, \mathcal{Q}_i^+$ and $\mathcal{Q}_i^-$ for $1 \leq i \leq k$,
          • numbers d_i for $1 \leq i \leq k$
with the properties asserted by Lemma 1.21.

split $\mathcal{P}$ into two sets $\mathcal{P}_1^+$ and $\mathcal{P}_1^-$ with disjoint convex hulls both of size n.

$i := 1$.
while $\mathcal{P}_i^- \neq \mathcal{P}_1^+$ **do**
   construct the common inner tangent ℓ_i oriented from $\mathcal{P}_i^-$ to $\mathcal{P}_i^+$ such that $\mathcal{P}_i^-$ lies to the right and $\mathcal{P}_i^+$ lies to the left of ℓ_i.
   $d_i := \min\{\#\mathcal{P}_i^- \cap \ell_i, \#\mathcal{P}_i^+ \cap \ell_i\}$.
   let $\mathcal{Q}_i^-$ contain the first d_i points of $\mathcal{P}_i^- \cap \ell_i$ and $\mathcal{Q}_i^+$ contain the last d_i points of $\mathcal{P}_i^+ \cap \ell_i$ along ℓ_i.
   $\mathcal{P}_{i+1}^- := \mathcal{P}_i^- \setminus \mathcal{Q}_i^- \cup \mathcal{Q}_i^+$ and $\mathcal{P}_{i+1}^+ := \mathcal{P}_i^+ \setminus \mathcal{Q}_i^+ \cup \mathcal{Q}_i^-$.
   $i := i + 1$.
let k be the index where the **while** loop terminates
construct the common inner tangent ℓ_k oriented from $\mathcal{P}_k^-$ to $\mathcal{P}_k^+$ such that $\mathcal{P}_k^-$ lies to the right and $\mathcal{P}_k^+$ lies to the left of ℓ_k.

$d_k := \min\{\#\mathcal{P}_k^- \cap \ell_k, \#\mathcal{P}_k^+ \cap \ell_k\}$.
let $\mathcal{Q}_k^-$ contain the first d_k points of $\mathcal{P}_k^- \cap \ell_k$ and $\mathcal{Q}_k^+$ contain the last d_k points of $\mathcal{P}_k^+ \cap \ell_k$ along ℓ_k.

First we summarize how the moves of Ungar's proof and the sets of the Ungar algorithm are related:

Lemma 1.20. *The sets constructed by Algorithm 1.19 have the following properties for all $i = 1, \ldots, k$:*

1. *the line ℓ_i corresponds to a crossing move,*
2. *the sets $\mathcal{P}_i^+, \mathcal{P}_i^-$ correspond to left and right halves of the permutations before ℓ_i,*
3. *the sets $\mathcal{Q}_i^+, \mathcal{Q}_i^- \subset \ell_i$ correspond to the beginning and the end of the middle word and contain the elements, that change sides in the move ℓ_i,*
4. *the numbers d_i correspond to the number of elements, that change sides in the move ℓ_i,*
5. *ℓ_k is a reorientation of ℓ_1.*

Proof. Follows directly from Ungar's proof using Lemma 1.18.   □

The following Lemma shows parallels and differences to the PPS algorithm.

Lemma 1.21. *The sets constructed by Algorithm 1.19 have the following properties for all $i = 1, \ldots, k$:*

1. *$\#\mathcal{P}_i^+ = \#\mathcal{P}_i^- = n$*
2. *$\operatorname{conv} \mathcal{P}_i^+ \cap \operatorname{conv} \mathcal{P}_i^- = \emptyset$*
3. *$\mathcal{P}_i^- \subset \overline{\ell_i^-}$ and $\mathcal{P}_i^+ \subset \overline{\ell_i^+}$*
4. *$\mathcal{Q}_i^- \subset \mathcal{P}_i^- \cap \ell_i,\ \mathcal{Q}_i^+ \subset \mathcal{P}_i^+ \cap \ell_i$*
5. *At least one of the following assertions holds:*
    (a) *$\mathcal{Q}_i^- \cap \mathcal{Q}_{i+1}^+ = \emptyset$*
    (b) *$\mathcal{Q}_i^+ \cap \mathcal{Q}_{i+1}^- = \emptyset$*
6. *$\#\mathcal{Q}_i^+ = \#\mathcal{Q}_i^- = d_i \geq 1$*
7. *$\sum_{i=1}^{k-1} d_i \geq n$*
8. *$d_k = d_1$*

Proof. All these guarantees also follow from the translation of Ungar's proof with the help of Lemma 1.18. Especially (5) follows from the fact that a touching move occurs on at least one side. But it can be derived directly from $\ell_i \neq \ell_{i+1}$.   □

Remark 1.22. *We don't prove that the **while**-loop terminates, but rely for this fact on Ungar's proof.*

1.4.3   Ungar Algorithm Phase 2

In Phase 2 we find $d_i + d_{i+1} - 1$ lines between ℓ_i and ℓ_{i+1}, $i = 1, \ldots, k-1$. These lines correspond to moves that dismantle the middle word after the crossing move corresponding to ℓ_i and build up the middle word before the crossing move corresponding to ℓ_{i+1}. So by Lemma 1.18 they are common inner tangents to $\{k_1, \ldots, k_j\}$ and $\{k_{j+1}, \ldots, k_{2n}\}$ with k_{j+1} in the middle word $\ell_i \cap \mathcal{P}$.

The conditions $\mathcal{Q}_i^+ \cap \mathcal{Q}_{i+1}^- = \emptyset$ and $\mathcal{Q}_i^- \cap \mathcal{Q}_{i+1}^+ = \emptyset$ respectively are weaker than the requirement of a touching move. Nevertheless each of them is sufficient to guarantee enough moves between ℓ_i and ℓ_{i+1} and is easier to check in the algorithm. If the first condition is satisfied the sets we need can be viewed in terms of the sets already constructed as follows:

$$
\overbrace{\qquad\qquad}^{\mathcal{P}_{i+1}^-} \quad \overbrace{\qquad\qquad}^{\mathcal{P}_{i+1}^+}
$$
$$
\overbrace{\qquad}^{\ell_i}
$$
$$
\underbrace{k_1 \; \ldots}_{\mathcal{P}_{i+1}^- \setminus \ell_i} \; \underbrace{\overbrace{\mathcal{Q}_i^+ \; \ldots \; | \; \ldots \; \mathcal{Q}_i^- \; \ldots \; k_{2n}}}_{\mathcal{P}_{i+1}^+ \cup (\mathcal{P}_{i+1}^- \cap \ell_i) \setminus \mathcal{Q}_i^+}
$$

The sets to which common inner tangents correspond to moves shortening the middle word are constructed by distributing $\mathcal{Q}_i^+$ onto the halves we see in the sketch. The moves which make the middle word longer are constructed analoguously.

Algorithm 1.23 (Ungar Phase 2).
Input: lines and sets as described by Lemma 1.21
Output: $d_i + d_{i+1} - 1$ lines between ℓ_i and ℓ_{i+1} for each $i = 1, \ldots k-1$

    for $i = 1$ to $k-1$ **do**
      if $\mathcal{Q}_i^+ \cap \mathcal{Q}_{i+1}^- = \emptyset$ **then**
        $\mathcal{Q} := \mathcal{Q}_i^+,\ \widetilde{\mathcal{Q}} := \mathcal{Q}_{i+1}^-,$
        $\mathcal{R} := \mathcal{P}_{i+1}^- \setminus \ell_i,\ \widetilde{\mathcal{R}} := \mathcal{P}_{i+1}^+ \cup (\mathcal{P}_{i+1}^- \cap \ell_i) \setminus \mathcal{Q}_i^+,$
        $\mathcal{S} := \mathcal{P}_{i+1}^- \setminus \ell_{i+1},\ \widetilde{\mathcal{S}} := \mathcal{P}_{i+1}^+ \cup (\mathcal{P}_{i+1}^- \cap \ell_{i+1}) \setminus \mathcal{Q}_{i+1}^-$
      else
        $\mathcal{Q} := \mathcal{Q}_i^-,\ \widetilde{\mathcal{Q}} := \mathcal{Q}_{i+1}^+,$
        $\mathcal{R} := \mathcal{P}_{i+1}^+ \setminus \ell_i,\ \widetilde{\mathcal{R}} := \mathcal{P}_{i+1}^- \cup (\mathcal{P}_{i+1}^+ \cap \ell_i) \setminus \mathcal{Q}_i^-,$
        $\mathcal{S} := \mathcal{P}_{i+1}^+ \setminus \ell_{i+1},\ \widetilde{\mathcal{S}} := \mathcal{P}_{i+1}^- \cup (\mathcal{P}_{i+1}^+ \cap \ell_{i+1}) \setminus \mathcal{Q}_{i+1}^+$
      sort $\mathcal{Q} = \{q_1, \ldots, q_d\}$ such that q_1 ist nearest to $\ell_i \cap \ell_{i+1}$.

sort $\widetilde{\mathcal{Q}} = \{\widetilde{q}_1, \ldots, \widetilde{q}_{\widetilde{d}}\}$ such that $\widetilde{q}_1$ ist nearest to $\ell_i \cap \ell_{i+1}$.
for $j = 1, \ldots, d_i$ **do**
    construct the common inner tangent $s_{ij} \neq \ell_i$ to $\mathcal{R} \cup \{q_1, \ldots q_{j-1}\}$ and $\{q_j, \ldots q_{d_i}\} \cup \widetilde{\mathcal{R}}$.
for $j = 1, \ldots, d_{i+1} - 1$ **do**
    construct the common inner tangent $\widetilde{s}_{ij} \neq \ell_{i+1}$ to $\mathcal{S} \cup \{\widetilde{q}_1, \ldots \widetilde{q}_{j-1}\}$ and $\{\widetilde{q}_j, \ldots \widetilde{q}_{d_{i+1}}\} \cup \widetilde{\mathcal{S}}$.

Remark 1.24. *This algorithm finds*

$$k - 1 + \sum_{i=1}^{k-1}(d_i + d_{i+1} - 1) = \sum_{i=1}^{k} 2d_i \geq 2n$$

lines with different directions because it translates Ungar's combinatoric proof.

1.4.4 The Ungar Algorithm does not find *non-avoiding* segments

The segments on the lines found by the Ungar algorithm can in general *not* all be chosen pairwise non-avoiding as the following example shows.

Example 1.25. In the following point configuration the segments $\overline{12}$, $\overline{34}$ and $\overline{56}$ correspond to crossing moves and are pairwise avoiding.
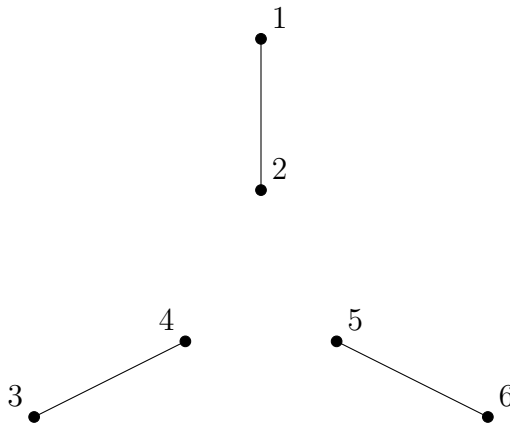
In this configuration the Ungar algorithm finds the following set of 12 primitive segments:
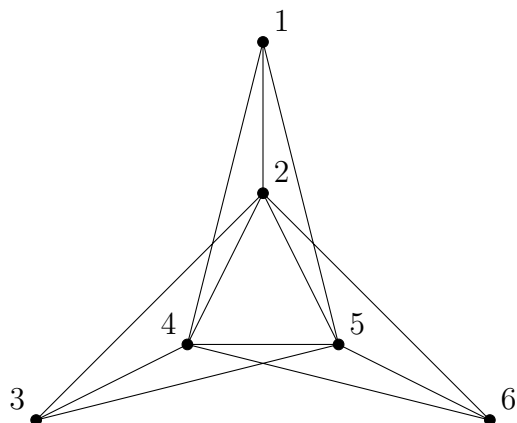
which has the following system of 6 non-avoiding primitive segments as a subset:
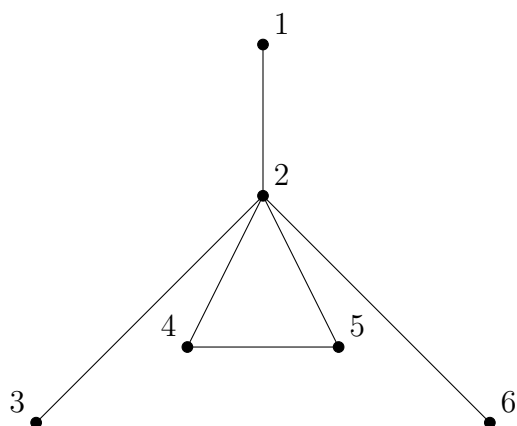
The PPS algorithm with $p_0 = 3$ and thus $\mathcal{P}_0^- = \{1, 2, 3\}$ and $\mathcal{P}_0^+ = \{4, 5, 6\}$ finds:
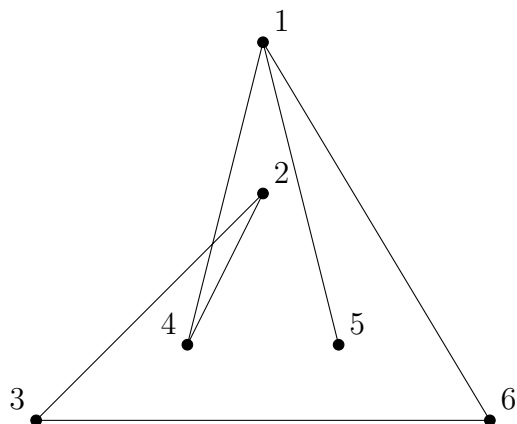
Open question: Is there a configuration with $2n < 14$ points such that the lines found by the Ungar algorithm do not contain a set of $2n$ non-avoiding primitive segments?

1.5   SYSTEMS OF NON-AVOIDING PRIMITIVE SEGMENTS IN SLOPE–CRITICAL CONFIGURATIONS

A point configuration with $2n+1$ points is *slope–critical* if it defines exactly $2n$ different slopes. In particular slope–critical point configurations contain an odd number of points. A system of $2n$ non-avoiding primitive segments in a slope–critical configuration represents all possible directions. We call such a system *complete*.

In [20] Jamison and Hill gave a survey of all known slope–critical point configurations comprising three infinite families and 97 sporadic examples. In the following we present the results of our study of these examples.

1.5.1   THE INFINITE FAMILIES

1.5.1.1   The Centered Polygons

The family of *centered polygons* is given by

$$P_0(k) := \{(0,0)\} \cup \{(\cos \tfrac{2\pi\ell}{k}, \sin \tfrac{2\pi\ell}{k} \mid \ell = 1, \ldots, k\}$$

$P_0(k)$ consists of $k+1$ points and is slope critical for all even $k \geq 2$.

A complete system of non-avoiding primitive segments is given by all segments emanating from one vertex and the chord joining its two neighbors. (See Figure 1.9)

1.5.1.2   The Exponential Crosses

For positive integers s and t and $\lambda \in \mathbb{R}, \lambda > 1$ the *exponential cross* $EX_\lambda(s,t)$ is given by

$$EX_\lambda(s,t) := \{(0,0)\} \cup \{(\pm\lambda^\ell, 0) \mid 0 \leq \ell \leq s\} \cup \{(0, \pm\lambda^\ell) \mid 0 \leq \ell \leq t\}$$

$EX_\lambda(s,t)$ consists of $2(s+t+2)+1$ points and is slope critical for all choices of s, t and λ.

A complete system of non-avoiding primitive segments is given by the segments
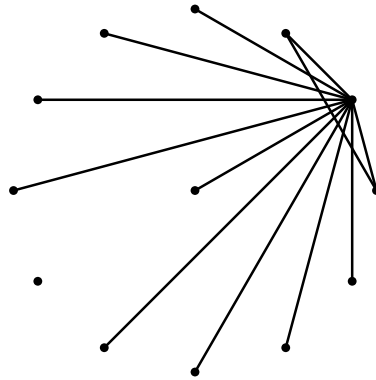
Figure 1.9: $P_0(12)$

- joining $(0,1)$ with all points of the form $(x,0)$,
- joining the two points $(\pm 1, 0)$ with all the points of the form $(0, y)$ with $y > 1$ and
- the segment joining $(0,0)$ and $(1,0)$.

See Figure 1.10.
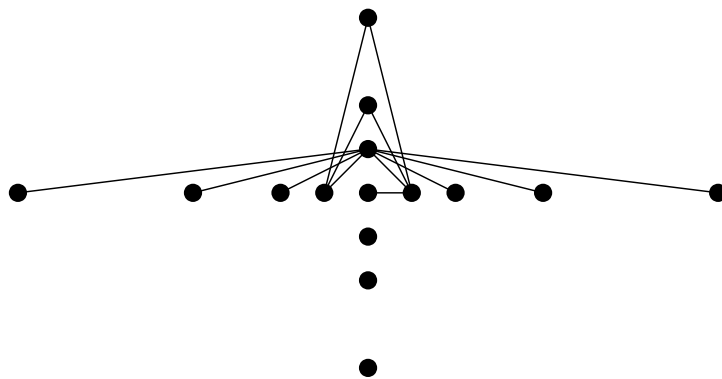
Figure 1.10: $EX_2(3,2)$

1.5.1.3 The Tricolumnar Arrays

For nonnegative integer parameters s, t and h the *tricolumnar array* $TC(s, t, h)$ is given by

$$TC(s, t, h) = \begin{aligned} &\{(\pm 1, k) \mid k = 0, \dots, s\} \\ \cup\ &\{(0, \tfrac{s}{2} \pm k) \mid k = 0, \dots, t\} \\ \cup\ &\{(0, \tfrac{s \pm (2k+1)}{2}) \mid k = 0, \dots, h - 1\}. \end{aligned}$$

$TC(s, t, h)$ consists of $2(s+t+h)+3$ points and is slope–critical for all choices of s, t and h, not all 0. The family of *bipencils* is the special case $TC(0, t, 0)$.

A complete system of non-avoiding primitive segments is given by the primitive segments

1. emanating from $(-1, 0)$ with nonnegative slope (and thus ending in points of the form $(0, y)$ or $(1, y)$ with $y \geq 0$),
2. emanating from $(1, 0)$ with negative slope (and thus ending in points of the form $(0, y)$ or $(-1, y)$ with $y > 0$) and
3. (a) one of the segments on the y-axis or
   (b) if $t = h = 0$ by the primitive segment joining $(-1, s)$ and $(-1, s - 1)$.

The different possibilities are illustrated in Figure 1.11.

(a) TC(4,0,0) (b) TC(4,1,0) (c) TC(4,3,1)

Figure 1.11: Tricolumnar Arrays

1.5.2   The Sporadic Examples

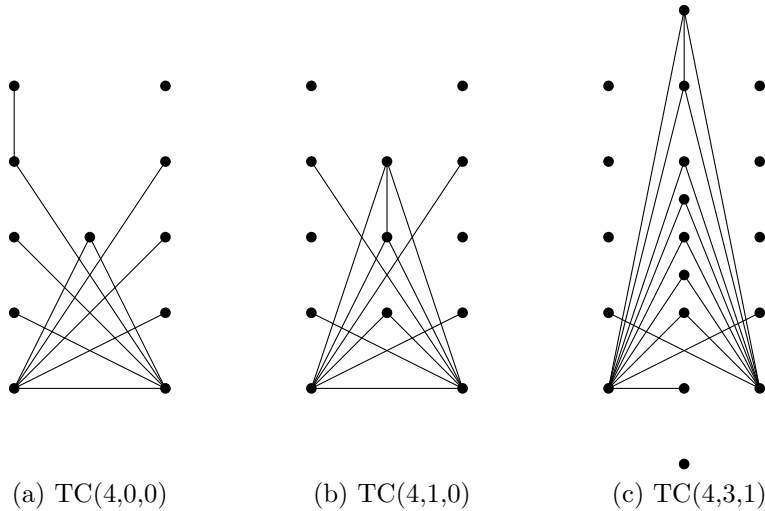As the known algorithms for finding directions or non-avoiding segments in a point configuration are not suited for finding non-avoiding *primitive* segments we implemented a heuristic and a complete search for such systems. The result of this search were three point configurations which do not admit a complete system of non-avoiding primitive segments and complete systems of non-avoiding segments for all other configurations of the Jamison–Hill catalogue.

1.5.2.1   Reduction to a stable set problem

Given a point configuration $\mathcal{P}$ in the plane, find first the primitive segments of $\mathcal{P}$. Define the non avoiding matrix (m_{ij}) indexed by the primitive segments by

$$m_{ij} := \left\{ \begin{array}{ll} 1 & \text{if } i \text{ and } j \text{ are non-avoiding} \\ 0 & \text{else} \end{array} \right.$$

This matrix can be interpreted as the incidence matrix of a graph. We call this graph the non-avoiding graph of $\mathcal{P}$. To find a maximal system of non-avoiding primitive segments in $\mathcal{P}$ translates into finding a maximal stable set in the non-avoiding graph of $\mathcal{P}$. The stable set problem is $\mathcal{NP}$-hard in general.

It is not known whether non-avoiding graphs have a special structure, that simplifies this problem.

1.5.2.2   Greedy heuristic

We implemented a heuristic using the rule "Take always the segment that excludes the least number of other segments." This heuristic found complete systems of non-avoiding primitive segments in 76 of the 97 sporadic examples.

1.5.2.3   Branch and Bound

A branch is abandoned if the number of remaining segments is to small to admit a complete system of non-avoiding primitive segments. This thorough search found 13 complete systems of non-avoiding primitive segments and gave three configurations not admitting such a system. Five configurations where too large for our implementation of Branch and Bound.

1.5.2.4   Computer Aided Search

For the last five configurations we found systems of non-avoiding primitive
segments through choosing segments from all classes by hand and letting the
computer do the non-avoiding check.

1.5.2.5   Pictures

The positive results found by the methods described in the last three sections
are summarized in the following table.

Table 1.1: Systems of non-avoiding primitive segments in the sporadic slope-
critical configurations

Table 1.1 – *Continued from previous page*

$\mathbb{Z}$ 11 4 *

$\mathbb{Z}$ 11 4 A

$\mathbb{Z}$ 11 4 B

$\mathbb{Z}$ 11 4 C

$\mathbb{Z}$ 11 4 D

$\mathbb{Z}$ 11 6 A

$\mathbb{Z}$ 11 6 B

$\mathbb{Z}$ 13 4 A

$\mathbb{Z}$ 13 4 B

$\mathbb{Z}$ 13 4 C

$\mathbb{Z}$ 13 4 D

$\mathbb{Z}$ 13 6 A

Table 1.1 – *Continued from previous page*

$\mathbb{Z}$ 13 6 B

$\mathbb{Z}$ 13 6 C

$\mathbb{Z}$ 13 8

$\mathbb{Z}$ 15 4 A

$\mathbb{Z}$ 15 4 B

$\mathbb{Z}$ 15 4 C

$\mathbb{Z}$ 15 6 A

$\mathbb{Z}$ 15 6 B

$\mathbb{Z}$ 15 8 A

$\mathbb{Z}$ 15 8 B

$\mathbb{Z}$ 15 8 C

$\mathbb{Z}$ 17 4 A

Continued on next page

Table 1.1 – *Continued from previous page*

$\mathbb{Z}$ 17 4 B

$\mathbb{Z}$ 17 4 C

$\mathbb{Z}$ 17 4 D

$\mathbb{Z}$ 17 4 E

$\mathbb{Z}$ 17 6 A

$\mathbb{Z}$ 17 6 B

$\mathbb{Z}$ 17 6 C

$\mathbb{Z}$ 17 8 A

$\mathbb{Z}$ 17 8 B

$\mathbb{Z}$ 17 8 C

$\mathbb{Z}$ 19 4

$\mathbb{Z}$ 19 6

Table 1.1 – *Continued from previous page*

$\mathbb{Z}$ 19 8

$\mathbb{Z}$ 21 4 A

$\mathbb{Z}$ 21 4 B

$\mathbb{Z}$ 21 4 C

$\mathbb{Z}$ 21 6

$\mathbb{Z}$ 21 8 A

$\mathbb{Z}$ 21 8 B

$\mathbb{Z}$ 23 4 B

$\mathbb{Z}$ 23 6 A

$\mathbb{Z}$ 23 6 B

$\mathbb{Z}$ 23 6 C

$\mathbb{Z}$ 23 8

Continued on next page

Table 1.1 – *Continued from previous page*

$\mathbb{Z}$ 25 4 A $\mathbb{Z}$ 25 4 B $\mathbb{Z}$ 25 6

$\mathbb{Z}$ 25 8 $\mathbb{Z}$ 27 8 $\mathbb{Z}$ 29 4 A

$\mathbb{Z}$ 29 4 B $\mathbb{Z}$ 29 4 C $\mathbb{Z}$ 29 6

$\mathbb{Z}$ 31 12 $\mathbb{Z}$ 33 10 $\mathbb{Z}$ 35 4

Table 1.1 – *Continued from previous page*

$\mathbb{Z}$ 35 8

$\mathbb{Z}$ 37 6

$\mathbb{Z}$ 45 8

$\mathbb{Z}$ 47 6

$\mathbb{Z}$ 49 4

$\mathbb{Z}_2$ 11 4 *

$\mathbb{Z}_2$ 13 6

$\mathbb{Z}_3$ 13 4
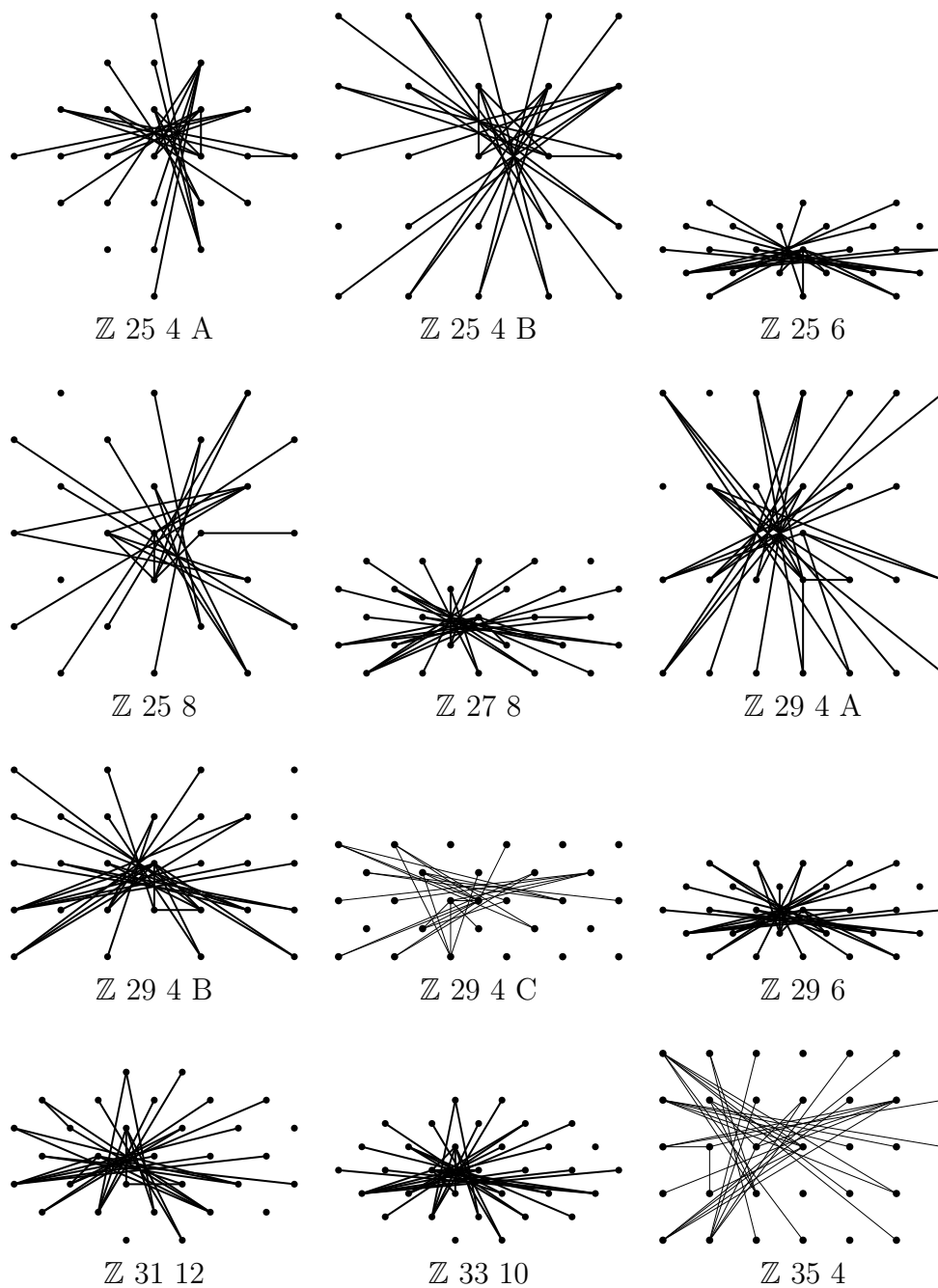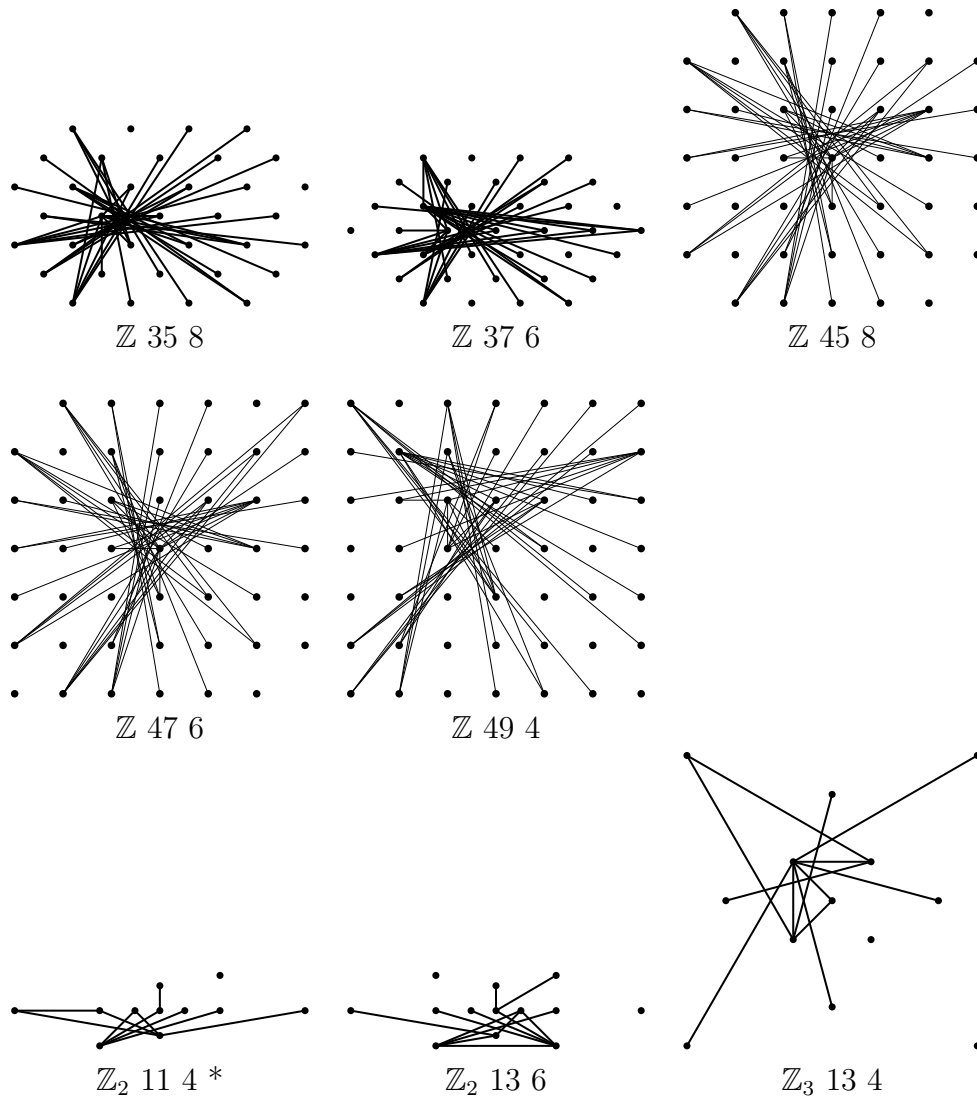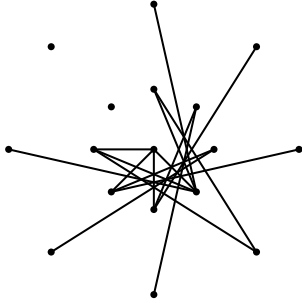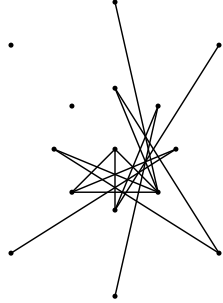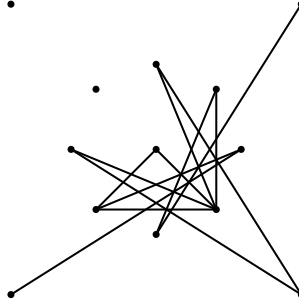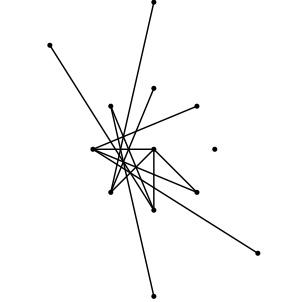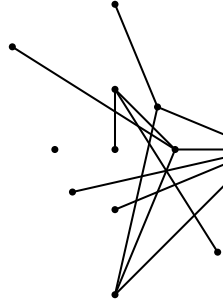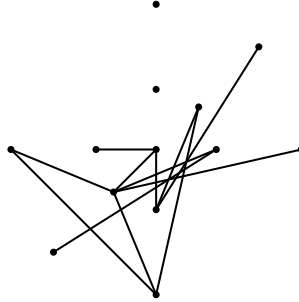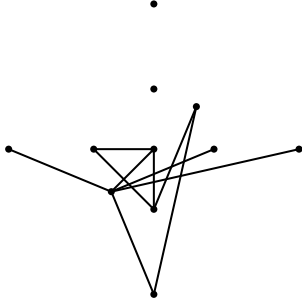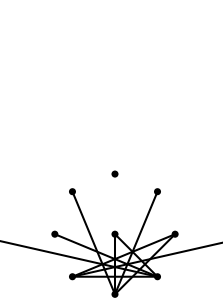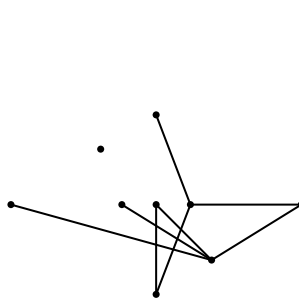
Table 1.1 – *Continued from previous page*

Grünbaum Octagon   Grünbaum(1111;1110)   Grünbaum(1111;1010)

Grünbaum(1111;1100)   Grünbaum(1110;1011)   Grünbaum(1110;1110)

Grünbaum(1110;1010)   Grünbaum(1111;1000) $\mathbb{Z}_5$ 9 4 *

Table 1.1 – *Continued from previous page*

$\mathbb{Z}_5$ 9 6

$\mathbb{Z}_5$ 11 4

$\mathbb{Z}_5$ 11 6

$\mathbb{Z}_5$ 13 4

$\mathbb{Z}_5$ 13 6

$\mathbb{Z}_5$ 13 8

$\mathbb{Z}_5$ 15 6 A

$\mathbb{Z}_5$ 15 6 B

$\mathbb{Z}_5$ 15 8

Continued on next page

Table 1.1 – *Continued from previous page*

$\mathbb{Z}_5$ 17 6 $\mathbb{Z}_5$ 17 8
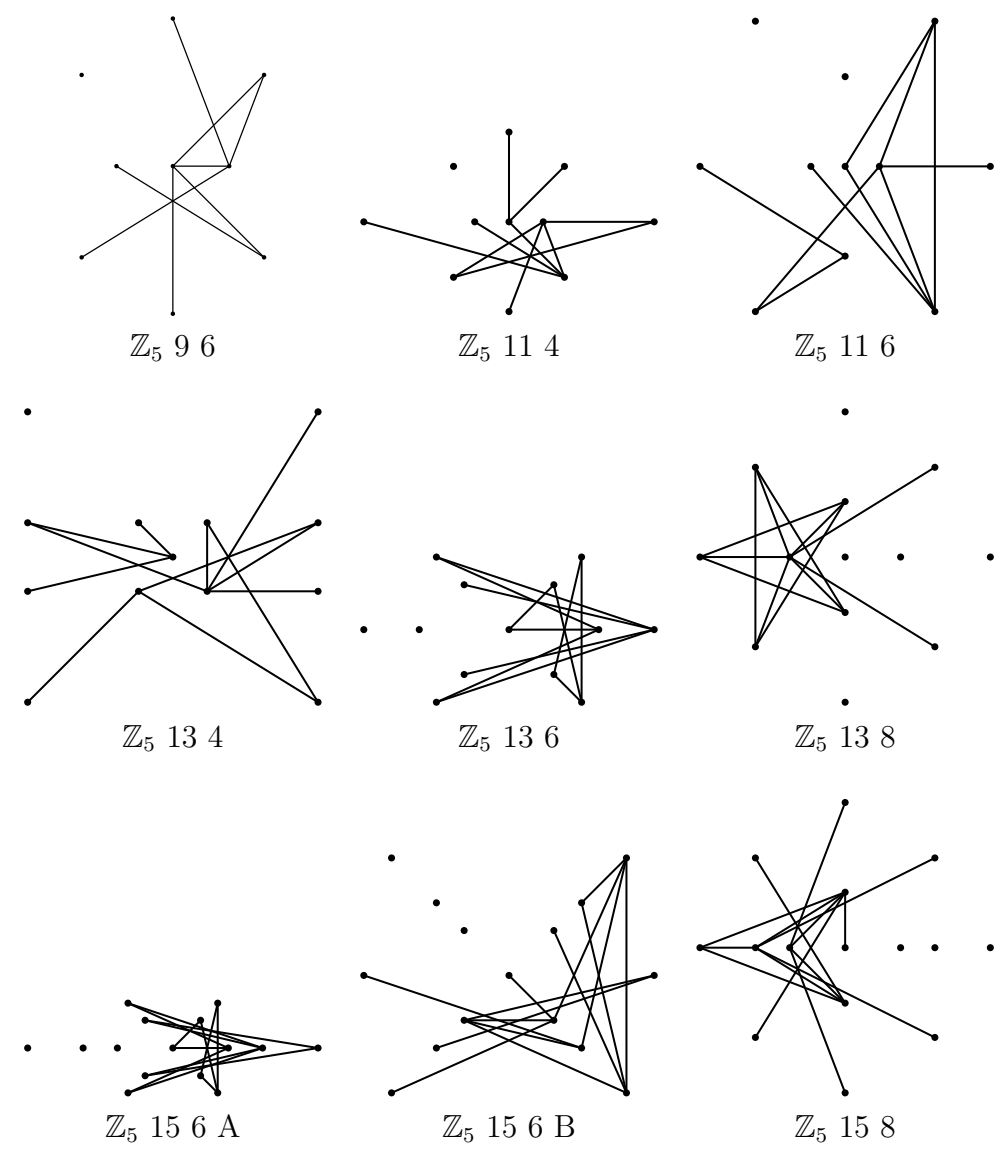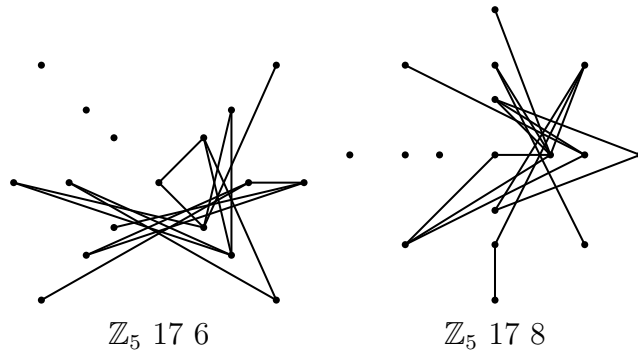
1.6   COUNTEREXAMPLES

The computer search yielded that the configurations $\mathbb{Z}\_15\_4D$, $\mathbb{Z}_5\_17\_4$ and $\mathbb{Z}\_23\_4A$ do not admit complete systems of non-avoiding primitive segments. The two larger examples are shown in Figure 1.12

(a) $\mathbb{Z}_5\_17\_4$ (b) $\mathbb{Z}\_23\_4A$
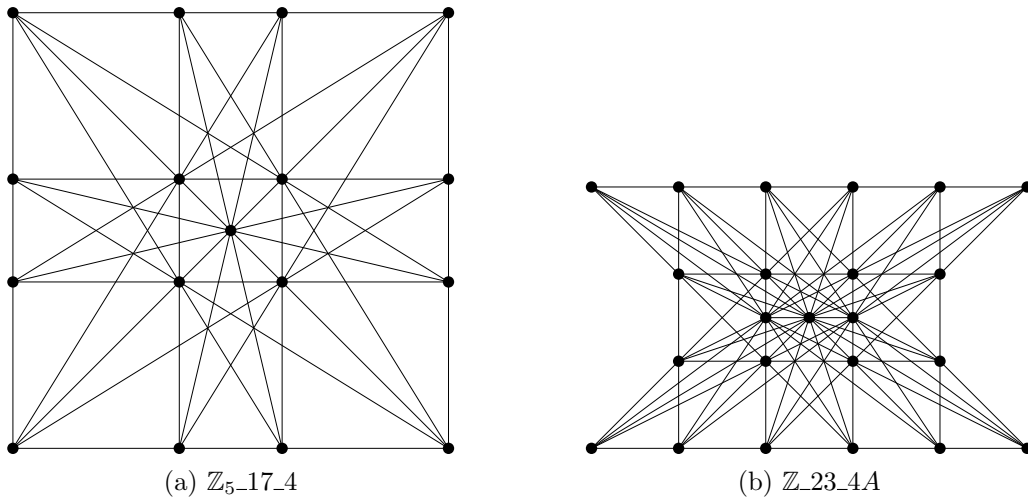
Figure 1.12: The large counterexamples

For the smallest example we here give a proof by hand.

Theorem 1.26. *The configuration number $\mathbb{Z}\_15\_4D$ in the Jamison–Hill*
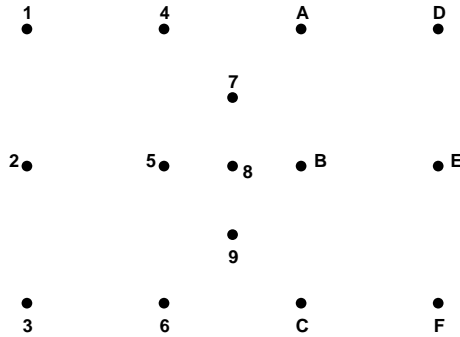
Figure 1.13: The smallest Counterexample $\mathbb{Z}\_15\_4D$

catalogue (see Figure 1.13) consisting of the 15 *points*

1	$(-3, 2)$	4	$(-1, 2)$	7	$(0, 1)$	A	$(1, 2)$	D	$(3, 2)$
2	$(-3, 0)$	5	$(-1, 0)$	8	$(0, 0)$	B	$(1, 0)$	E	$(3, 0)$
3	$(-3, -2)$	6	$(-1, -2)$	9	$(0, -1)$	C	$(1, -2)$	F	$(3, -2)$

does not admit a system of 14 non-avoiding primitive segments.

Proof. The configuration $\mathcal{P}$ has 15 points and is slope–critical because it defines only 14 directions. So in a system of 14 non-avoiding primitive segments there has to be one for each direction.

We show that there is no system of non-avoiding primitive segments representing all the 9 directions $\mathcal{A}, \ldots, \mathcal{I}$ in Table 1.2.

We observe that the following segments cannot be in a system representing all slopes:

- $\overline{16}$ and $\overline{AF}$ because they avoid both segments $\overline{49}$ and $\overline{7C}$ of $\mathcal{H}$.
- $\overline{34}$ and $\overline{CD}$ because they avoid both segments $\overline{67}$ and $\overline{9A}$ of $\mathcal{I}$.
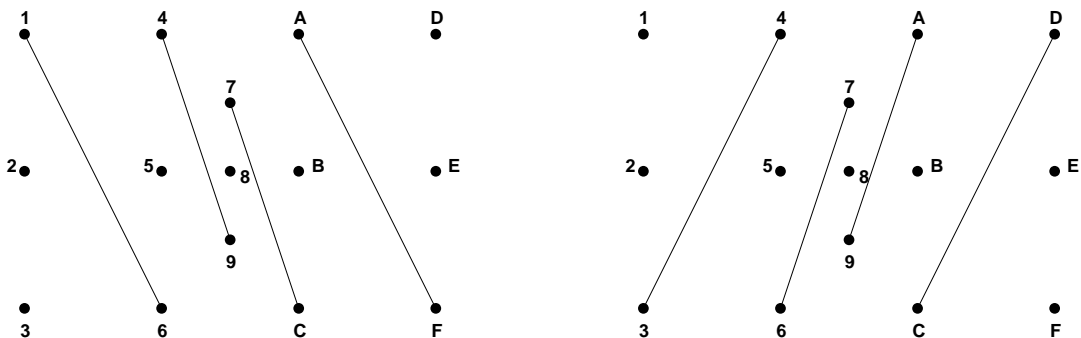
Based on the succesive combination of the directions $\mathcal{A}$, $\mathcal{B}$ and $\mathcal{C}$ taking into account which segments are mutually avoiding we get four cases. Each of the

direction	slope	primitive segments	
$\mathcal{A}$	$-\frac{2}{3}$	$\overline{18}, \overline{8F}$	
$\mathcal{B}$	$\frac{2}{3}$	$\overline{38}, \overline{8D}$	
$\mathcal{C}$	$\frac{1}{3}$	$\overline{27}, \overline{7D}, \overline{39}, \overline{9E}$	
$\mathcal{D}$	-1	$\overline{15}, \overline{59}, \overline{9C}, \overline{26}, \overline{47}, \overline{7B}, \overline{BF},$ $\overline{AE}$	
$\mathcal{E}$	1	$\overline{24}, \overline{35}, \overline{57}, \overline{7A}, \overline{69}, \overline{9B}, \overline{BD},$ $\overline{CE}$	
$\mathcal{F}$	-2	$\overline{16}, \overline{48}, \overline{8C}, \overline{AF}$	
$\mathcal{G}$	2	$\overline{34}, \overline{68}, \overline{8A}, \overline{CD}$	
$\mathcal{H}$	-3	$\overline{49}, \overline{7C}$	
$\mathcal{I}$	3	$\overline{67}, \overline{9A}$	

Table 1.2: Slope classes of segments in the Counterexample of Theorem 1.26

cases leads to the necessity of adding one of the forbidden segments 16, AF, 34 or CD.

Start with direction $\mathcal{A}$. Without loss of generality we choose segment $\overline{18}$ because $\mathcal{P}$ is centrally symmetric.

Next we choose a segment from direction $\mathcal{B}$. For this we get two cases.

    1. $\overline{18}$, $\overline{38}$:
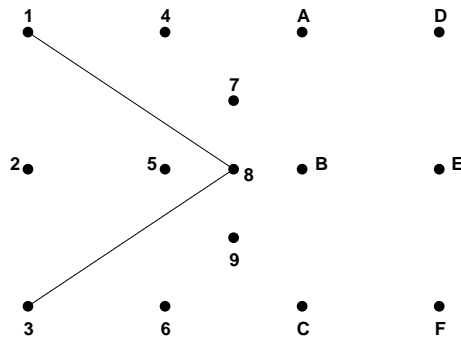
    2. $\overline{18}$, $\overline{8D}$:
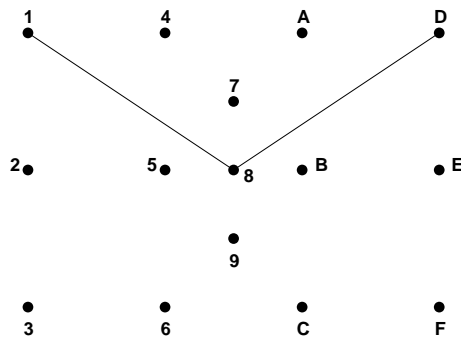
As $\overline{18}$ avoids $\overline{39}$, $\overline{38}$ avoids $\overline{27}$ and $\overline{8D}$ avoids $\overline{9E}$, adding a segment in direction $\mathcal{C}$ gives the following four cases:

    1.   (a) $\overline{18}$, $\overline{38}$, $\overline{7D}$:
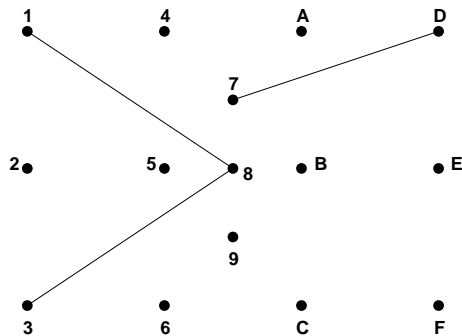
(b) $\overline{18}$, $\overline{38}$, $\overline{9E}$:
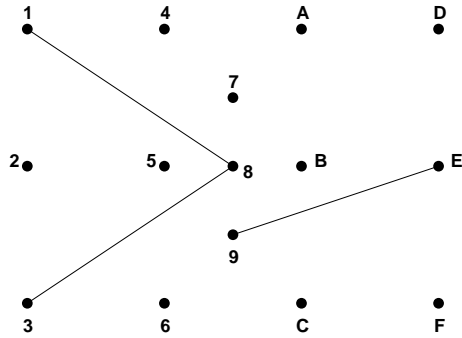
2. (a) $\overline{18}$, $\overline{8D}$, $\overline{7D}$:
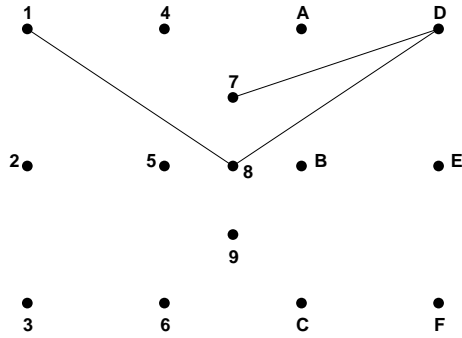
(b) $\overline{18}$, $\overline{8D}$, $\overline{27}$:
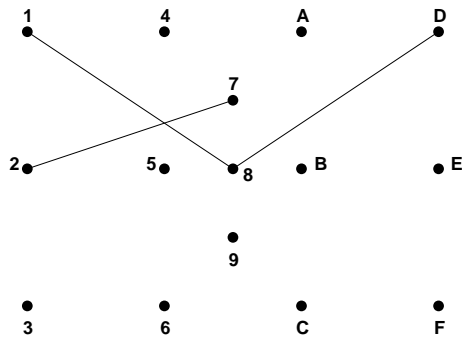
In each of the four cases we give now an order of directions of which we can add only one segment each and which leads to the choice of a forbidden segment.

1. (a) Direction $\mathcal{D}$: $\overline{18}$ avoids $\overline{26}$, $\overline{47}$, $\overline{7B}$ and $\overline{AE}$; $\overline{38}$ avoids $\overline{BF}$; $\overline{7D}$ avoids $\overline{59}$ and $\overline{9C}$; So we have to add $\overline{15}$:
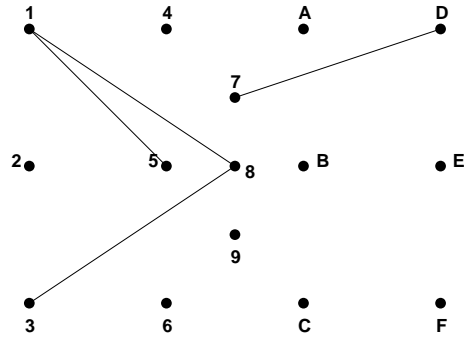
Direction $\mathcal{F}$: $\overline{7D}$ avoids $\overline{8C}$; $\overline{15}$ avoids $\overline{48}$ and $\overline{AF}$; So we would have to add the forbidden segment $\overline{16}$.

(b) Direction $\mathcal{E}$: $\overline{18}$ avoids $\overline{BD}$ and $\overline{69}$; $\overline{38}$ avoids $\overline{24}$, $\overline{9B}$ and $\overline{CE}$; $\overline{9E}$ avoids $\overline{57}$ and $\overline{7A}$; So we have to add $\overline{35}$:
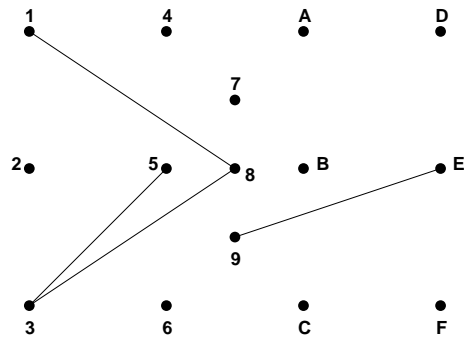
Direction $\mathcal{G}$: $\overline{9E}$ avoids $\overline{8A}$; $\overline{35}$ avoids $\overline{68}$ and $\overline{CD}$; So we would have to add the forbidden segment $\overline{34}$.

2. In both these cases we take the directions $\mathcal{D}$ and $\mathcal{E}$ first.
   Direction $\mathcal{D}$: $\overline{18}$ avoids $\overline{26}$, $\overline{47}$, $\overline{7B}$ and $\overline{AE}$; $\overline{8D}$ avoids $\overline{15}$ and $\overline{9C}$;
   Direction $\mathcal{E}$: $\overline{18}$ avoids $\overline{69}$ and $\overline{BD}$; $\overline{8D}$ avoids $\overline{24}$, $\overline{37}$, $\overline{7A}$ and $\overline{CE}$;

   (a) Direction $\mathcal{D}$: $\overline{7D}$ avoids $\overline{59}$. So we have to take $\overline{BF}$.
       Direction $\mathcal{E}$: $\overline{BF}$ avoids $\overline{35}$. So we have to take $\overline{9B}$:
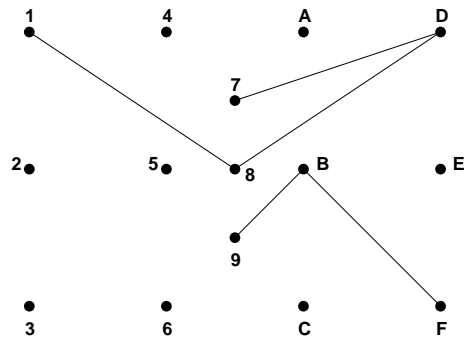
Direction $\mathcal{G}$: $\overline{BF}$ avoids $\overline{68}$; $\overline{9B}$ avoids $\overline{8A}$ and $\overline{34}$; So we would have to add the forbidden segment $\overline{CD}$.

(b) Direction $\mathcal{E}$: $\overline{27}$ avoids $\overline{9B}$. So we have to take $\overline{35}$.
Direction $\mathcal{D}$: $\overline{35}$ avoids $\overline{BF}$. So we have to take $\overline{59}$:
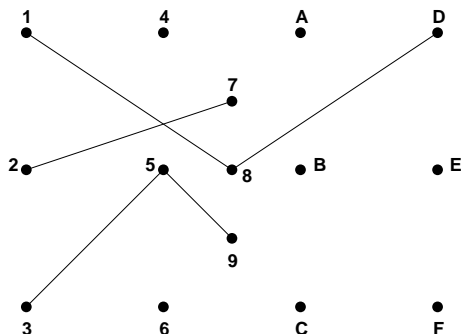
Direction $\mathcal{F}$: $\overline{35}$ avoids $\overline{8C}$; $\overline{59}$ avoids $\overline{48}$ and $\overline{AF}$; So we would have to add the forbidden segment $\overline{16}$.

Every case was shown to be non-extensible so there is no complete system of non-avoiding primitive segments. □

Remark 1.27. *The configuration number $\mathbb{Z}\_15\_4D$ in the Jamison-Hill catalogue does admit a system of 13 non-avoiding primitive segments. (See Figure 1.14)*
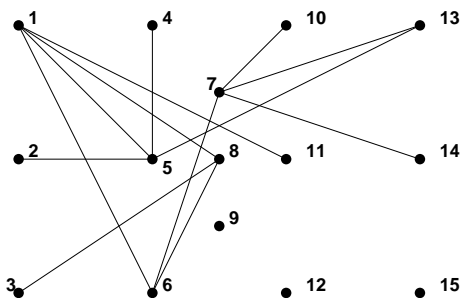
Figure 1.14: A system of 13 non-avoiding primitive segments for the configuration $\mathbb{Z}\_15\_4D$

1.6.1   Variants of the Counterexample

1. To get a counterexample with only 14 points we can drop any extreme vertex. As there are no new primitive segments generated and the number of directions is still 14 the proof stays valid for this example.

2. To get a counterexample with 15 points that is not slope–critical we
   apply a projective transformation. Under this transformation segments
   stay avoiding or non-avoiding respectively. Especially the parallel seg-
   ments of the slope classes become avoiding segments after the transfor-
   mation. (See Figure 1.15)
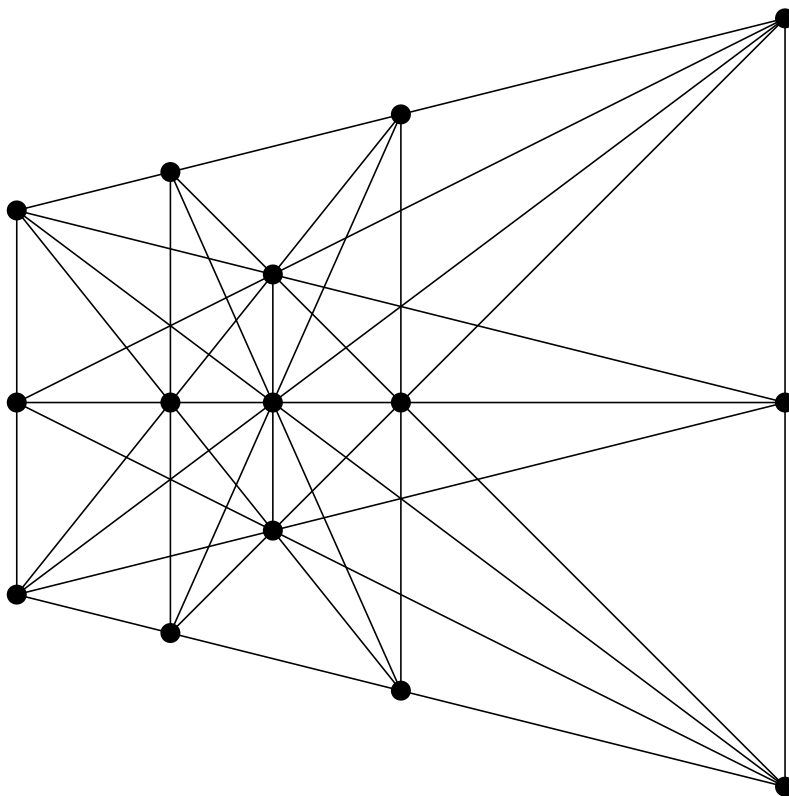
Figure 1.15: A non-slope–critical configuration of 15 points without a system
of 14 non-avoiding primitive segments

Polyhedral surfaces of high genus in cubes of Klee–Minty type

In this chapter we bring together two lines of research concerning interesting deformed d-cubes.

One direction goes back to the construction of counterexamples to the polynomiality of deterministic pivot rules for the simplex algorithm of linear programming. As a bad example for Dantzig's rule in 1972 Klee and Minty [22] presented a deformed realization of the d-cube such that there is an ascending Hamiltonian path with respect to the last coordinate. The vertex ordering induced by this height function has a particularly nice combinatorial description as Avis and Chvátal [5] as well as Gärtner, Henk and Ziegler [14] pointed out. This was the starting point for a series of similarly constructed deformed cubes as surveyed by Amenta and Ziegler [4]. Among these there are the cubes by Murty [28] and Goldfarb [16] which prove the nonpolynomiality of the Gass-Saaty pivot rule [15], which was interpreted geometrically as the shadow vertex rule by Borgwardt [10]. This result ensures a projection of a d-dimensional cube to $\mathbb{R}^2$ that keeps all vertices of the cube, while all the edges of the resulting 2^d-gon are projected cube edges. Moreover, all but one edge of the resulting 2^d-gon are projections of the Klee-Minty Hamilton path. Secondly this means that the resulting 2^d-gon may be further projected to $\mathbb{R}^1$ giving a polytopal complex with one edge less.

The other direction yields cubes with interesting projections into $\mathbb{R}^4$. Joswig and Ziegler [21] constructed neighborly cubical polytopes in $\mathbb{R}^4$ by projecting deformed d-cubes such that all vertices and edges are preserved. Their methods were used and refined by Rörig in his thesis [31] such that special polytopal surfaces in the 2-skeleton of the d-cube survive the projection as well. Especially he embedded the family of quadrilateral surfaces F_d which McMullen, Schulz and Wills constructed in [26] realized in $\mathbb{R}^3$ with genus $\Theta(d2^d)$ on 2^d vertices. The surfaces survive not only the projection into $\mathbb{R}^4$ but also a further orthogonal projection to $\mathbb{R}^3$. His construction however does not take care of the Klee-Minty and Goldfarb properties. In Theorem

2.13 we give explicit inequality descriptions of deformed d-cubes $C_d \subset \mathbb{R}^d$ for $d \geq 4$ such that the chain of projections

$$\mathbb{R}^d \longrightarrow \mathbb{R}^4 \to \mathbb{R}^3 \to \mathbb{R}^2 \to \mathbb{R}^1$$

onto the last $4, 3, 2$ and 1 coordinates respectively has the properties of the beforementioned results simultaneously:

(4) The MSW surfaces F_d survive the projection into $\mathbb{R}^4$.

(3) As polyhedral complexes the surfaces F_d are preserved by the projection onto the 3 last coordinates because their images after the projection into $\mathbb{R}^4$ lie in the upper convex hull with respect to the fourth-to-last coordinate.

(2) All vertices of F_d are strictly preserved by the projection to $\mathbb{R}^2$.

(1) The vertex ordering induced by the height function x_d is also preserved because all vertices of F_d are projected into the upper convex hull with respect to the second-to-last coordinate.

2.1   Cubes

2.1.1   Combinatorics

We follow the notation of Ziegler [40] for the cube based on the inequality description of the standard d-cube.

The standard d-dimensional cube $\mathcal{C}_d = [0, 1]^d$ is described by the inequalities

$$0 \leq x_j \leq 1, \qquad \text{for } j = 1, \ldots, d$$

For a vertex of $\mathcal{C}_d$ all coordinates are fixed at the upper or lower bounds, i.e. $V(\mathcal{C}_d) = \{0, 1\}^d$. Every other non-empty face of $\mathcal{C}_d$ consists of those points in $\mathbb{R}^d$ for which some coordinates lie in the interval $[0, 1]$ while the others are fixed to one of their bounds. Thus the set of non-empty faces of $\mathcal{C}_d$ may be identified with $\{0, 1, *\}^d$. In this notation $011*010$ represents the edge between 0110010 and 0111010. Each facet has exactly one non-$*$ entry corresponding to the coordinate that is fixed at one of its bounds.

The observation $\mathcal{C}_d = \mathrm{prism}(\mathcal{C}_{d-1}) = \mathrm{conv}(\mathcal{C}_{d-1} \times \{0\}, \mathcal{C}_{d-1} \times \{1\})$ yields a recursive definition of the cube.

2.1.2   Realizations

Any (lower) triangular matrix gives rise to a realization of the cube by the following construction.

Notation. For any lower triangular matrix

$$
T = \begin{pmatrix}
t_{11} & 0 & \cdots & \cdots & 0 \\
t_{21} & \ddots & \ddots & & \vdots \\
\vdots & \ddots & \ddots & \ddots & \vdots \\
\vdots & \ddots & \ddots & \ddots & 0 \\
t_{d1} & \cdots & \cdots & t_{d,d-1} & t_{dd}
\end{pmatrix} \in \mathbb{R}^{d \times d}
$$

let

$$
T^{\pm} = \begin{pmatrix}
t_{11} & 0 & \cdots & \cdots & & \cdots & 0 \\
-t_{11} & 0 & \cdots & \cdots & & \cdots & 0 \\
t_{21} & t_{22} & 0 & & & & \vdots \\
t_{21} & -t_{22} & 0 & \ddots & & & \vdots \\
\vdots & & \ddots & \ddots & \ddots & & \vdots \\
\vdots & & & \ddots & \ddots & 0 \\
\vdots & & & & \ddots & 0 \\
\vdots & & & & t_{d-1,d-1} & \vdots \\
\vdots & & & & -t_{d-1,d-1} & 0 \\
t_{d1} & \cdots & \cdots & \cdots & t_{d,d-1} & t_{dd} \\
t_{d1} & \cdots & \cdots & \cdots & t_{d,d-1} & -t_{dd}
\end{pmatrix} \in \mathbb{R}^{2d \times d}
$$

and for any column vector

$$
b = \begin{pmatrix} b_1 \\ b_2 \\ \vdots \\ b_d \end{pmatrix} \in \mathbb{R}^d
\qquad \text{let} \qquad
\tilde{b} = \begin{pmatrix} b_1 \\ b_1 \\ b_2 \\ b_2 \\ \vdots \\ b_d \\ b_d \end{pmatrix} \in \mathbb{R}^{2d}.
$$

In this notation the cube $[-1,1]^d$ is described by the system $E_d^{\pm} x \leq \tilde{\mathbf{1}}_d$.

Lemma 2.1. *Let $M > m > 0$ and let*

$$
T_d := \begin{pmatrix}
t_{11} & 0 & \cdots & \cdots & 0 \\
t_{21} & \ddots & \ddots & & \vdots \\
\vdots & \ddots & \ddots & \ddots & \vdots \\
\vdots & \ddots & \ddots & \ddots & 0 \\
t_{d1} & \cdots & \cdots & t_{d,d-1} & t_{dd}
\end{pmatrix} \in \mathbb{R}^{d \times d}
$$

be a lower triangular matrix with $t_{ii} \geq m > 0$ for $1 \leq i \leq d$ and $|t_{ij}| \leq M$ for all $1 \leq j < i \leq d$. Let $c = \frac{2dM}{m}$ and let

$$
b_d := \frac{m}{2} \begin{pmatrix} c \\ c^2 \\ \vdots \\ \vdots \\ c^d \end{pmatrix} \in \mathbb{R}^d.
$$

Then the polytope defined by

$$
T_d^{\pm} x \leq \tilde{b}_d
$$

is combinatorially equivalent to the d-cube. The coordinates of the points in the cube are bounded from above by $|x_j| < c^k$ for $j \leq k$. Every pair of inequalities that differ only in the sign of the diagonal entry defines a pair of disjoint facets.

Proof by induction. We show by induction that $C_k := \left\{ x \in \mathbb{R}^k \mid T_k^{\pm} x \leq \tilde{b}_k \right\}$ is a cube and that $|x_k| \leq c^k$. With $c > 1$ the bound $|x_j| \leq c^k$ for $j < k$ follows.

$\underline{k = 1}$: The inequalities

$$
\pm t_{11} x_1 \leq b_1
$$

define a 1-cube and

$$
|x_1| \leq \frac{b_1}{t_{11}} \leq \frac{b_1}{m} = \frac{1}{2} c < c
$$

establishes the upper bound for x_1.

$\underline{k \to k+1}$: By the induction hypothesis the first k pairs of inequalities define a cube in $\mathbb{R}^k$ and its coordinates are bounded by c^k.

The $(k+1)$st pair of inequalities may be written as

$$
|x_{k+1}| \leq \frac{1}{t_{k+1,k+1}} \left(b_{k+1} - \sum_{j=1}^{k} t_{k+1,j} x_j \right).
$$

Now we show that the right hand side is positive by bounding the sum from above

$$\left|\sum_{j=1}^{k} t_{k+1,j} x_j\right| \leq \sum_{j=1}^{k} |t_{k+1,j}||x_j|$$

$$< kMc^k$$

$$\leq dMc^k = \frac{m}{2}\frac{2dM}{m}c^k = \frac{m}{2}c^{k+1} = b_{k+1}.$$

So the $(k+1)$st pair of inequalities cannot be simultaneously satisfied with equality but any one of them can. Therefore they define a disjoint pair of facets. This shows that the polytope defined by the first $k+1$ pairs of inequalities is again a cube.

Finally we establish the new upper bound

$$|x_{k+1}| \leq \frac{1}{t_{k+1,k+1}}\left(b_{k+1} - \sum_{j=1}^{k} t_{k+1,j} x_j\right)$$

$$\leq \frac{1}{m}\left(\frac{m}{2}c^{k+1} + \sum_{j=1}^{k} |t_{k+1,j}||x_j|\right)$$

$$< \frac{1}{m}\left(\frac{m}{2}c^{k+1} + dMc^k\right) = c^k\left(\frac{1}{2}c + \frac{1}{2}\cdot\frac{2dM}{m}\right) = c^{k+1}.$$

$\square$

Remark 2.2. *In this setting the facet with combinatorial representation*

$$* \ldots * v_k * \ldots * \in \{0, 1, *\}^d$$

corresponds to the facet supported by the hyperplane

$$(t_{k1}, \ldots, (-1)^{v_k+1} t_{kk}, 0, \ldots, 0)x = b_k.$$

The vertex $x \in C_d$ with combinatorial coordinates

$$v_1 \ldots v_d \in \{0, 1\}^d$$

is the solution of the linear system of equations

$$\begin{pmatrix} (-1)^{v_1+1}t_{11} & 0 & \cdots & \cdots & & 0 \\ t_{21} & \ddots & \ddots & & & \vdots \\ \vdots & & \ddots & \ddots & \ddots & & \vdots \\ \vdots & & \ddots & \ddots & \ddots & & 0 \\ t_{d1} & \cdots & \cdots & t_{d,d-1} & (-1)^{v_d+1}t_{dd} \end{pmatrix} x = b.$$

2.1.3   Cubes of Klee–Minty type

In 1972 Klee and Minty [22] constructed d-dimensional cubes $C_d \subset \mathbb{R}^d$ that have a Hamiltonian path increasing with respect to the last coordinate. Following the recursive construction of the cube they described the Hamiltonian path in C_1 as $0 < 1$ and in C_d as the concatenation of the Hamiltonian path in $C_{d-1} \times \{0\}$ and the reversed Hamiltonian path in $C_{d-1} \times \{1\}$. For example the Hamiltonian path for $d = 3$ is

$$000, \ 100, \ 110, \ 010, \ 011, \ 111, \ 101, \ 001.$$

Thus for $d = 4$ we get

$$0000, \ 1000, \ 1100, \ 0100, \ 0110, \ 1110, \ 1010, \ 0010,$$
$$0011, \ 1011, \ 1111, \ 0111, \ 0101, \ 1101, \ 1001, \ 0001.$$

The combinatorial essence of this height function is the induced vertex ordering. We use the criterion of Gärtner, Henk and Ziegler [14] which goes back to Avis and Chvátal [5].

Definition 2.3 (Cube of Klee–Minty type)**.** A *cube of Klee-Minty type* is a polytope in $\mathbb{R}^d$ that is combinatorially equivalent to the d-cube and that satisfies the following condition for every two neighboring vertices with combinatorial coordinates $v_1 \ldots v_d$ and $w_1 \ldots w_d$ with $v_k \neq w_k$ and $v_j = w_j$ for $1 \leq j \leq d, j \neq k$:

$$v > w \quad \Leftrightarrow \quad \sum_{j=k}^{d} v_j \equiv 1 \bmod 2$$

$$\Leftrightarrow \quad \big((v_k = 1 \text{ and } \sum_{j=k+1}^{d} v_j \equiv 0 \bmod 2) \text{ or }$$

$$(v_k = 0 \text{ and } \sum_{j=k+1}^{d} v_j \equiv 1 \bmod 2)\big).$$

From this combinatorial description of the height function, we derive an explicit description of the ascending Hamiltonian path:

Proposition 2.4. *In a cube of Klee–Minty type the ascending Hamiltonian path has the following properties:*

    1. The first vertex is $0 \ldots 00$.

2. *The last vertex is $0\ldots01$.*

3. *For every other vertex the two neighbors are the vertex that differs only in the first coordinate and the vertex that differs only in the coordinate after the first 1.*

Proof. First observe that $0\ldots00$ and $0\ldots01$ are the only vertices that don't have a coordinate after the first 1. So we can use property 3 as a rule to construct a path in both directions from any other vertex. This path will reach $0\ldots00$ and $0\ldots01$ eventually. It is ascending from $0\ldots00$ to $0\ldots01$ as for all $v_1,\ldots,v_k \in \{0,1\}$ we have $10\ldots01v_1v_2\ldots v_k < 00\ldots01v_1v_2\ldots v_k \Leftrightarrow \sum_{j=1}^{k} v_j$ is even $\Leftrightarrow 00\ldots01v_1v_2\ldots v_k < 00\ldots01(1-v_1)v_2\ldots v_k$. The path is Hamiltonian as we can start from any vertex and there is no ambiguity in the rules. $\qquad\square$

Remark 2.5. *From this description of the Hamiltonian path it follows that two arbitrary vertices can be compared by comparing only their "tails". Every pair of vertices with combinatorial coordinates $v_1\ldots v_d$ and $w_1\ldots w_d$ with $v_k \neq w_k$ and $v_j = w_j$ for $k+1 \leq j \leq d$ satisfies*

$$v > w \quad \Leftrightarrow \quad \sum_{j=k}^{d} v_j \equiv 1 \bmod 2$$

$$\Leftrightarrow \quad \Big((v_k = 1 \text{ and } \sum_{j=k+1}^{d} v_j \equiv 0 \bmod 2) \text{ or}$$

$$(v_k = 0 \text{ and } \sum_{j=k+1}^{d} v_j \equiv 1 \bmod 2)\Big).$$

2.2 Inequalities for cubes of Klee-Minty type

In this section we show that the construction of cubes via lower triangular matrices yields cubes of Klee-Minty type for the special case of matrices with subdiagonal 1 and small diagonal values ε.

Theorem 2.6. *Let $1 > \varepsilon > 0$. Further let $t_{ij} \in \mathbb{R}$ and $M > 1$ with $M \geq |t_{ij}|$ for $i = 1,\ldots,d$ and $1 \leq j \leq i-2$. Write $c = \frac{2dM}{\varepsilon}$.*

Then

$$
A_\varepsilon = \begin{pmatrix}
\varepsilon & 0 & \ldots & \ldots & 0 \\
1 & \ddots & \ddots & & \vdots \\
t_{31} & \ddots & \ddots & \ddots & \vdots \\
\vdots & \ddots & \ddots & \ddots & 0 \\
t_{d1} & \ldots & t_{d,d-2} & 1 & \varepsilon
\end{pmatrix} \in \mathbb{R}^{d \times d}
\quad and \quad
b_\varepsilon = \frac{\varepsilon}{2} \begin{pmatrix}
c \\ c^2 \\ \vdots \\ \vdots \\ c^d
\end{pmatrix} \in \mathbb{R}^d
$$

via $A_\varepsilon^\pm x \le \tilde{b}_\varepsilon$ define a cube of Klee–Minty type.

Proof. As already shown in Section 2.1.2, $\{x \in \mathbb{R}^d \mid A_\varepsilon^\pm x \le \tilde{b}_\varepsilon\}$ is a d-cube. It remains to show that the vertex order with respect to the height function induced by the last coordinate is correct.

We show this in two steps. First we show that the cube defined by the matrix A'_ε with $t_{ij} = 0$ for $i = 1, \ldots, d$ and $1 \le j \le i - 2$ with the right hand side b_ε has the correct height function. After that we will show that every other cube defined by A_ε and b_ε has the same height function whenever ε is small enough.

For the first step we recall from Remark 2.2 that the coordinate vector x of a vertex $v = v_1 \ldots v_d$ in this realization of the cube is the solution of the linear system

$$
\begin{pmatrix}
(-1)^{v_1+1}\varepsilon & 0 & \ldots & \ldots & & 0 \\
1 & \ddots & \ddots & & & \vdots \\
0 & \ddots & \ddots & \ddots & & \vdots \\
\vdots & \ddots & \ddots & \ddots & & 0 \\
0 & & \ldots & 0 & 1 & (-1)^{v_d+1}\varepsilon
\end{pmatrix} x = b.
$$

Then for every $k = 2, \ldots, d$

$$
\begin{aligned}
x_d &= \frac{1}{\varepsilon}(-1)^{v_d+1}(b_d - x_{d-1}) \\
&= \frac{1}{\varepsilon}(-1)^{v_d+1}b_d + \frac{1}{\varepsilon}(-1)^{v_d}x_{d-1} \\
&= \frac{1}{\varepsilon}(-1)^{v_d+1}b_d + \frac{1}{\varepsilon}(-1)^{v_d}\frac{1}{\varepsilon}(-1)^{v_d+1}(b_d - x_{d-1}) \\
&= \frac{1}{\varepsilon}(-1)^{v_d+1}b_n + \frac{1}{\varepsilon^2}(-1)^{v_d+v_{d-1}+1}b_{d-1} + \frac{1}{\varepsilon^2}(-1)^{v_d+v_{d-1}}x_{d-2} \\
&= -\sum_{j=k+1}^{d} \frac{1}{\varepsilon^{d-j+1}}(-1)^{\sum_{i=j}^{d} v_i}b_j + \frac{1}{\varepsilon^{d-k+1}}(-1)^{\sum_{i=k}^{d} v_i}(x_{k-1} - b_k).
\end{aligned}
$$

We now examine two neighboring vertices v and $w \in \{0,1\}^d$ that differ in the kth combinatorial coordinate only. For the coordinates x of v and y of w in this realization we have

$$
x_d - y_d \;=\; \frac{1}{\varepsilon^{d-k+1}}(-1)^{\sum_{i=k+1}^{d} v_i}(x_{k-1} - b_k)((-1)^{v_k} - (-1)^{w_k})
$$

$$
\begin{cases}
< 0 & \text{for } \sum_{i=k}^{d} v_i \text{ even and} \\
> 0 & \text{for } \sum_{i=k}^{d} v_i \text{ odd,}
\end{cases}
$$

which is the desired height function.

From this calculation we see that the difference of the heights of two neighboring vertices is

$$
\begin{aligned}
|x_d - y_d| \;&=\; \frac{2}{\varepsilon^{d-k+1}}|x_{k-1} - b_k| = \frac{2}{\varepsilon^{d-k+1}}(b_k - |x_{k-1}|) \\
&>\; \frac{2}{\varepsilon^{d-k+1}}\left(\frac{\varepsilon}{2} \cdot c^k - c^{k-1}\right) = \frac{2}{\varepsilon^{d-k+1}}\left(\frac{\varepsilon}{2}c - 1\right)c^{k-1} \\
&=\; \frac{2}{\varepsilon^{d-k+1}}\left(\frac{\varepsilon}{2}\frac{2dM}{\varepsilon} - 1\right)\left(\frac{2dM}{\varepsilon}\right)^{k-1} = \frac{2}{\varepsilon^{d-k+1}}(dM - 1)\left(\frac{2dM}{\varepsilon}\right)^{k-1} \\
&>\; \frac{(2dM)^{k-1}}{\varepsilon^d}.
\end{aligned}
$$

So $|x_d - y_d| = \Omega\left(\frac{1}{\varepsilon^d}\right)$.

We now show that the height of a vertex v with respect to A_ε differs from its height with respect to A'_ε at most by $\mathcal{O}\left(\frac{1}{\varepsilon^{d-1}}\right)$. This implies that A_ε and A'_ε define the same vertex ordering for ε small enough.

If x' are the coordinates of v with respect to A_ε then $x'_1 = x_1$, $x'_2 = x_2$ and for $i > 2$

$$
\begin{aligned}
|x_i - x'_i| \;&=\; \frac{1}{\varepsilon}|x_{i-1} - x'_{i-1} + \sum_{j=1}^{i-2} t_{dj} x'_j| \\
&\leq\; \frac{1}{\varepsilon}\left(|x_{i-1} - x'_{i-1}| + \sum_{j=1}^{i-2} |t_{dj}||x'_j|\right) \\
&<\; \frac{1}{\varepsilon}\left(|x_{i-1} - x'_{i-1}| + (d-2)Mc^{i-2}\right) \\
&=\; \frac{1}{\varepsilon}\left(|x_{i-1} - x'_{i-1}| + \mathcal{O}\left(\frac{1}{\varepsilon^{i-2}}\right)\right) \\
&=\; \frac{1}{\varepsilon}|x_{i-1} - x'_{i-1}| + \mathcal{O}\left(\frac{1}{\varepsilon^{i-1}}\right).
\end{aligned}
$$

So we get

$$|x_d - x'_d| = \frac{1}{\varepsilon}\left(\frac{1}{\varepsilon}\left(\ldots\left(\frac{1}{\varepsilon}|x_2 - x'_2| + \mathcal{O}\left(\frac{1}{\varepsilon^2}\right)\right)\ldots\right)\right) = \mathcal{O}\left(\frac{1}{\varepsilon^{d-1}}\right),$$

which completes the proof. □

2.3   MSW surfaces

2.3.1   Combinatorial model of the MSW surfaces

The following combinatorial model for the surfaces F_d constructed by Mc-Mullen, Schulz and Wills in [26] is found in Rörig [31]. He describes this family of surfaces by applying the mirror surface construction.

For $d \geq 3$ combinatorially the MSW surface F_d is a subcomplex of the d-cube. The vertices of F_d are all the vertices of the cube $\{0,1\}^d$. Also the edges are all edges of the cube. They exist between vertices that differ in a single entry. The 2-faces of F_d are quadrilaterals and have vertices that differ in exactly 2 *cyclically neighboring* digits. In the notation of Section 2.1.1 the quad $011**10$ has the vertices

$$011\mathbf{00}10, 011\mathbf{10}10, 011\mathbf{01}10 \text{ and } 011\mathbf{11}10.$$

From this combinatorial description we read off the f-vector of F_d:

$$(2^d, d2^{d-1}, d2^{d-2}).$$

Therefore its Euler characteristic is $\chi(F_d) = (4-d)2^{d-2}$ and its genus is $g = (d-4)2^{d-3} + 1$.

In particular, for $d \geq 12$ the surface F_d has a genus that is larger than the number of vertices. F_{12} has only 4096 vertices and genus 4097.

2.3.2   Strictly preserved faces and upper convex hulls

The image $\pi(P)$ of a polytope P after a linear projection π is again a polytope. In general we have no control of what happens to the faces of P under π: The image of a face G of P may be an arbitrary polytopal subset of $\pi(P)$. It needs not even be a subset of a proper face of the projected polytope $\pi(P)$.

For our construction we therefore consider only "strictly preserved" faces as introduced by Ziegler in [40] and used by Rörig [31].
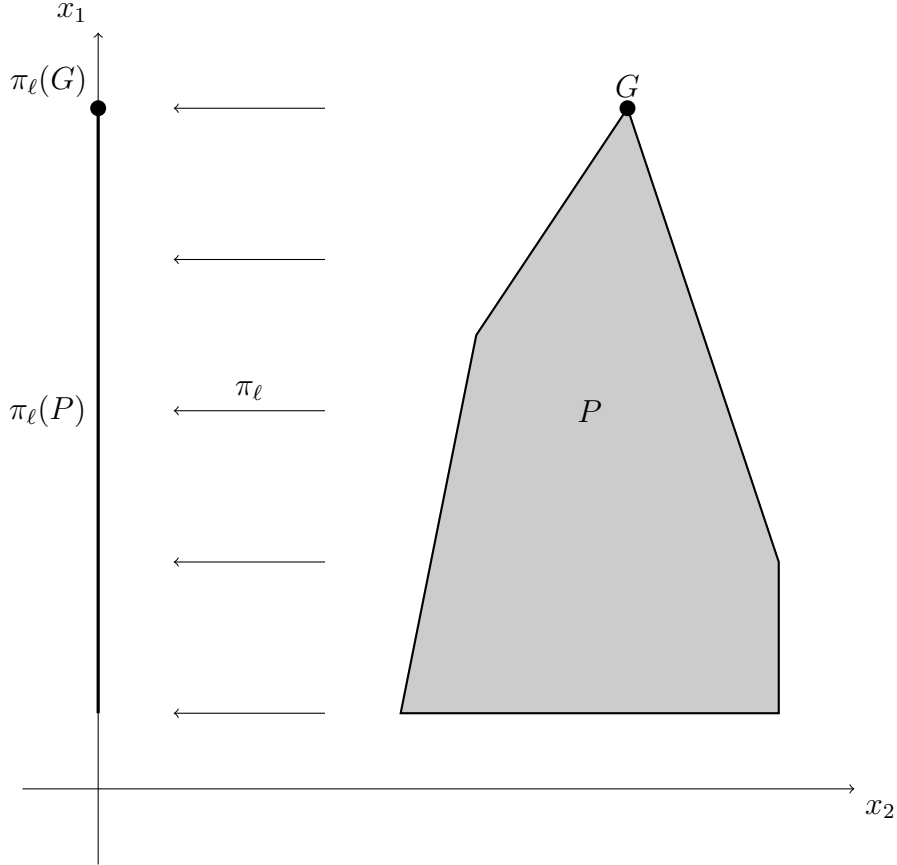
Figure 2.1: Only the face G is strictly preserved under π_ℓ

Definition 2.7 (Faces strictly preserved by a projection). Let $\pi : P \to Q = \pi(P)$ be a projection of polytopes. Then a proper face G of P is *strictly preserved by π* if

1. the image $\pi(G)$ is a face of Q,

2. the map $G \to \pi(G)$ is a bijection, and

3. The preimage of the image is G, i.e. $\pi^{-1}(\pi(G)) = G$.

To facilitate the formulation of linear algebra conditions for the strict preservation of faces, in the following we consider only projections to the last few coordinates. The general situation may be transformed to this special setting by a suitable change of coordinates.

Notation 2.8. *For k and $\ell \in \mathbb{N}$ let $\pi'_k : \mathbb{R}^{k+\ell} \to \mathbb{R}^k, (x', x'') \mapsto x'$ be the projection to the first k coordinates. Also let $\pi''_\ell : \mathbb{R}^{k+\ell} \to \mathbb{R}^\ell, (x', x'') \mapsto x''$*

be the projection to the last ℓ coordinates, i.e. it deletes the first k coordinates. For any ambient dimension d let $\bar{k} = d-k+1$ so that $x_{\bar{k}}$ denotes the $(k-1)$st-to-last coordinate.

Lemma 2.9 (Linear algebra conditions for strict preservation of faces [40])**.**
Let $P \subset \mathbb{R}^d$ be a full-dimensional polytope, and let G be a proper face of P. Denote by $\mathcal{I}_G$ the set of facets of P that contain G.
Then G is strictly preserved by the projection $\pi''_\ell : P \to \pi''_\ell(P)$ if and only if the vectors $\pi'_{d-\ell}(n_F)$, given by omitting the last ℓ components of the normal vectors n_F to all facets $F \in \mathcal{I}_G$, are stricly positively dependent and span $\mathbb{R}^{d-\ell}$.

With the help of this lemma it is possible to obtain realizations of the MSW surfaces in $\mathbb{R}^4$ in the boundary of a projected high dimensional cube. However, we want to project further down orthogonally so we have to take care that the combinatorial structure is kept when projecting further.

Definition 2.10 (Upper convex hull with respect to the x_i-coordinate)**.** A face G of a polytope $P \subset \mathbb{R}^d$ lies in the *upper convex hull of P with respect to the x_i-coordinate* if it has a defining normal vector with a positive x_i-coordinate. We denote the geometric polyhedral complex of all faces lying in the upper convex hull of P with respect to the x_i-coordinate by $U_i(P)$.

Lemma 2.11. *The restriction of the projection π''_{k-1} to the upper convex hull $U_{\bar{k}}(\pi''_k(P))$ of the projected polytope with respect to the $x_{\bar{k}}$-coordinate is piecewise linear and bijective so the image $\pi''_{k-1}(U_{\bar{k}}(\pi''_k(P))) = \pi''_{k-1}(P)$ is a geometric polytopal complex that is combinatorially equivalent to $U_{\bar{k}}(\pi''_k(P))$.*

To check whether a face is strictly preserved in the upper convex hull with respect to the first coordinate of the projected polytope we use the following refined linear algebra condition:

Lemma 2.12 (Linear algebra condition for strict preservation of faces in the upper convex hull [31])**.** *Let $P \subset \mathbb{R}^d$ be a full-dimensional polytope, and let G be a proper face of P. Denote by $\mathcal{I}_G$ the set of facets of P that contain G. Then G is strictly preserved in the upper convex hull with respect to $x_{\bar{\ell}}$ by the projection $\pi''_\ell : P \to \pi''_\ell(P)$ if and only if the projections $\pi'_{d-\ell}(n_F)$ of the normal vectors n_F to facets F in $\mathcal{I}_G$ span $\mathbb{R}^{d-\ell}$ and admit a strictly positive linear combination $n = \sum_{F \in \mathcal{I}_G} \lambda_F n_F$ with $\lambda_F > 0$ for all $F \in \mathcal{I}_G$ such that $\pi'_{d-\ell}(n) = 0$ and $n_{\bar{\ell}} > 0$.*

2.3.3 MSW CUBES

In this section we establish the main result of this chapter. For every MSW surface F_d we construct a deformed cube C_d in $\mathbb{R}^d$ such that the projection of $F_d \subset C_d$ to the last three coordinates yields a realization of F_d in $\mathbb{R}^3$.

The main ingredient for this construction is the convex $(d+1)$-gon $\mathcal{C}_2(d+1)$ shown in Figure 2.2.
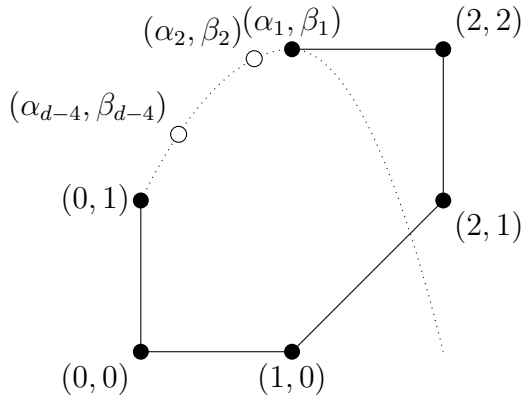
Figure 2.2: The $(d+1)$-gon $\mathcal{C}_2(d+1)$

In the following theorem we give concrete rational values for $(\alpha_i, \beta_i), i = 1, \ldots, d-4$ by choosing them on a parabola. However, any function f that parametrizes a convex arc that joins $(0,1)$ and $(1,2)$ could be used.

Theorem 2.13 (Inequalities for MSW cubes)**.** *Let $d \geq 5$, $1 > \varepsilon > 0$ and $\alpha_1 = 1 > \alpha_2 > \cdots > \alpha_{d-4} > 0$. For $j = 1, \ldots, d-4$ set $\beta_j := 2 - ((alpha_j - 1)^2$, and $\gamma_j := \alpha_j + \beta_j - 1$ as well as $c := \frac{4d}{\varepsilon}$. Let*

$$
A_\varepsilon := \begin{pmatrix}
\varepsilon & 0 & \ldots & & \ldots & \ldots & \ldots & 0 \\
1 & \ddots & \ddots & & & & & \vdots \\
0 & \ddots & \ddots & \ddots & & & & \vdots \\
\vdots & \ddots & \ddots & \ddots & \ddots & & & \vdots \\
0 & \ldots & 0 & 1 & \ddots & \ddots & & \vdots \\
-\beta_1 & \ldots & \ldots & -\beta_{d-4} & 1 & \ddots & \ddots & \vdots \\
\gamma_1 & \ldots & \ldots & \gamma_{d-4} & -2 & 1 & \ddots & 0 \\
-\alpha_1 & \ldots & \ldots & -\alpha_{d-4} & 2 & -2 & 1 & \varepsilon
\end{pmatrix} \in \mathbb{R}^{d \times d} \quad and \quad b_\varepsilon := \frac{\varepsilon}{2} \begin{pmatrix} c \\ c^2 \\ \vdots \\ \vdots \\ \vdots \\ \vdots \\ \vdots \\ c^d \end{pmatrix} \in \mathbb{R}^d.
$$

Then

1. *The polytope*
$$C_d = \{x \in \mathbb{R}^d \mid A_\varepsilon^\pm x \leq \tilde{b}_\varepsilon\}$$
   is a cube of Klee–Minty type.

2. *All 2-faces of the MSW surfaces are strictly preserved in the upper convex hull with respect to $x_{\bar{4}}$ by the projection of C_d to $\mathbb{R}^4$.*

3. *All the vertices are strictly preserved in the upper convex hull with respect to $x_{\bar{2}}$ by the projection of C_d to $\mathbb{R}^2$.*

Proof. As all entries of A_ε are bounded from above by $M = 2$, the results of Section 2.1.2 imply that the matrix A_ε together with the right hand side b_ε defines a realization of the d-cube. In Section 2.2 it was shown that a cube corresponding to a matrix of the form A_ε induces the Klee–Minty vertex ordering. So it only remains to show that the quads and vertices are strictly preserved in the upper convex hull by the projections to the last four and two coordinates respectively.

The algebraic conditions of Lemma 2.12 for the preservation of the faces in question follow from the fact that the auxiliary matrix

$$\tilde{A}_0 := \begin{pmatrix} 0 & \cdots & \cdots & \cdots & \cdots & 0 \\ 1 & \ddots & & & & \vdots \\ 0 & \ddots & \ddots & & & \vdots \\ \vdots & \ddots & \ddots & \ddots & & \vdots \\ 0 & \cdots & 0 & 1 & \ddots & \vdots \\ -\beta_1 & \cdots & \cdots & -\beta_{d-4} & 1 & 0 \\ \gamma_1 & \cdots & \cdots & \gamma_{d-4} & -2 & 1 \\ -\alpha_1 & \cdots & \cdots & -\alpha_{d-4} & 2 & -2 \\ 0 & \cdots & \cdots & 0 & -1 & 2 \\ 0 & \cdots & \cdots & \cdots & 0 & -1 \end{pmatrix} \in \mathbb{R}^{(d+2)\times(d-2)}$$

is a Gale diagram of

$$\begin{pmatrix} 1 & 1 & 1 & \cdots & 1 & 1 & 1 & 1 & 1 & 1 \\ 0 & 1 & 1 & \cdots & 1 & 1 & 1 & 1 & 1 & 1 \\ 0 & \alpha_1 & \alpha_2 & \cdots & \alpha_{d-4} & 0 & 0 & 1 & 2 & 2 \\ 0 & \beta_1 & \beta_2 & \cdots & \beta_{d-4} & 1 & 0 & 0 & 1 & 2 \end{pmatrix} \in \mathbb{R}^{4\times(d+2)},$$

which is the matrix representation of the pyramid with apex $(0,0,0)$ over the $(d+1)$-gon $\mathcal{C}_2(d+1)$ of Figure 2.2 lifted to the $\{1\} \times \mathbb{R}^2$ plane.

First we look at the 2-faces under the projection π_4'': The inequality description of any 2-face of $\mathcal{F}_d$ is given by two consecutive rows of A_ε that correspond to the pairs of inequalities that are not satisfied with equality and by a choice of one inequality to be satisfied with equality from each pair of inequalities, i.e. a sign for the diagonal entry, that correspond to the other rows of A_ε. The normal vectors in the subset of the inequalities satisfied with equality have to be strictly positively dependent, spanning and the fourth-to-last coordinate of this linear combination has to be positive. The edges from i to $i+1$ and from 1 to d respectively in the pyramid above imply a positive linear combination of 0 using all other rows of $\tilde{A}_0$. The images of the last two rows of $\tilde{A}_0$ under π_{d-4}' are 0, so they may be omitted to get a positive linear combination of 0 using the projected rows $1, \dots, d$ without two cyclically consecutive rows. The fourth-to-last coordinate of this combination of rows is positive because the $d+1, d+1$ entry of $\tilde{A}_0$ is -1 and in the larger combination used with a positive weight. The relevant projected rows of $A_\varepsilon^\pm$ are a small perturbation of these rows of $\tilde{A}_0$. So the conditions of Lemma 2.12 are satisfied for the matrix that we are really interested in whenever ε is small enough.

At last we consider the vertices under the projection π_2. The edge from $d+1$ to $d+2$ in the pyramid above implies a positive linear combination of 0 using all the other rows of $\tilde{A}_0$. This yields the conditions of Lemma 2.12 for the vertices by an analogous argument. $\qquad\square$

COMBINATORIAL MORSE THEORY FOR
POLYHEDRAL SURFACES

In the case of surfaces Classical Morse Theory as described by Milnor [27] examines how the global complexity measured by the Euler characteristic is reflected by the local changes at critical points when the surface is built along an increasing Morse function. In this setting nondegenerate critical points of surfaces are isolated and of very simple types: (local) maxima, (local) minima and ordinary saddles. Therefore each critical point contributes at most 1 to the Euler characteristic and we have $2g \leq \#$critical points.

Polyhedral surfaces are not differentiable submanifolds of $\mathbb{R}^3$ and therefore not directly accessible to Classical Morse Theory. Our approach uses the fact that they are Whitney stratified spaces. So we can apply Stratified Morse Theory, developed by Goresky and MacPherson [18]. In this framework general position linear functionals are Morse functions and all vertices are critical points.

For every vertex v we get a parameter – the Morse number μ – which is the difference in the Euler characteristic of the partial surfaces before and after v. The higher the Morse number the more possibilities there are to explain μ in terms of the change in the number of connected components, boundary components and handles. We combine these detailed information in the notion of the *type* of v. Then we derive conditions for feasible types and construct examples. Afterwards we give a detailed analysis of the MSW surfaces F_d described in Section 2.3. In the end we look at vertices with maximal possible Morse number together with a complete graph.

3.1   STRATIFIED MORSE THEORY

Stratified Morse theory was developed by M. Goresky and R. MacPherson in their book [18] to which we refer for details and proofs omitted here. It is a generalization of classical Morse theory to Whitney stratified spaces. Whitney stratified spaces are subsets of manifolds that are built of submanifolds

fitting together nicely not only regarding the submanifolds themselves but also the tangent spaces of the submanifolds.

We give a short review of the definitions needed to formulate the main theorem of stratified Morse theory.

Definition 3.1 (General notions of Morse theory)**.** Let f be a smooth function on a Whitney stratified subspace X of a d-dimensional manifold M.

- Denote
$$X_{\leq c} \quad := \quad \{x \in X \mid f(x) \leq c\}$$

- A *critical point* p of f is a critical point of the restriction of f to any stratum S of X in the sense of classical Morse Theory. The value $f(p)$ is called *critical value*.

- The function f is a *Morse function* iff
  1. its critical values are distinct.
  2. the restriction of f to each stratum is non-degenerate.
  3. the differential of f at p does not annihilate any limit of tangent spaces to any stratum other than the one containing p. This is a non-degeneracy condition for f in directions normal to the strata as well.

- *Morse data* at a critical point p consists of a pair (A, B) of topological spaces with $B \subset A$ such that as c crosses the critical value $v = f(p)$, the change in $X_{\leq c}$ can be described by gluing in A along B.

In particular we see that all 0-dimensional strata are critical points for *every* Morse function.

In classical Morse theory the *Morse index* λ of a critical point contains all information needed to retain the complete Morse data, which is the handle

$$(D^\lambda \times D^{d-\lambda}, (\partial D^\lambda) \times D^{d-\lambda}).$$

In stratified Morse theory we can construct Morse data for a critical point out of a tangential and a normal building block.

Definition 3.2 (Tangential and normal Morse data)**.** Let f be a Morse function on a Whitney stratified subspace X of a manifold M. Let p be a critical point of f and S the stratum of X that contains p.

- *Tangential Morse data* is the classical Morse data for $f|_S$ at p.

- Denote by $D(p)$ a small disk in M transverse to the stratum S containing p such that $D(p) \cap S = \{p\}$. The intersection of $D(p) \cap X$ is called the *normal slice* at p and is denoted by $N(p)$.

- For any critical point p in X with critical value v *normal Morse data* at p is the pair (A, B) of spaces, where $A = N(p) \cap \{x \in X \mid v - \varepsilon \leq f(x) \leq v + \varepsilon\}$ and $B = N(p) \cap \{x \in X \mid v - \varepsilon = f(x)\}$.

Remark 3.3. *Normal Morse data is Morse data of the restriction of f to the normal slice.*

Theorem 3.4 (Main Theorem of stratified Morse theory)**.** *Let f be a Morse function on a compact Whitney stratified space X.*

1. *As c varies within the open interval between two adjacent critical values, the topological type of $X_{\leq c}$ remains constant.*
2. *Let p be a critical point. Denote the tangential Morse data at p by (A_t, B_t) and the normal Morse data at p by (A_n, B_n). Then the product*

$$(A_t, B_t) \times (A_n, B_n) = (A_t \times A_n, A_t \times B_n \cup A_n \times B_t)$$

is Morse data at the critical point p.

3.2 Geometric Polyhedral Complexes as Whitney stratified spaces

Let Δ be a geometric polyhedral complex in $\mathbb{R}^d$ and $f : \mathbb{R}^d \to \mathbb{R}$ a linear functional in general position with respect to Δ. (i.e. it does not evaluate to the same value on to distinct vertices.) Then Δ is a Whitney stratified subspace of its ambient $\mathbb{R}^d$ and f is a Morse function. So we can apply stratified Morse Theory.

All vertices are critical and only vertices are critical points. This does not depend on the particular choice of the linear functional but follows from the fact that linear functionals on polytopes attain their maxima and minima on vertices. The tangential Morse data at each vertex is $(\cdot, \emptyset)$, as the tangent space to a vertex is 0-dimensional. Morse data in this situation is thus completely determined by the normal Morse data.

In contrast to classical Morse theory critical points in which the topological type does not change are possible. We call such critical points *trivial*.

Proposition 3.5. *Let Δ be a geometric polyhedral complex in $\mathbb{R}^d$ and $f : \mathbb{R}^d \to \mathbb{R}$ a linear functional in general position with respect to Δ. Without*

loss of generality assume that the vertices of Δ are numbered according to the order induced by f. The normal Morse data at a vertex v is homotopy equivalent to

$$(\overline{\mathrm{star}_\Delta v}, \mathrm{link}_\Delta v \cap \Delta_{\{1,\dots,v-1\}})$$

Proof. The normal slice $N(v)$ is a retract of the closed star $\overline{\mathrm{star}_\Delta v}$ in Δ. The second space $B = N(v) \cap \{x \in X \mid f(v) - \varepsilon = f(x)\}$ is transformed by this homotopy into $\mathrm{link}_\Delta v \cap \{x \in X \mid f(x) < f(v)\}$ which in turn retracts to $\mathrm{link}_\Delta v \cap \Delta_{\{1,\dots,v-1\}}$. $\qquad\qquad\square$

Remark 3.6. *If we fix a linear functional we get the induced order of the vertices of Δ. Proposition 3.5 assures that in that case all Morse data can be obtained in a purely combinatorial way from the combinatorics of Δ together with a vertex ordering.*

3.3   POLYHEDRAL SURFACES IN $\mathbb{R}^3$

We now turn our attention to embedded surfaces in $\mathbb{R}^3$. By the Classification Theorem for surfaces every compact orientable surface (with boundary) is homeomorphic to a finite collection of spheres, each with a finite number of handles and punctures (see Francis and Weeks [13] for a nice proof).

Let M be a (not necessarily connected) polyhedral surface with f_0 vertices, f_1 edges and f_2 2-faces. Then the Euler characteristic $\chi(M) = f_0 - f_1 + f_2$ is a homotopy type invariant and can alternatively be expressed by

$$\chi(M) = 2c - 2h - b,$$

where c is the number of connected components of M, h the total number of handles and b the total number of boundary components. If M is connected the topological type is completely determined by h and b. Otherwise handles and boundary components could be distributed among the connected components in an arbitrary way.

Notation 3.7. *Let f be a linear functional in general position with respect to M, v a vertex of M and $\varepsilon > 0$ small enough, i.e. there is no vertex w with $|f(w) - f(v)| \leq \varepsilon$. Write*

$$M_v^\pm = M_{\leq f(v)\pm\varepsilon}$$

and let $c_v^\pm$, $h_v^\pm$, $b_v^\pm$ and $\chi_v^\pm$ the number of connected components, the total number of handles, the total number of boundary components and the Euler characteristic of $M_v^\pm$ respectively.

Section 3.2 yields in particular that the first component of normal Morse data at a vertex v of a surface is always a disc. For the second component there are the several possibilities and we describe the effects on c, h, b and χ of the transition from M_-^v to M_+^v.

Opening a new connected component. $c_v^+ = c_v^- + 1$, $b_v^+ = b_v^- + 1$, $h_v^+ = h_v^-$ and thus $\chi_v^+ = \chi_v^- + 1$.

Closing a hole. $b_v^+ = b_v^- - 1$, $c_v^+ = c_v^-$, $h_v^+ = h_v^-$ and thus $\chi_v^+ = \chi_v^- + 1$.

Trivial critical point. No changes.

"The classical saddle point". $\chi_v^+ = \chi_v^- - 1$ There are three possibilities:

1. Connect two connected components. $c_v^+ = c_v^- - 1$, $b_v^+ = b_v^- - 1$, $h_v^+ = h_v^-$
2. Split a boundary component. $b_v^+ = b_v^- + 1$, $c_v^+ = c_v^-$, $h_v^+ = h_v^-$
3. Close a handle. $h_v^+ = h_v^- + 1$, $b_v^+ = b_v^- - 1$, $c_v^+ = c_v^-$

A "wild" critical point where the disc is attached along $k > 2$ paths. $\chi_v^+ = \chi_v^- - k + 1$. The effect can be thought of repeatedly attaching discs along two paths. Any combination of the possibilities of the previous point is combinatorially possible.

Remark 3.8. *The number k of paths is the number of changes from a higher to a lower neighbor in the star of the vertex. This includes the two cases with $k = 0$ which correspond to $\emptyset$ where all neighbors are higher and $\bigcirc$ where all neighbors are lower.*

Definition 3.9 (Morse number)**.** Let M be a polyhedral surface in $\mathbb{R}^3$, let f be a general position linear functional on $\mathbb{R}^3$. We denote by

$$\mu(v) := \chi(M_v^-) - \chi(M_v^+)$$

the change in the Euler characteristic when passing v and call it the *Morse number* of v.

Remark 3.10. *Any trivial critical point has Morse number 0.*

Remark 3.11. *The number of connected components increases at critical points with Morse number -1 and may decrease in other critical points. The number of handles only increases along f. The number of boundary components increases if boundary components split and decreases as a side effect when the number of handles or connected components changes.*

Definition 3.12 (Type of a critical point)**.** With Notation 3.7 define

$$c_v := -(c_v^+ - c_v^-), \quad h_v := h_v^+ - h_v^-, \quad b_v := b_v^+ - b_v^- + h + c$$

We call b_v the *net change in boundary components* and (c_v, h_v, b_v) the *type of v*.

Lemma 3.13 (Elementary properties of the type of a vertex)**.** *Let v be a vertex of M of type (c, h, b) with respect to the linear functional f and denote by $(\tilde{c}, \tilde{h}, \tilde{b})$ the type of v w.r.t. $-f$.*

Then

1. *$b \geq -1$, $c \geq -1$ and $h \geq 0$*

2. *$c + h + b = \mu(v)$*

3. *If $b = -1$ or $c = -1$ then the other two numbers are zero.*

4. *$\tilde{b} = c + h$ and $b = \tilde{c} + \tilde{h}$.*

Proof. Follows directly from Definitions 3.9 and 3.12 and Remark 3.11. $\quad\square$

Example 3.14 (The Möbius Torus)**.** As a first example we analyze Császár's realization of the Möbius torus. The EG model [23] of the Császár torus uses the coordinates $A = (3, -3, 0)$, $B = (-3, 3, 0)$, $C = (-3, -3, 1)$, $D = (3, 3, 1)$, $E = (-1, -2, 3)$, $F = (1, 2, 3)$ and $G = (0, 0, 15)$.

With the height function $f(x, y, z) = y + 7z$ we get the alphabetical order of the vertices. There are four nontrivial critical points where the topology changes, as listed in Table 3.1, which is the same behavior as in classical Morse theory.

With the height function $f(x, y, z) = x + 2y + 3z$ on the other hand we get the vertex ordering and the Morse data listed in Table 3.2. Here vertex E is a monkey saddle. Passing E results in closing a handle and opening a new boundary component at the same time. Its type $(0, 1, 1)$ isn't possible in classical Morse theory.
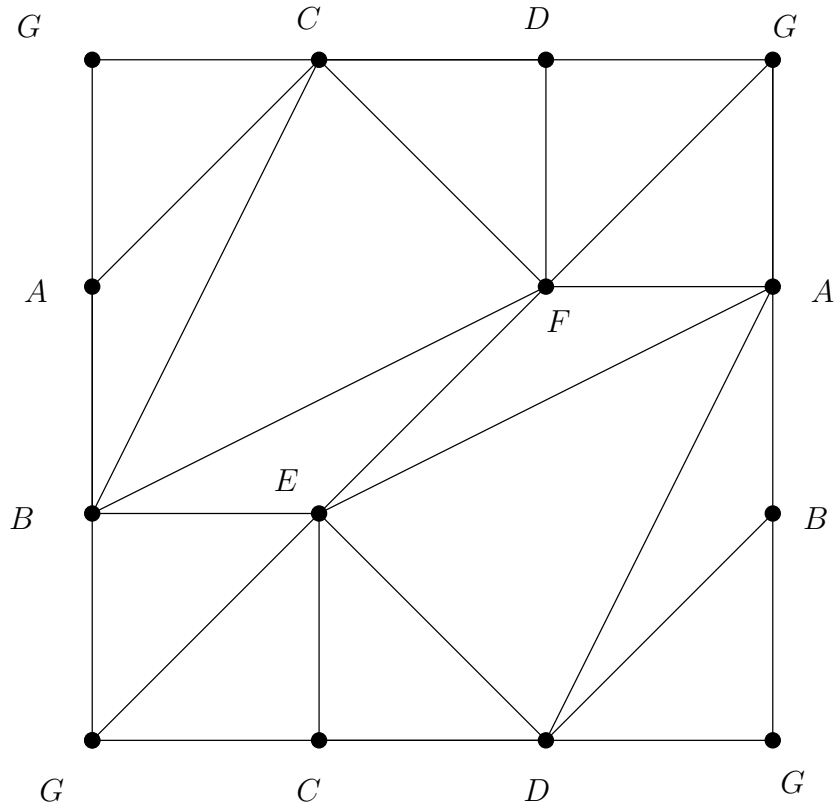
Figure 3.1: The Möbius torus

vertex	height	Morse number	Morse data	M_v^-	h_v^-	b_v^-	χ
A	-3	-1	$(\bullet, \emptyset)$	$\emptyset$	0	1	1
B	3	0	$(\bullet, \rightarrowtail)$		0	1	1
C	4	0	$(\bullet, \rightarrowtail)$		0	1	1
D	10	1	$(\bullet, \updownarrow\updownarrow)$		0	2	0
E	19	1	$(\bullet, \updownarrow\updownarrow)$		1	1	-1
F	23	0	$(\bullet, \rightarrowtail)$		1	1	-1
G	105	-1	$(\bullet, \circ)$		1	0	0

Table 3.1: Morse data and topological changes with the vertex ordering induced by $f(x, y, z) = y + 7z$

vertex	height	Morse number	Morse data	M_v^-	h_v^-	b_v^-	χ
C	-6	-1	(●,∅)	∅	0	1	1
A	-3	0	(●,↦)	●	0	1	1
B	3	0	(●,↦)	●	0	1	1
E	4	2	(●,≺!)	●	1	1	-1
D	12	0	(●,↦)	⊖	1	1	-1
F	13	0	(●,↦)	⊖	1	1	-1
G	45	-1	(●,○)	⊖	1	0	0

Table 3.2: Morse data and topological changes with respect to the vertex ordering induced by $f(x,y,z) = x + 2y + 3z$

3.4 A sphere with a critical point of high Morse number

In this example we look at a triangulated 2-sphere on $2n + 2$ vertices in $\mathbb{R}^3$ with a dent (see Figure 3.2). Combinatorially it is the boundary of the bipyramid over an $2n$-gon. Let

$$
\begin{aligned}
w_1 &:= (0,0,0), \\
w_2 &:= (0,0,1) \text{ and} \\
v_k &:= (\cos\phi_k, \sin\phi_k, \tfrac{k}{2n+1}(-1)^k) \text{ for } k = 1, \ldots, 2n
\end{aligned}
$$

where $\phi_k := \frac{k}{n}\pi$.

With respect to the last coordinate as a height function we get the following induced vertex ordering:

$$v_{2n-1}, v_{2n-3}, \ldots, v_1, w_1, v_2, v_4, \ldots, v_{2n}, w_2$$

The vertices have the Morse numbers

$$
\mu(w_1) = n - 1, \quad \mu(w_2) = -1 \quad \text{and} \quad \mu(v_k) = \begin{cases} -1 & k \text{ odd}, \\ 0 & k \text{ even}. \end{cases}
$$

The Morse numbers add up to the negative Euler characteristic

$$n - 1 + (-1) + n \cdot (-1) = -2 = -\chi.$$

So we see that every Morse number $k \geq -1$ can be realized in $\mathbb{R}^3$.

The intersection figures

$$
M \cap \left\{ \begin{pmatrix} x \\ y \\ z \end{pmatrix} \in \mathbb{R}^3 \mid z = \pm\varepsilon \right\}
$$
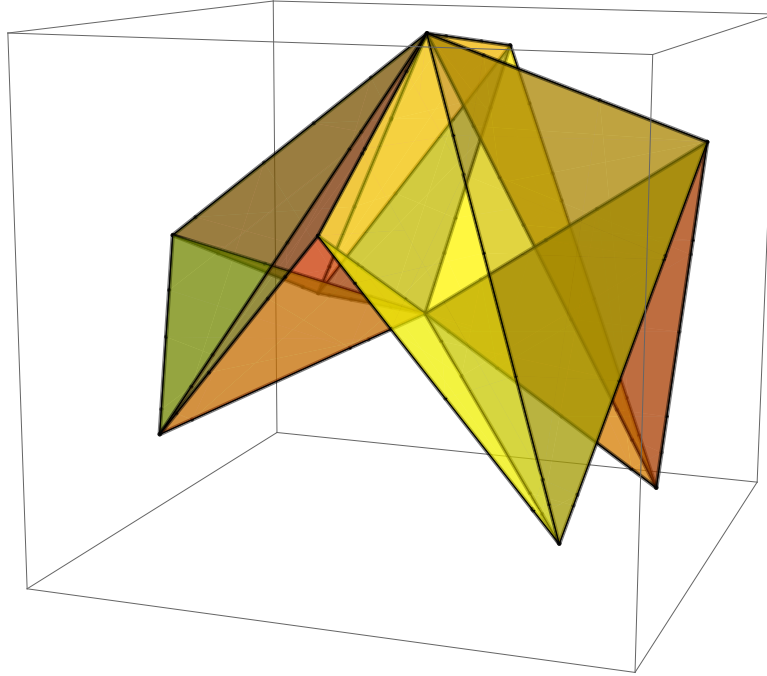
Figure 3.2: A sphere with 10 vertices and a vertex of Morse number 3

are the boundary components of $M^{\pm}_{w_1}$ and are shown schematically in Figure 3.3.
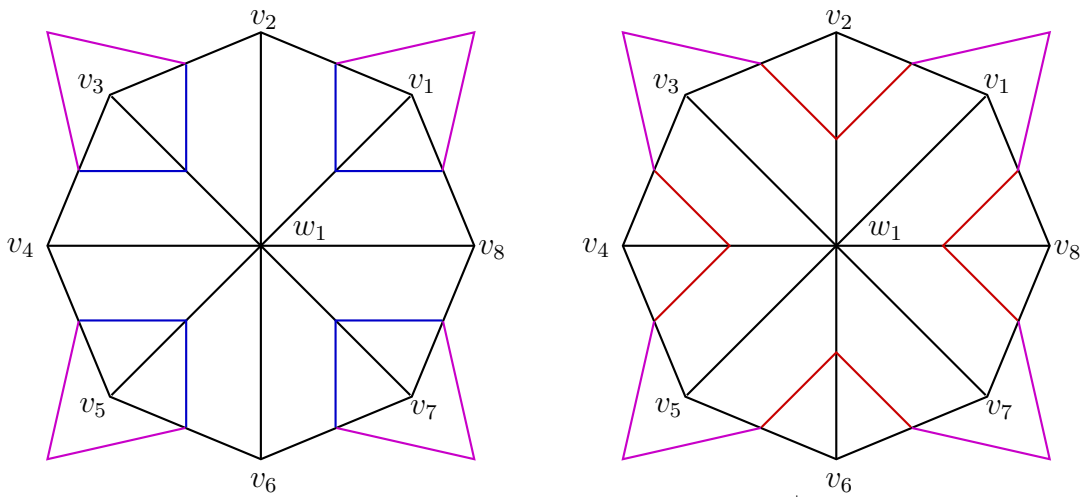
Figure 3.3: Boundary components of $M^{\pm}_{w_1}$

The vertices v_k for odd k are of type $(-1, 0, 0)$, w_1 has type $(n-1, 0, 0)$ and

w_2 has type $(0, 0, -1)$.

It is not necessary for a realization of this triangulation of S^2 to have a vertex with a high Morse number as boundary of the standard convex realization of the bipyramid over a polygon shows.

3.5   REALIZING CRITICAL POINTS OF ARBITRARY TYPE

Theorem 3.15. *Let $\mu \geq 2$ with $\mu = c + h + b$, $c, h, b \geq 0$. Then there is a triangulated surface M in $\mathbb{R}^3$ with a vertex v with Morse number $\mu(v) = \mu$ with respect to the height function z and with $c_v = c$, $h_v = h$ and $b_v = b$.*

Proof. By construction.

We start with the star of the vertex $v = (0, 0, 0)$ with vertex coordinates for $v_1, \ldots, v_{2\mu+2}$ as in the previous example. Therefore $\mu(v) = \mu$.

- First we describe the construction in the case $c + h \leq b$.

  In this case prescribe the intersection figures $M_v^{\pm}$ as follows: Below v we schematically draw $b_v^- = c + h + 1$ boundary components as shown in Figure 3.4 by drawing $c + h$ boundary components for the $4(c + h)$ triangles on the left and one boundary component for the remaining triangles on the right.
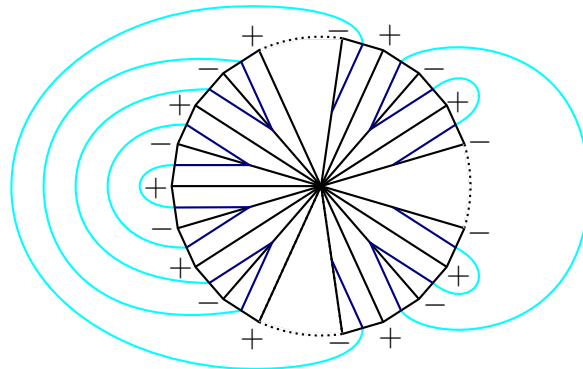
Figure 3.4: Intersection figures ∂M_v^-

  Above v we then have the situation of Figure 3.5 and therefore

  $$b_v^+ = c + h + 1 + \frac{1}{2}(2\mu + 2 - 4(c + h) - 2) = \mu - (c + h) + 1 = b + 1$$
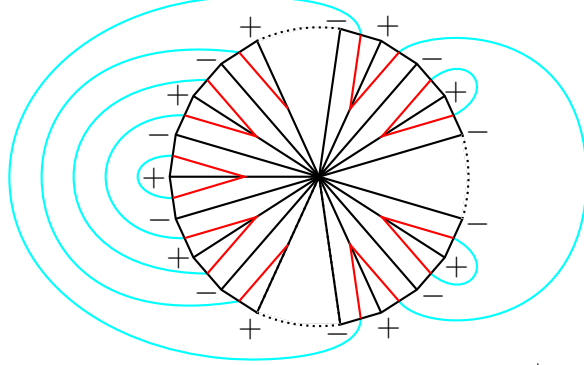
Figure 3.5: Intersection figures ∂M_v^+

boundary components.

With these prescriptions we get

$$2(c_v + h_v) = \mu(v) - b_v + c_v + h_v = \mu - b_v^+ + b_v^- = \mu - (b - (c+h)) = 2(c+h)$$

and

$$b_v = \mu(v) - (c_v + h_v) = \mu - (c+h) = b.$$

Now complete the surface below v such that there are $c + 1$ connected components. M_v^+ is connected as there is a path from every point to v. So we have $c_v = c$ and $h_v = h$.

- For the case $b < c + h$ we modify the construction as follows: Figure 3.4 with $+$ and $-$ exchanged becomes ∂M_v^+ with $b_v^+ = b + 1$ boundary components. In this case we group $4b$ triangles on the left. Then Figure 3.5 with $+$ and $-$ exchanged becomes ∂M_v^- and has $b_v^+ = c + h + 1$ boundary components. The rest of the construction stays the same.

$\square$

Remark 3.16. *In these examples the high Morse number is again not forced by the combinatorics. The surface outside the star of v can be constructed outside the prism $\operatorname{conv}\{(\cos \phi_k, \sin \phi_k) \mid k = 1, \ldots, 2n\} \times [-1, 1]$. If we choose $v = (0, 0, 1)$ as the central point it is higher than all its neighbors. Therefore it has Morse number -1 and for each of the even neighbors $v_2, \ldots, v_{2n}$ the Morse number is increased by 1.*

3.6   The MSW-surfaces

In Chapter 2 we presented an embedding of the MSW surfaces into cubes of Klee–Minty type such that the surfaces and the height function x_n survive the projection to $\mathbb{R}^3$. In the following we calculate Morse numbers and analyzethe types of critical points in these realizations.

3.6.1   Morse number of a vertex in an MSW surface

To calculate the Morse number of a vertex v we need to compare the vertices of $\overline{\mathrm{star}_{F_d} v}$ with v. These vertices are the vertices of the quads that contain v. In every quad there are not only two neighbors of v but also the vertex diagonally opposite to v. Nevertheless the relevant changes appear in the neighbors already.

Example 3.17. With the combinatorial description of Subsection 2.3.1 the vertex $v = 011011101 \in F_9$ lies in the quad $0110**101$. The other three vertices of this quad are $011\mathbf{00}101$, $011\mathbf{0}1\mathbf{0}101$ and $0110\mathbf{0}11101$. Comparing these to v using the combinatorial description of the height function in Remark 2.5 we see that the non-neighbor $011\mathbf{00}101$ has the same differing tail 0101 as the neighbor $0110\mathbf{1}0101$ and these two vertices are thus lower than v. The other neighbor $0110\mathbf{0}11101$ is higher than v.

Now all neighbors of v are

vertex	compared to v
$\mathbf{1}11011101$	$>$
$0\mathbf{0}1011101$	$>$
$01\mathbf{0}011101$	$<$
$011\mathbf{1}11101$	$>$
$0110\mathbf{0}1101$	$>$
$01101\mathbf{0}101$	$<$
$011011\mathbf{0}01$	$>$
$0110111\mathbf{1}1$	$<$
$01101110\mathbf{0}$	$<$.

Proposition 3.18. *Let $v = v_1 \ldots v_d \in F_d$. Then*

$$\mu(v) = \left\lceil \frac{\sum_{j=1}^{d-1} v_j}{2} \right\rceil - 1.$$

Proof. From the combinatorial description of the height function on F_d we see that there is a change in direction from the neighbor that differs from v in the combinatorial coordinate v_k to the neighbor that differs in v_{k+1} if and only if

$$\sum_{j=k}^{d} v_j \not\equiv \sum_{j=k+1}^{d} v_j \mod 2.$$

This happens if and only if $v_k = 1$. There is an additional change from neighbor d to neighbor 1 if

$$\sum_{j=1}^{d-1} v_j \equiv 1 \mod 2.$$

Half of these changes are up-down changes, so the Morse number of a vertex $v_1 \dots v_d$ is

$$\left\lceil \frac{\sum_{j=1}^{d-1} v_j}{2} \right\rceil - 1.$$

$\square$

Remark 3.19. *The vertices with maximal Morse number are $1 \dots 11$ and $1 \dots 10$. They have Morse number*

$$\left\lceil \frac{d-1}{2} \right\rceil - 1.$$

If d is even there is a directional change from each neighbor of v to the next.

However, in F_d there are no further edges between the neighbors of v. Some of these edges intersect the surface. This has been verified for small d by a calculation in SAGE [36].

3.6.2 Types of critical points in F_d

In order to determine the types of the critical points, we have to take a closer look at the structure of the surfaces. Following the recursive definition of the cube C_d we give a recursive description of the MSW surface F_d. This is the combinatorial essence of the geometric construction of McMullen, Schulz and Wills.

Start with the 2-skeleton of the 3-cube $C_3 =: F_3$, which is a 2-sphere.

For the step $d \to d+1$ we observe how the union of the two copies $F_d \times \{0\}$ and $F_d \times \{1\}$ differs from F_{d+1}. The union of these two copies contains the quads $*v_2 \ldots v_{d-1} * v_{d+1}$ which are not present in F_{d+1}. Instead F_{d+1} contains the quads

$$*v_2 \ldots v_{d-1}0*, \quad *v_2 \ldots v_{d-1}1*, \quad 0v_2 \ldots v_{d-1}** \quad \text{and} \quad 1v_2 \ldots v_{d-1}**.$$

These quads form 'tunnels' between $F_d \times \{0\}$ and $F_d \times \{1\}$. So we obtain F_{d+1} from two copies of F_d by deleting the quads $*v_2 \ldots v_{d-1} * v_{d+1})$ and adding the tunnels. So all the handles of F_d are present in F_{d+1} twice and there are $2^{d-2} - 1$ additional handles coming from the tunnels.

Figure 3.6 shows a schematic picture of F_5. On the left the vertices are enumerated along the hamiltonian path. Quads are represented by vertical line segments with "pearls" on the heights of their vertices. Edges are the complete line segments and the parts between pearls. All pearls on the same height represent one vertex. At heights between vertices the intersection figures are represented schematically by curves.

Theorem 3.20. *In the MSW–surface F_d there are only vertices of pure types $(0, \mu, 0)$ and $(0, 0, \mu)$, $\mu = -1, \ldots, \lfloor \frac{d}{2} \rfloor$ with the only exception of $0 \ldots 0$ which has type $(-1, 0, 0)$.*

Proof. All the surfaces $(F_d)_{\leq c}$ are connected. So every vertex with has type $(0, h, b)$. Let $v = v_1 \ldots v_d \in F_d$ be a vertex with Morse number $\mu > 0$ gives rise to two vertices in F_{d+1}. Denote the type of v by $(0, h, b)$. Then there are two possibilities:

1. If $v_1 \ldots v_d v_{d+1}$ has the same Morse number as v then $v_1 \ldots v_d 0$ has the same type $(0, h, b)$ as v and $v_1 \ldots v_d 1$ is of type $(0, b, h)$.

2. If the Morse number of $(v_1, \ldots, v_d, v_{d+1})$ is greater than $(v_1, \ldots, v_d)$ then $(v_1, \ldots, v_d, 0)$ has type $(0, h, b+1)$ and $(v_1, \ldots, v_d, 1)$ is of type $(0, b+1, h)$. That means an additional boundary component is opened in $v_1 \ldots v_d 0$ which is closed into a handle symmetrically in $v_1 \ldots v_d 1$.

So for each digit that contributes to the Morse number (i.e. the 3rd, 5th and so on 1) there is a partner vertex in the same subcube with the bit after the contributing 1 flipped. Now *all* these partners are either higher or lower, as the parity of the respective tails is the same. So either only boundary components are opened or only handles are closed.   □
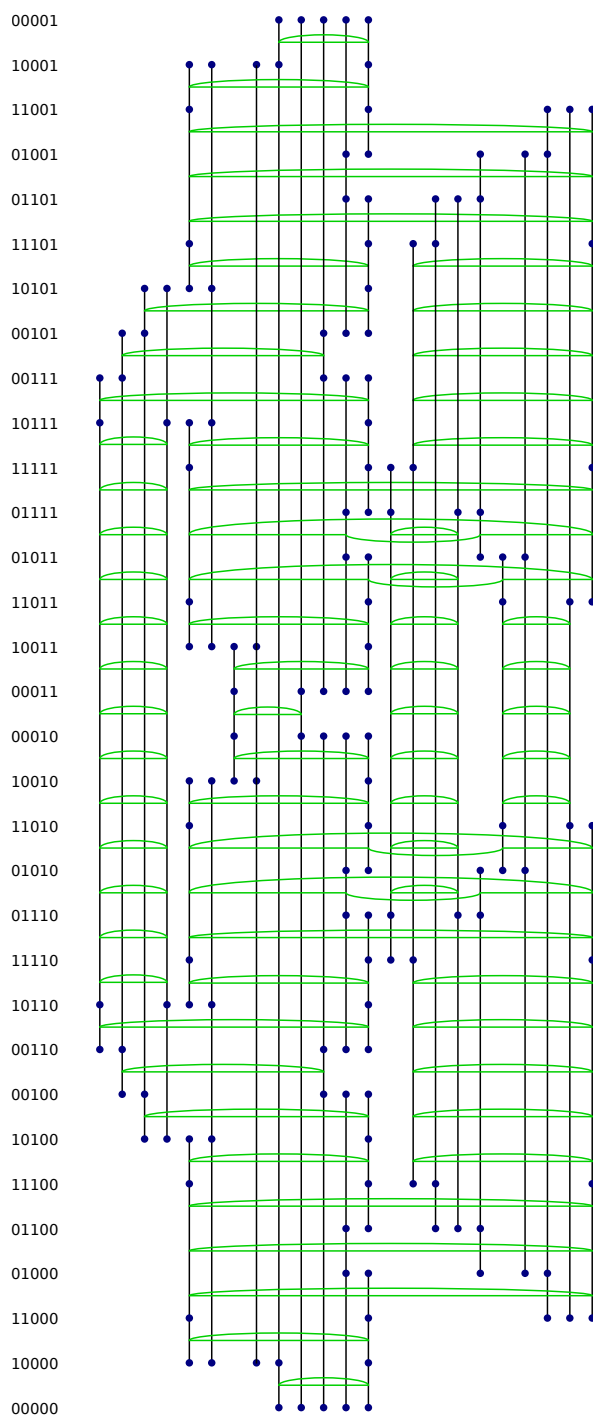
Figure 3.6: MSW surface F_5

3.7   The star of a vertex together with a complete graph

We have seen that all types (c, h, b) with $c, h, b \geq 0$ of critical points occur in triangulated surfaces embedded in $\mathbb{R}^3$. However, the graphs of the surfaces constructed for $\mu = c + b + h \geq 2$ in Section 3.5 are far from complete.

A surface on n vertices with complete graph has genus $\Theta(n^2)$. Thus the average contribution of a vertex towards the Euler characteristic is $\Theta(n)$. Therefore there is at least one vertex in which a Morse number linear in the number of vertices is attained.

So in this section we look at the interplay of a vertex star with high Morse number and the complete graph.

Problem 3.21. *Let n be odd. Is there a geometric realization in $\mathbb{R}^3$ of the (abstract, impure) simplicial complex*

$$\Delta_n := \{123, 134, \ldots, 1n2\} \cup K_n$$

under the additional condition that there is a plane containing 1 such that $2, 4, \ldots, n-1$ are on the positive side and $3, 5, \ldots, n$ are on the negative side?

The vertex star of vertex E of the Császár torus in Example 3.14 together with the plane $x + 2y + 3z = 4$ gives a solution of this problem for $n = 7$.

For $n = 9$ the points

1	$(0, 0, 0)$	2	$(-45, 1, 58)$	3	$(37, -83, -1)$
4	$(-64, -98, 39)$	5	$(-11, -82, -96)$	6	$(-25, 67, 24)$
7	$(-26, 23, -100)$	8	$(49, 11, 75)$	9	$(64, -31, -47)$

realize Δ_9 with the additional condition satisfied with respect to the x-y-plane. (See Figure 3.7) This solution was found generating and checking random coordinates in MATHEMATICA and SAGE [36].

For Δ_{11} the generation of some millions of random examples did *not* yield an example.

Schewe ([32], [33]) described how to associate a SAT problem to a given simplicial complex Δ such that a solution gives rise to an oriented matroid that is compatible with Δ. For Δ_{11} and Δ_{13} we found compatible oriented matroids using an extension of Schewe's program.

U. Brehm claimed that it is easy to find a realization, and indeed here is one:

Proposition 3.22 (Coordinates for Δ_n)**.**
Let $n \in \mathbb{N}$ and $M \geq 2$.
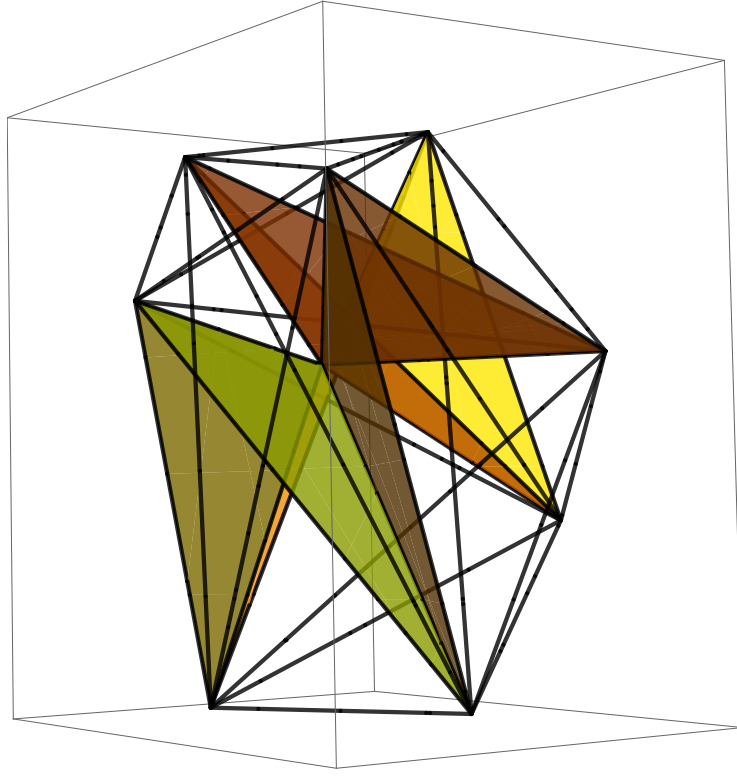
Figure 3.7: Realization of Δ_9

Then

1	$(0,0,0)$
2	$(-1,0,1)$
3	$(0,1,-M)$
j	$(1-2^{-j+3}, 1-(1-2^{-j+3})^2, (-M)^{j-2}), j = 1, \ldots, n-2$
$n-1$	$(1,0,(-M)^{n-3}$
n	$(0,-1,(-M)^{n-2})$

is a geometric realization of Δ_n.

Proof. We check that every pair consisting of an edge ij, $1 \leq i < j \leq n$ and a triangle $1\ell(\ell+1)$, $1 < \ell \leq n-1$ or $12n$ with disjoint vertex sets is completely disjoint.
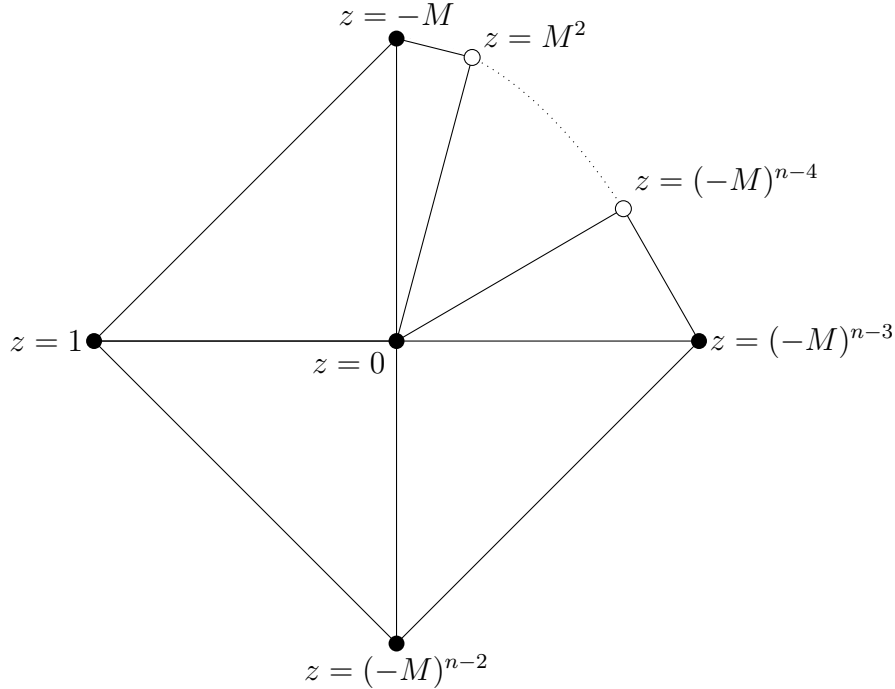
Figure 3.8: Coordinates for Δ_n

First we see that all edges $1j$, $j(j+1)$ and $2n$ only intersect the triangles they are a part of and no edge intersects the triangle $12n$.

So look at an edge $ij, 2 \leq i < i+1 < j \leq n$ and a triangle $1\ell(\ell+1), 1 < \ell \leq n-1$ that have disjoint vertex sets. These intersect in the projection to the x-y-plane only if $i < \ell$ and $j > \ell + 1$. In this case the vertex j lies far above/below the triangle $1\ell(\ell+1)$ and therefore the triangle and the edge don't intersect. $\qquad\square$

GEOMETRIC REALIZABILITY OF POLYHEDRAL SURFACES

4.1 INTRODUCTION

In general, it is difficult to prove for a simplicial complex K that it does *not* have a simplicial embedding (or not even a simplicial immersion) into $\mathbb{R}^m$.

For example, the question whether any neighborly simplicial surface on $n \geq 12$ vertices can be realized in $\mathbb{R}^3$ leads to problems of this type. Specifically, Altshuler [3] enumerated the 59 combinatorial types of neighborly simplicial 2-manifolds of genus 6. Bokowski & Guedes de Oliveira [9] employed oriented matroid enumeration methods to show that one specific instance, number 54 from Altshuler's list, does not have a simplicial embedding; the other 58 cases were shown not to have simplicial embeddings only recently by Lars Schewe ([32], [33]).

For *piecewise linear* non-embeddability proofs there is a classical setup via obstruction classes, due to Shapiro [35] and Wu [38]. In 2000, Isabella Novik [29] refined these obstructions for simplicial embeddability: She showed that if a *simplicial embedding* of K in $\mathbb{R}^m$ exists, then a certain polytope in the cochain space $C^m(\mathsf{K}_\Delta^2; \mathbb{R})$ must contain an integral point. Thus, infeasibility of a certain integer program might prove that a complex K has no geometric realization.

In the following, we present Novik's approach (cf. parts 1 and 4 of Theorem 4.26) in a reorganized way, so that we can work out more details, which allow us to sharpen some inequalities defining the polytope in $C^m(\mathsf{K}_\Delta^2; \mathbb{R})$ (cf. Theorem 4.26.2c). Further we interpret this polytope as a projection of a polytope in $C^m(\mathsf{S}_\Delta^2; \mathbb{R})$, where S denotes the simplicial complex consisting of all faces of the N-simplex. The latter polytope is easier to analyze. This setup is the right framework to work out the relations between variables (cf. Theorem 4.26.2) and to express linking numbers (cf. Theorem 4.26.3b), which are intersection numbers of cycles and empty simplices of K (which are present

in S and therefore need no extra treatment.) Using the extensions based on linking numbers we can reprove for a first example (Brehm's triangulated Möbius strip [11]) that it is not simplicially embeddable in $\mathbb{R}^3$.

4.2   A quick walk-through

Let K be a finite (abstract) simplicial complex on the vertex set V, and fix a geometric realization $|K|$ in some Euclidean space. Further let $f : V \to \mathbb{R}^m$ be any general position map (that is, such that any $m + 1$ points from V are mapped to affinely independent points in $\mathbb{R}^m$). Any such general position map extends affinely on every simplex to a *simplicial map* $f : |K| \to \mathbb{R}^m$ which we also denote by f. Such a simplicial map is a special case of a piecewise linear map.

Every piecewise linear general position map f defines an *intersection cocycle*

$$\varphi_f \ \in \ C^m(K_\Delta^2; \mathbb{Z}). \tag{4.1}$$

Here K_Δ^2 denotes the *deleted product* complex, which consists of all faces $\sigma_1 \times \sigma_2$ of the product $K \times K$ such that σ_1 and σ_2 are disjoint simplices (in K). As the deleted product is a polytopal complex we have the usual notions of homology and cohomology. For a detailed treatment of the deleted product complex we refer to Matoušek [25].

The values of the intersection cocycle are given by

$$\varphi_f(\sigma_1 \times \sigma_2) \ = \ (-1)^{\dim \sigma_1} \mathcal{I}\big(f(\sigma_1), f(\sigma_2)\big),$$

where $\mathcal{I}$ denotes the signed intersection number of the oriented simplicial chains $f(\sigma_1)$ and $f(\sigma_2)$ of complementary dimensions in $\mathbb{R}^m$. These intersection numbers (and thus the values of the intersection cocycle) have the following key properties:

1. In the case of a simplicial map, all values $(-1)^{\dim \sigma_1} \mathcal{I}\big(f(\sigma_1), f(\sigma_2)\big)$ are ± 1 or 0. (In the greater generality of piecewise linear general position maps $f : K \to \mathbb{R}^m$, as considered by Shapiro and by Wu, $\mathcal{I}\big(f(\sigma_1), f(\sigma_2)\big)$ is an integer.)
2. If f is an embedding, then $\mathcal{I}\big(f(\sigma_1), f(\sigma_2)\big) = 0$ holds for any two disjoint simplices $\sigma_1, \sigma_2 \in K$.
3. In the case of the "cyclic map" which maps V to the monomial curve of order m (the "moment curve"), the coefficients $(-1)^{\dim \sigma_1} \mathcal{I}\big(f(\sigma_1), f(\sigma_2)\big)$ are given combinatorially.

The intersection cocycle is of interest since it defines a cohomology class $\Phi_K = [\varphi_f]$ that does not depend on the specific map f. Thus, if some piecewise linear map $g : K \to \mathbb{R}^m$ is an embedding, then $\varphi_g \equiv 0$ and therefore Φ_K is zero.

But a simplicial embedding is a special case of a piecewise linear embedding. So the information Φ_K is not strong enough to establish simplicial non-embeddability for complexes that admit a piecewise linear embedding — such as, for example, orientable closed surfaces in $\mathbb{R}^3$.

According to Novik we should therefore study the specific coboundaries $\delta\lambda_{f,c}$ that establish equivalence between different intersection cocycles.

So, *Novik's Ansatz* is to consider

$$\boxed{\varphi_f - \varphi_c = \delta\lambda_{f,c}} \tag{4.2}$$

where

- $\varphi_f \in C^m(K_\Delta^2; \mathbb{Z})$ is an integral vector, representing the intersection cocycle of a hypothetical embedding $f : K \to \mathbb{R}^m$, so $\varphi_f \equiv 0$. (i.e. for every pair $\sigma_1, \sigma_2 \in K$ of disjoint simplices, that $\varphi_f(\sigma_1 \times \sigma_2) = 0$),
- $\varphi_c \in C^m(K_\Delta^2; \mathbb{Z})$ is an integral vector, whose coefficients $\varphi_c(\sigma_1 \times \sigma_2)$ are known explicitly, representing the intersection cochain of the cyclic map $c : K \to \mathbb{R}^m$,
- δ is a known integral matrix with entries from $\{1, -1, 0\}$ that represents the coboundary map $\delta : C^{m-1}(K_\Delta^2; \mathbb{Z}) \to C^m(K_\Delta^2; \mathbb{Z})$, and finally
- $\lambda_{f,c} \in C^{m-1}(K_\Delta^2; \mathbb{Z})$ is an integral vector, representing the *deformation cochain*, whose coefficients are determined by f and c, via

$$\lambda_{f,c}(\tau_1 \times \tau_2) = \mathcal{I}\big(h_{f,c}(\tau_1 \times I), h_{f,c}(\tau_2 \times I)\big),$$

where $h_{f,c}(x, t) = tf(x) + (1 - t)c(x)$ interpolates between f and c, for $t \in I := [0, 1]$.

Thus if K has a simplicial embedding, then the linear system (4.2) in the unknown vector $\lambda_{f,c}$ has an *integral* solution. Moreover, Novik derived explicit bounds on the coefficients of $\lambda_{f,c}$, that is, on the signed intersection numbers between the parametrised surfaces $h_{f,c}(\tau_1 \times I)$ and $h_{f,c}(\tau_2 \times I)$.

The intersection cocycles and deformation cochains induced by the general position maps $f, g : V \to \mathbb{R}^m$ on *different* simplicial complexes K and $\tilde{K}$ on the *same* vertex set V coincide on $K_\Delta^2 \cap \tilde{K}_\Delta^2$. They are projections of the same intersection cocycle or deformation cochain on S_Δ^2, where S denotes the full face lattice of the simplex with vertex set V. We therefore investigate these

largest cochains and get Novik's results back as well as some stronger results
even in the original setting; see Theorem 4.21 and Remark 4.22.

In the following, we

- derive the validity of the basic equation (4.2), in Section 4.3,
- examine deformation cochains induced by general position maps on the
  vertex set in Section 4.4, and
- exhibit an obstruction system to geometric realizability in Section 4.5.

Furthermore, in Section 4.6 we discuss subsystems and report about compu-
tational results.

4.3   OBSTRUCTION THEORY

We state and prove the results of this section for *simplicial* maps only. They
hold in the more general framework of *piecewise linear* maps as well. For
proofs and further details in this general setting we refer to Wu [38].

4.3.1   INTERSECTIONS OF SIMPLICES AND SIMPLICIAL CHAINS

Definition 4.1. Let σ and τ be affine simplices of complementary dimensions
$k + \ell = m$ in $\mathbb{R}^m$ with vertices $\sigma_0, \ldots, \sigma_k$ and $\tau_0, \ldots, \tau_\ell$ respectively. Suppose
that $\sigma_0, \ldots, \sigma_k$ and $\tau_0, \ldots, \tau_\ell$ are in general position and the simplices
are oriented according to the increasing order of the indices. Then σ and τ
intersect in at most one point. The *intersection number* $\mathcal{I}(\sigma, \tau)$ is defined
to be zero if σ and τ don't intersect and ± 1 according to the orientation of
the full dimensional simplex $(p, \sigma_1, \ldots, \sigma_k, \tau_1, \ldots, \tau_\ell)$ if σ and τ intersect in
p. This definition extends bilinearly to simplicial chains in $\mathbb{R}^m$. (We consider
integral chains, that is, formal combinations of affine simplices in $\mathbb{R}^m$ with
integer coefficients.)

Lemma 4.2. *Let x, y be simplicial chains in $\mathbb{R}^m$ with $\dim x = k$ and
$\dim y = \ell$.*

(a) *If $k + \ell = m$ then $\mathcal{I}(x, y) = (-1)^{k\ell}\mathcal{I}(y, x)$.*

(b) *If $k + \ell = m + 1$ then $\mathcal{I}(\partial x, y) = (-1)^k\mathcal{I}(x, \partial y)$.*

Now we use intersection numbers to associate a cocycle to each general po-
sition map.

Notation 4.3. *For $N \in \mathbb{N}$ denote $[N] := \{1, \ldots, N\}$ and $\langle N \rangle := [N] \cup \{0\}$.*

Lemma and Definition 4.4. *Let $f : \langle N \rangle \to \mathbb{R}^m$ be a general position map. The cochain defined by*

$$\varphi_f(\sigma_1 \times \sigma_2) := (-1)^{\dim \sigma_1} \mathcal{I}\big(f(\sigma_1), f(\sigma_2)\big) \qquad \text{for } m\text{-cells } \sigma_1 \times \sigma_2 \in \mathsf{K}_\Delta^2$$

is a cocycle. It is called the intersection cocycle *of f.*

The intersection cocycle has the following symmetries. For every m-cell $\sigma_1 \times \sigma_2$, with $\dim \sigma_1 = k$ and $\dim \sigma_2 = \ell$,

$$\varphi_f(\sigma_1 \times \sigma_2) = (-1)^{(k+1)(\ell+1)+1} \varphi_f(\sigma_2 \times \sigma_1).$$

Remark 4.5. *Wu calls this cocycle the* imbedding cocyle *[38, p. 183]. If f is a piecewise linear embedding, then $\varphi_f = 0$. When we look at simplicial maps we even have an equivalence: A simplicial map f is an embedding of K if and only if the intersection cocycle is 0. So φ_f measures the deviation of f from a geometric realization. This makes the intersection cocycle quite powerful.*

<div align="center">

4.3.2   Intersections of parametrized surfaces

</div>

In this section we sort out definitions, fix orientations and establish the fundamental relation in Proposition 4.9 (cf. [38, pp. 180 and 183]). Wu uses a simplicial homology between two different piecewise linear maps to establish the independence of the homology class of the particular piecewise linear map. We use a straight line homotopy instead.

Definition 4.6. Let $U \subset \mathbb{R}^k$ and $V \subset \mathbb{R}^\ell$ be sets that are closures of their interiors and $\varphi : U \to \mathbb{R}^m$ and $\psi : V \to \mathbb{R}^m$ smooth parametrized surfaces. The surfaces φ and ψ *intersect transversally* at $p = \varphi(\alpha) = \psi(\beta)$ with $\alpha \in \overset{\circ}{U}$ and $\beta \in \overset{\circ}{V}$, if

$$T_p \mathbb{R}^m = d\varphi(T_\alpha U) \oplus d\psi(T_\beta V)$$

In other words $k + \ell = m$ and the vectors

$$\left. \frac{\partial \varphi}{\partial u_1} \right|_\alpha, \ldots, \left. \frac{\partial \varphi}{\partial u_k} \right|_\alpha, \left. \frac{\partial \psi}{\partial v_1} \right|_\beta, \ldots, \left. \frac{\partial \psi}{\partial v_\ell} \right|_\beta$$

span $\mathbb{R}^m$. In this situation the index of intersection of φ and ψ in p is defined by

$$\mathcal{I}_p(\varphi, \psi) \quad := \quad \operatorname{sgn} \det \left(\left. \frac{\partial \varphi}{\partial u_1} \right|_\alpha, \ldots, \left. \frac{\partial \varphi}{\partial u_k} \right|_\alpha, \left. \frac{\partial \psi}{\partial v_1} \right|_\beta, \ldots, \left. \frac{\partial \psi}{\partial v_\ell} \right|_\beta \right).$$

The surfaces φ and ψ are in *general position* if they intersect transversally only. In particular there are no intersections at the boundary. Surfaces in general position intersect in finitely many points only and the *intersection number* is defined by

$$\mathcal{I}(\varphi, \psi) \quad := \sum_{p = \varphi(\alpha) = \psi(\beta)} \mathcal{I}_p(\varphi, \psi).$$

We also write $\mathcal{I}\big(\varphi(U), \psi(V)\big)$ for $\mathcal{I}(\varphi, \psi)$ when we want to emphasize the fact that the images intersect.

We now give parametrizations of simplices so that the two definitions coincide.

Notation 4.7. *Denote by $(e_1, \ldots, e_m)$ the standard basis of $\mathbb{R}^m$ and let $e_0 := 0$. For $I \subseteq \langle m \rangle$ let Δ_I denote the simplex $\mathrm{conv}\{e_i \mid i \in I\}$. Finally let $J = \{j_0, \ldots, j_k\}_<$ denote the set $\{j_0, \ldots, j_k\}$ with $j_0 < \ldots < j_k$.*

For a simplex $\sigma = \mathrm{conv}\{\sigma_0, \ldots, \sigma_k\}$ the parametrization $\varphi_\sigma : \mathbb{R}^k \supset \Delta_{[k]} \to \sigma \subset \mathbb{R}^m, (u_1, \ldots, u_k) \mapsto \sigma_0 + \sum_{i=1}^{k} u_i(\sigma_i - \sigma_0)$ induces the orientation corresponding to the increasing order of the indices. Now consider two simplices $\sigma = \mathrm{conv}\{\sigma_0, \ldots, \sigma_k\}$ and $\tau = \mathrm{conv}\{\tau_0, \ldots, \tau_\ell\}$. If $\{\sigma_0, \ldots, \sigma_k, \tau_0, \ldots, \tau_\ell\}$ is in general position then also φ_σ and φ_τ are in general position. Let σ and τ intersect in

$$p = \sum_{i=0}^{k} \alpha_i \sigma_i = \sigma_0 + \sum_{i=1}^{k} \alpha_i(\sigma_i - \sigma_0) = \varphi_\sigma(\alpha)$$

$$= \sum_{i=0}^{\ell} \beta_i \tau_i = \tau_0 + \sum_{i=1}^{\ell} \beta_i(\tau_i - \tau_0) = \varphi_\tau(\beta).$$

Then we have by a straightforward calculation:

$$\mathcal{I}(\sigma, \tau) = \mathrm{sgn} \det \left(\begin{pmatrix} 1 \\ p \end{pmatrix}, \begin{pmatrix} 1 \\ \sigma_1 \end{pmatrix}, \ldots, \begin{pmatrix} 1 \\ \sigma_k \end{pmatrix}, \begin{pmatrix} 1 \\ \tau_1 \end{pmatrix}, \ldots, \begin{pmatrix} 1 \\ \tau_\ell \end{pmatrix} \right)$$

$$= \mathrm{sgn} \det \left(\frac{\partial \varphi_\sigma}{\partial u_1}\bigg|_\alpha, \ldots, \frac{\partial \varphi_\sigma}{\partial u_k}\bigg|_\alpha, \frac{\partial \varphi_\tau}{\partial v_1}\bigg|_\beta, \ldots, \frac{\partial \varphi_\tau}{\partial v_\ell}\bigg|_\beta \right)$$

$$= \mathcal{I}(\varphi_\sigma, \varphi_\tau) .$$

In the following we use the parametrization $\varphi_{|J|} \times \mathrm{id}$ that induces the product orientation on $|J| \times \mathbb{R}$.

Definition 4.8. Let $f, g : \langle N \rangle \to \mathbb{R}^m$ be two general position maps such that $\{f(i) : i \in \langle N \rangle\} \cup \{g(i) : i \in \langle N \rangle\}$ is in general position, where $f(i) = g(j)$ is permitted only if $i = j$. Define the *deformation map*

$$h_{f,g} : \ |\mathsf{K}| \times \mathbb{R} \ \to \ \mathbb{R}^m \times \mathbb{R}$$

$$h_{f,g}(x, t) \ := \ (tf(x) + (1-t)g(x), t).$$

and the *deformation cochain* $\lambda_{f,g} \in \mathcal{C}^{m-1}(\mathsf{K}_\Delta^2)$ of f and g by

$$\lambda_{f,g}(\tau_1 \times \tau_2) \ := \ \mathcal{I}\big(h_{f,g}(|\tau_1| \times [0,1]), h_{f,g}(|\tau_2| \times [0,1])\big)$$

for $(m-1)$-cells $\tau_1 \times \tau_2 \in \mathsf{K}_\Delta^2$.

Proposition 4.9. *The cohomology class of φ_f is independent of the general position map f: For two general position maps f and g we have*

$$\delta \lambda_{f,g} \ = \ \varphi_f - \varphi_g.$$

Therefore the cohomology class $\Phi_\mathsf{K} := [\varphi_f] \in H^m(\mathsf{K}_\Delta^2; \mathbb{Z})$ is an invariant of the complex K itself.

Proof. Let $\sigma \times \tau \in \mathsf{K}_\Delta^2$, $\dim \sigma \times \tau = m$. In the following we omit the index f, g from $\lambda_{f,g}$ and $h_{f,g}$. We get the boundary of $h(\sigma \times [0,1])$ by taking the boundary first and then applying h. The intersections $h(\partial \sigma \times [0,1]) \cap h(\tau \times [0,1])$ are inner intersections. We extend the surface patch $h(\tau \times [0,1])$ to $h(\tau \times [-\varepsilon, 1+\varepsilon])$ so that the intersections $h(\sigma \times \{0\}) \cap h(\tau \times \{0\})$ and $h(\sigma \times \{1\}) \cap h(\tau \times \{1\})$ become inner intersections of $h(\partial(\sigma \times [0,1])) \cap h(\tau \times [-\varepsilon, 1+\varepsilon])$ as well but no new intersections occur. Then

$$
\begin{aligned}
\lambda(\partial \sigma \times \tau) &= \mathcal{I}\big(h(\partial \sigma \times [0,1]), h(\tau \times [0,1])\big) \\
&= \mathcal{I}\big(h(\partial \sigma \times [0,1]), h(\tau \times [-\varepsilon, 1+\varepsilon])\big) \\
&= \mathcal{I}\big(h(\partial(\sigma \times [0,1])), h(\tau \times [-\varepsilon, 1+\varepsilon])\big) \\
&\quad + (-1)^{\dim \sigma} \mathcal{I}\big(h(\sigma \times \{0\}), h(\tau \times [-\varepsilon, 1+\varepsilon])\big) \\
&\quad - (-1)^{\dim \sigma} \mathcal{I}\big(h(\sigma \times \{1\}), h(\tau \times [-\varepsilon, 1+\varepsilon])\big) \\
&= (-1)^{\dim \sigma+1} \mathcal{I}\big(h(\sigma \times [0,1]), h(\partial(\tau \times [-\varepsilon, 1+\varepsilon]))\big) \\
&\quad + (-1)^{\dim \sigma} \mathcal{I}\big(f(\sigma), f(\tau)\big) - (-1)^{\dim \sigma} \mathcal{I}\big(g(\sigma), g(\tau)\big) \\
&= (-1)^{\dim \sigma+1} \big[\mathcal{I}\big(h(\sigma \times [0,1]), h(\partial \tau \times [-\varepsilon, 1+\varepsilon])\big) \\
&\qquad\qquad + \mathcal{I}\big(h(\sigma \times [0,1]), h(\tau \times \{-\varepsilon\})\big) \\
&\qquad\qquad - \mathcal{I}\big(h(\sigma \times [0,1]), h(\tau \times \{1+\varepsilon\})\big) \big] \\
&\quad + (-1)^{\dim \sigma} \mathcal{I}\big(f(\sigma), f(\tau)\big) - (-1)^{\dim \sigma} \mathcal{I}\big(g(\sigma), g(\tau)\big) \\
&= (-1)^{\dim \sigma+1} \lambda(\sigma \times \partial \tau) + \varphi_f(\sigma \times \tau) - \varphi_g(\sigma \times \tau)
\end{aligned}
$$

$\square$

The deformation cochain has symmetries as well:

Lemma 4.10. *If $\tau_1 \times \tau_2$ is an $(m-1)$-cell of K_Δ^2 then $\tau_2 \times \tau_1$ is also an $(m-1)$-cell of K_Δ^2 and*

$$\lambda_{f,g}(\tau_1 \times \tau_2) \;\;=\;\; (-1)^{(\dim \tau_1 + 1)(\dim \tau_2 + 1)} \lambda_{f,g}(\tau_2 \times \tau_1).$$

Proof.

$$
\begin{aligned}
\lambda_{f,g}(\tau_1 \times \tau_2) &= \mathcal{I}\big(h_{f,g}(\tau_1 \times [0,1]), h_{f,g}(\tau_2 \times [0,1])\big) \\
&= (-1)^{(\dim \tau_1 + 1)(\dim \tau_2 + 1)} \mathcal{I}\big(h_{f,g}(\tau_2 \times [0,1]), h_{f,g}(\tau_1 \times [0,1])\big) \\
&= (-1)^{(\dim \tau_1 + 1)(\dim \tau_2 + 1)} \lambda_{f,g}(\tau_2 \times \tau_1)
\end{aligned}
$$

$\square$

Remark 4.11. *Intersection cocycle and deformation cochain can also be defined for* piecewise linear *general position maps maintaining the same properties [38]. So the cohomology class $\Phi_\mathsf{K} := [\varphi_f] \in H^m(\mathsf{K}_\Delta^2)$ where $f : |\mathsf{K}| \to \mathbb{R}^m$ is any piecewise linear map, only serves as an obstruction to piecewise linear embeddability. It cannot distinguish between piecewise linear embeddability and geometric realizability.*

4.4   Distinguishing between simplicial maps and PL maps

In this section, we collect properties of deformation cochains between *simplicial* maps that do notnecessarily hold for deformation cochains between arbitrary *piecewise linear* maps. The values of the intersection cocycles φ_f, φ_g and the deformation cochain $\lambda_{f,g}$ of two simplicial maps f and g depend only on the values that f and g take on the vertex set $\langle N \rangle$ of the complex in question. The complex itself determines the products $\sigma \times \tau$ on which $\lambda_{f,g}$ may be evaluated. So we examine what values these cochains take on $\mathcal{C}^{m-1}(\mathsf{S}_\Delta^2)$, where S denotes the full face lattice of the N-simplex. In Section 4.5 we derive further properties for the case that we deform into a geometric realization.

4.4.1   Linking numbers

Definition 4.12. Let x, y be simplicial cycles in $\mathbb{R}^m$, $\dim x + \dim y = m+1$, with disjoint supports. As every cycle bounds in $\mathbb{R}^m$ we find a chain γ such that $\partial \gamma = x$. The *linking number* of x and y is defined as $\mathcal{L}(x,y) := \mathcal{I}(\gamma, y)$.

Lemma 4.13. *Let σ, τ be affine simplices in $\mathbb{R}^m$. Then:*

(a) $|\mathcal{I}(\sigma, \tau)| \leq 1$ *if* $\dim \sigma + \dim \tau = m$.

(b) $|\mathcal{L}(\partial\sigma, \partial\tau)| \leq 1$ *if* $\dim \sigma = 2$ *and* $\dim \tau = m - 1$.

The next two conditions follow from the estimates in Lemma 4.13 on the intersection numbers φ_f.

Proposition 4.14. *Let f, g be two general position maps of $\langle N \rangle$ into $\mathbb{R}^m$. Then*

(a) $-1 - \varphi_g(\sigma \times \tau) \leq \delta\lambda_{f,g}(\sigma \times \tau) \leq 1 - \varphi_g(\sigma \times \tau)$
for all $\sigma \times \tau \in \mathsf{S}_\Delta^2$, $\dim \sigma + \dim \tau = m$.

(b) $-1 - \varphi_g(\sigma \times \partial\tau) \leq \lambda_{f,g}(\partial\sigma \times \partial\tau) \leq 1 - \varphi_g(\sigma \times \partial\tau)$
for all $\sigma \times \tau \in \mathsf{S}_\Delta^2$, $\dim \sigma = m - 1$ *and* $\dim \tau = 2$.

Proof. (a) As $\varphi_f(\sigma \times \tau) = (-1)^{\dim \sigma}\mathcal{I}\big(f(\sigma), f(\tau)\big)$ we can bound φ_f in Proposition 4.9 by $|\varphi_f| \leq 1$.

(b) $\varphi_f(\sigma \times \partial\tau) = (-1)^{\dim \sigma}\mathcal{I}\big(f(\sigma), f(\partial\tau)\big) = (-1)^{\dim \sigma}\mathcal{L}\big(f(\partial\sigma), f(\partial\tau)\big)$ and
$\delta\lambda_{f,g}(\sigma \times \partial\tau) = \lambda_{f,g}(\partial\sigma \times \partial\tau)$.

$\square$

4.4.2 Deforming simplices

4.4.2.1 The simplest case

For the following, homotopies between images of a simplicial complex under different general position maps play a crucial rôle. In this section we look at the simplest case: The homotopy from the standard simplex of $\mathbb{R}^m$ to an arbitrary one.

Let $D \in \mathbb{R}^{m \times m}$ be an arbitrary matrix with columns d_i, $i \in [m]$ and set $d_0 := 0$. Associate with D the map

$$h : \mathbb{R}^{m+1} \to \mathbb{R}^{m+1}, h(x, t) := ((tD + (1 - t)E_m)x, t).$$

Then for every subset $I \subset \langle m \rangle$ the map $h|_{\Delta_I \times [0,1]}$ represents the homotopy of Δ_I into $\text{conv}\{d_i \mid i \in I\}$, moving all points along straight line segments to corresponding points, i.e. it is a ruled m-dimensional surface.
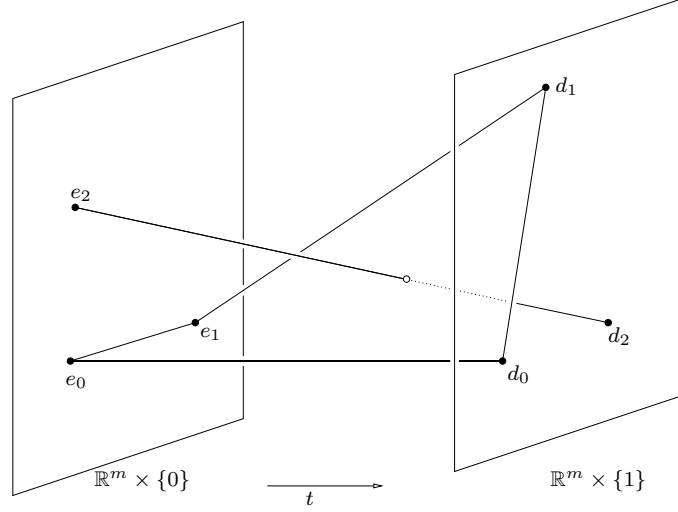
Figure 4.1: Intersecting surfaces $h(\Delta_{I_+} \times \mathbb{R})$ and $h(\Delta_{I_-} \times \mathbb{R})$ for the matrix (d_1, d_2) and the partition $I_+ = \{0,1\}$ and $I_- = \{2\}$

Definition 4.15. We call an eigenvalue of a square matrix *general* if it is simple, its eigenvector v has no vanishing components, and $\sum v_i \neq 0$.

This technical condition characterizes the situation where all pairs of ruled surfaces defined by disjoint subsets of the vertex set are transversal.

We begin by characterizing intersection points of pairs of surfaces in terms of eigenvalues of D.

Lemma 4.16. *Let $D \in \mathbb{R}^{m \times m}$ and $h : \mathbb{R}^{m+1} \to \mathbb{R}^{m+1}$ its associated map.*

(a) *Let $I_+, I_- \subset \langle m \rangle$ such that $I_+ \cap I_- = \emptyset$. If the surfaces $h(\Delta_{I_+} \times \mathbb{R})$ and $h(\Delta_{I_-} \times \mathbb{R})$ intersect at time t, then $1 - \frac{1}{t}$ is an eigenvalue of D.*

(b) *Let $u \neq 1$ be a general eigenvalue of D. Then u uniquely determines disjoint subsets I_+^u and $I_-^u \subset \langle m \rangle$ with $0 \in I_+^u$ such that $h(\Delta_{I_+^u} \times \mathbb{R})$ and $h(\Delta_{I_-^u} \times \mathbb{R})$ intersect at time*

$$t = \tfrac{1}{1-u}.$$

Another point of view: If $u \neq 1$ is an eigenvalue of D then $h(\Delta_{\langle m \rangle} \times \{t\})$ fails to span $\mathbb{R}^m \times \{t\}$. So we get a Radon partition in some lower dimensional subspace of $\mathbb{R}^m \times \{t\}$. If the eigenvector is general then we get a unique Radon partition.

Proof. (a) Let $(p,t) \in h(\Delta_{I_+} \times \mathbb{R}) \cap h(\Delta_{I_-} \times \mathbb{R})$ be an intersection point. Then p has the representation

$$p \ = \ h(\alpha, t) = h(\beta, t),$$

that is,

$$p \ = \ \sum_{i \in I_+} \alpha_i (td_i + (1-t)e_i) \ = \ \sum_{j \in I_-} \beta_j (td_j + (1-t)e_j)$$

with

$$\sum_{i \in I_+} \alpha_i = \sum_{j \in I_-} \beta_j = 1,$$

$\alpha_i, \beta_j > 0$ for all $i \in I_+$, $j \in I_-$. Because of $t \neq 0$ and $e_0 = d_0 = 0$ we can rewrite this as

$$t \left(\sum_{i \in I_+} \alpha_i \big(d_i - (1 - \tfrac{1}{t})e_i\big) + \sum_{j \in I_-} (-\beta_j)\big(d_j - (1 - \tfrac{1}{t})e_j\big) \right) \ = \ 0$$

Therefore $\sum_{i \in I_+} \alpha_i e_i + \sum_{j \in I_-} (-\beta_j)e_j$ is an eigenvector of D with eigenvalue $1 - \tfrac{1}{t}$.

(b) Let $u \neq 1$ be a general eigenvalue of D and v its eigenvector. Consider the sets $\tilde{I}_+^u := \{i \in [m] \mid v_i > 0\}$ and $I_-^u := \{i \in [m] \mid v_i < 0\}$ of positive and negative coefficients respectively. Without loss of generality assume that $V := -\sum_{i \in I_-^u} v_i > \sum_{i \in \tilde{I}_+^u} v_i$. Denote $I_+^u := \tilde{I}_+^u \cup \{0\}$, $\alpha_i := \frac{v_i}{V}$ for $i \in \tilde{I}_+^u$ and $\alpha_0 := 1 - \sum_{i \in \tilde{I}_+^u} \alpha_i$, $\beta_j := -\frac{v_j}{V}$ for $j \in I_-$ and $t := \frac{1}{1-u}$. Then (p,t) with

$$p \ = \ \sum_{i \in I_+^u} \alpha_i (td_i + (1-t)e_i) \ = \ \sum_{j \in I_-^u} \beta_j (td_j + (1-t)e_j)$$

is an intersection point of the two simplices $h(\Delta_{I_+^u} \times \{t\})$ and $h(\Delta_{I_-^u} \times \{t\})$. So the surfaces $h(\Delta_{I_+^u} \times \mathbb{R})$ and $h(\Delta_{I_-^u} \times \mathbb{R})$ intersect at time t.

$\square$

Remark 4.17. *If $u = 1$ is a general eigenvalue we can still find the sets I_+^u and I_-^u. Then the surfaces $h(\Delta_{I_+^u} \times \mathbb{R})$ and $h(\Delta_{I_-^u} \times \mathbb{R})$ have parallel ends. This complements the preceding lemma because they then 'meet at time $t = \infty$'.*

Denote by

$$\mathcal{P} := \{\{I_+, I_-\} \mid I_+ \cup I_- = \langle m \rangle, I_+ \cap I_- = \emptyset, 0 \in I_+\}$$

the set of all bipartitions of $\langle m \rangle$.

Corollary 4.18. *Let $D \in \mathbb{R}^{m \times m}$ and ℓ be the multiplicity of the eigenvalue 1 of D.*
Then

$$\sum_{\{I_+, I_-\} \in \mathcal{P}} \# \left(h(\Delta_{I_+} \times \mathbb{R}) \cap h(\Delta_{I_-} \times \mathbb{R}) \right) \quad \leq \quad m - \ell \ ,$$

that is, the total number of intersection points of pairs of surfaces of the form $h(\Delta_I \times \mathbb{R})$ and $h(\Delta_{\langle m \rangle \setminus I} \times \mathbb{R})$ can not exceed $m - \ell$.

Now we calculate intersection numbers of the surfaces found in Lemma 4.16. To this end we impose orientations on the surfaces in question. In the following let $h(\Delta_I \times \mathbb{R})$ carry the orientation induced by the parametrization $\psi := h \circ (\varphi_I \times \mathrm{id})$. Further let $I_+^u = \{i_0, \ldots, i_k\}_<$, $I_-^u = \{i_{k+1}, \ldots, i_m\}_<$ with $i_0 = 0$ and denote by (I_+^u, I_-^u) the 'shuffle' permutation $(i_0, \ldots, i_m) \mapsto (0, \ldots, m)$..

Lemma 4.19. *Let $D \in \mathbb{R}^{m \times m}$ and $u = 1 - \frac{1}{t}$ be an eigenvalue of D. Denote by (p, t) the intersection point of the surfaces $h(\Delta_{I_+^u} \times \mathbb{R})$ and $h(\Delta_{I_-^u} \times \mathbb{R})$. The surfaces intersect transversally and (p, t) is an inner point if and only if u is general. In this case we have*

$$\mathcal{I}\left(h(\Delta_{I_+^u} \times \mathbb{R}), h(\Delta_{I_-^u} \times \mathbb{R}) \right)\Big|_{(p,t)} = \mathrm{sgn}(I_+^u, I_-^u)\, \mathrm{sgn}(t^m \chi_D'(u)),$$

where χ_D' is the derivative of the characteristic polynomial $\chi_D(u) = \det(D - u E_m)$ of D.

Proof. Our calculations differ in so far from those of Novik in [29, Proof of Lemma 3.2] as we have to deal with the permutation $(I_+^u, I_-^u) : j \mapsto i_j$. Denote the intersection point of the surfaces in question by (p, t) where

$$p \quad = \quad t \sum_{j=0}^{k} \alpha_{i_j} d_{i_j}^u = t \sum_{j=k+1}^{m} \beta_{i_j} d_{i_j}^u \tag{4.3}$$

with $d_i^u := d_i - u e_i$.

For checking transversality as well as for the index of intersection at (p, t) we examine

$$\mathcal{D} := \det\left(\left(\frac{\partial \psi_+}{\partial \xi_1} \right), \ldots, \left(\frac{\partial \psi_+}{\partial \xi_k} \right), \left(\frac{\partial \psi_+}{\partial t} \right), \left(\frac{\partial \psi_-}{\partial \xi_1} \right), \ldots, \left(\frac{\partial \psi_-}{\partial \xi_{m-k}} \right), \left(\frac{\partial \psi_-}{\partial t} \right) \right),$$

where the first k derivatives are calculated at $(\alpha_{i_1}, \ldots, \alpha_{i_k}, t)$ and the last $m - k$ at $(\beta_{i_{k+2}}, \ldots, \beta_{i_m}, t)$. We therefore get

$$\mathcal{D} = \det\left(t\begin{pmatrix} d_{i_1}^u \\ 0 \end{pmatrix}, \ldots, t\begin{pmatrix} d_{i_k}^u \\ 0 \end{pmatrix}, \begin{pmatrix} \sum_{j=1}^{k} \alpha_{i_j}(d_{i_j} - e_{i_j}) \\ 1 \end{pmatrix}, \right.$$
$$\left. t\begin{pmatrix} d_{i_{k+2}}^u - d_{i_{k+1}}^u \\ 0 \end{pmatrix}, \ldots, t\begin{pmatrix} d_{i_m}^u - d_{i_{k+1}}^u \\ 0 \end{pmatrix}, \begin{pmatrix} \sum_{j=k+1}^{m} \beta_{i_j}(d_{i_j} - e_{i_j}) \\ 1 \end{pmatrix} \right).$$

With $i_0 = 0$, $d_0 = e_0 = 0$ we have

$$\begin{pmatrix} \sum_{j=1}^{k} \alpha_{i_j}(d_{i_j} - e_{i_j}) \\ 1 \end{pmatrix} - \begin{pmatrix} \sum_{j=k+1}^{m} \beta_{i_j}(d_{i_j} - e_{i_j}) \\ 1 \end{pmatrix} = \tfrac{1}{t} v \ ,$$

as $v = \sum_{j=1}^{k} \alpha_{i_j} e_{i_j} - \sum_{j=k+1}^{m} \beta_{i_j} e_{i_j}$ is also an eigenvector of $D - E$ with eigenvalue $\frac{1}{t}$. Subtracting the last column from the $(k + 1)$st and using Laplace expansion with respect to the last row we get

$$\mathcal{D} = t^{m-2} \det(d_{i_1}^u, \ldots, d_{i_k}^u, v, d_{i_{k+2}}^u - d_{i_{k+1}}^u, \ldots, d_{i_m}^u - d_{i_{k+1}}^u)$$
$$= t^{m-2} \sum_{j=1}^{m} v_j \det(d_{i_1}^u, \ldots, d_{i_k}^u, e_j, d_{i_{k+2}}^u - d_{i_{k+1}}^u, \ldots, d_{i_m}^u - d_{i_{k+1}}^u) \qquad (4.4)$$

From (4.3) we have

$$0 = \sum_{j=1}^{k} \alpha_{i_j} d_{i_j}^u - d_{i_{k+1}}^u - \sum_{j=k+2}^{m} \beta_{i_j}(d_{i_j}^u - d_{i_{k+1}}^u) \ .$$

Now we examine the summands of the last expression of $\mathcal{D}$ in three groups. In the first case, $j < k + 1$, we have $v_{i_j} = \alpha_{i_j}$. We substitute $\alpha_{i_j} d_{i_j}^u$, cancel all terms except $d_{i_{k+1}}^u$ and exchange $d_{i_{k+1}}^u$ and e_{i_j}:

$$\alpha_{i_j} \det(d_{i_1}^u, \ldots, d_{i_k}^u, e_{i_j}, d_{i_{k+2}}^u - d_{i_{k+1}}^u, \ldots, d_{i_m}^u - d_{i_{k+1}}^u)$$
$$= \det(d_{i_1}^u, \ldots, \alpha_{i_j} d_{i_j}^u, \ldots, d_{i_k}^u, e_{i_j}, d_{i_{k+2}}^u - d_{i_{k+1}}^u, \ldots, d_{i_m}^u - d_{i_{k+1}}^u)$$
$$= \det(d_{i_1}^u, \ldots, d_{i_{k+1}}^u, \ldots, d_{i_k}^u, e_{i_j}, d_{i_{k+2}}^u - d_{i_{k+1}}^u, \ldots, d_{i_m}^u - d_{i_{k+1}}^u)$$
$$= -\det(d_{i_1}^u, \ldots, e_{i_j}, \ldots, d_{i_m}^u) \ .$$

By an analogous calculation the second case, $j > k + 1$, yields

$$-\beta_{i_j} \det(d_{i_1}^u, \ldots, d_{i_k}^u, e_{i_j}, d_{i_{k+2}}^u - d_{i_{k+1}}^u, \ldots, d_{i_m}^u - d_{i_{k+1}}^u)$$
$$= -\det(d_{i_1}^u, \ldots, e_{i_j}, \ldots, d_{i_m}^u) \ .$$

For the remaining term, $j = k$, we use the same procedure on each of the summands after the first step and evaluate the telescope sum in the last step. Thus we get:

$$
\begin{aligned}
&- \beta_{i_{k+1}} \det(d_{i_1}^u, \ldots, d_{i_k}^u, e_{i_{k+1}}, d_{i_{k+2}}^u - d_{i_{k+1}}^u, \ldots, d_{i_m}^u - d_{i_{k+1}}^u) \\
&= - \det(d_{i_1}^u, \ldots, d_{i_k}^u, e_{i_{k+1}}, d_{i_{k+2}}^u - d_{i_{k+1}}^u, \ldots, d_{i_m}^u - d_{i_{k+1}}^u) \\
&\qquad + \sum_{j=k+2}^m \det(d_{i_1}^u, \ldots, d_{i_k}^u, e_{i_{k+1}}, d_{i_{k+2}}^u - d_{i_{k+1}}^u, \ldots, \beta_{i_j}(d_{i_j}^u - d_{i_{k+1}}^u), \ldots, d_{i_m}^u - d_{i_{k+1}}^u) \\
&= - \det(d_{i_1}^u, \ldots, d_{i_k}^u, e_{i_{k+1}}, d_{i_{k+2}}^u - d_{i_{k+1}}^u, \ldots, d_{i_m}^u - d_{i_{k+1}}^u) \\
&\qquad + \sum_{j=k+2}^m \det(d_{i_1}^u, \ldots, d_{i_k}^u, e_{i_{k+1}}, d_{i_{k+2}}^u - d_{i_{k+1}}^u, \ldots, -d_{i_{k+1}}^u, \ldots, d_{i_m}^u - d_{i_{k+1}}^u) \\
&= - \det(d_{i_1}^u, \ldots, d_{i_k}^u, e_{i_{k+1}}, d_{i_{k+2}}^u - d_{i_{k+1}}^u, \ldots, d_{i_m}^u - d_{i_{k+1}}^u) \\
&\qquad - \sum_{j=k+2}^m \det(d_{i_1}^u, \ldots, d_{i_k}^u, e_{i_{k+1}}, d_{i_{k+2}}^u, \ldots, d_{i_{j-1}}^u, d_{i_{k+1}}^u, d_{i_{j+1}}^u - d_{i_{k+1}}^u \ldots, d_{i_m}^u - d_{i_{k+1}}^u) \\
&= - \det(d_{i_1}^u, \ldots, d_{i_k}^u, e_{i_{k+1}}, d_{i_{k+2}}^u, , \ldots, d_{i_m}^u) \ .
\end{aligned}
$$

So in every single case we have

$$
v_{i_j} \det(d_{i_1}^u, \ldots, d_{i_k}^u, e_{i_j}, d_{i_{k+2}}^u - d_{i_{k+1}}^u, \ldots, d_{i_m}^u - d_{i_{k+1}}^u) = - \det(d_{i_1}^u, \ldots, e_{i_j}, \ldots, d_{i_m}^u) \ .
$$

To complete the calculation we insert these results into (4.4):

$$
\begin{aligned}
\mathcal{D} &= -t^{m-2} \sum_{j=1}^m \det(d_{i_1}^u, \ldots, e_{i_j}, \ldots, d_{i_m}^u) \\
&= \operatorname{sgn}(I_+^u, I_-^u) t^{m-2} \sum_{j=1}^m \det(d_1^u, \ldots, -e_j, \ldots, d_m^u) \\
&= \operatorname{sgn}(I_+^u, I_-^u) t^{m-2} \chi_D'(u).
\end{aligned}
$$

We have $\chi'(u) \neq 0$ since u is simple. Therefore the intersection is transversal and the index of intersection at the point under consideration is $\operatorname{sgn} \mathcal{D}$.. $\quad \square$

Corollary 4.20. *Let D be nonsingular, all its negative eigenvalues be general and ℓ_- the number of negative eigenvalues. Denote $\tilde{h}(J) := h(\Delta_J \times [0,1])$. Then we have*

$$
\sum_{\{I_+, I_-\} \in \mathcal{P}} \operatorname{sgn}(I_+, I_-) \ \mathcal{I}\big(\tilde{h}(I_+), \tilde{h}(I_-)\big) \quad = \quad \begin{cases} 0 & \text{if } \det D > 0 \ , \\ -1 & \text{if } \det D < 0 \ . \end{cases} \quad (4.5)
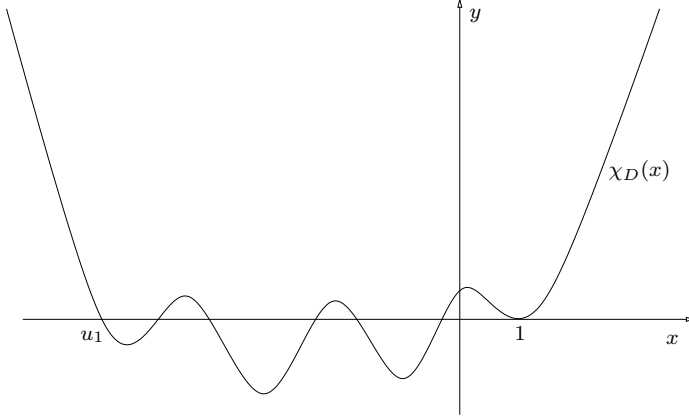$$

Figure 4.2: A characteristic polynomial with simple negative roots

For every subset $S \subset \mathcal{P}$ we have

$$-\left\lceil \frac{\ell_-}{2} \right\rceil \quad \leq \quad \sum_{\{I_+, I_-\} \in S} \mathrm{sgn}(I_+, I_-)\, \mathcal{I}\big(\tilde{h}(I_+), \tilde{h}(I_-)\big) \quad \leq \quad \left\lfloor \frac{\ell_-}{2} \right\rfloor \ . \tag{4.6}$$

As a special case we have for every individual pair $\{I_+, I_-\} \in \mathcal{P}$ the estimates

$$-\left\lceil \frac{\ell_-}{2} \right\rceil \quad \leq \quad \mathrm{sgn}(I_+, I_-)\, \mathcal{I}\big(\tilde{h}(I_+), \tilde{h}(I_-)\big) \quad \leq \quad \left\lfloor \frac{\ell_-}{2} \right\rfloor \ . \tag{4.7}$$

Proof. Intersection times $t \in [0, 1]$ correspond to eigenvalues $u < 0$ of D. The first root u_1 of χ_D satisfies $\chi'_D(u_1) < 0$ and two consecutive roots $u, \hat{u}$ of χ_D satisfy $\mathrm{sgn}\,\chi'_D(u) = -\mathrm{sgn}\,\chi'_D(\hat{u})$. So χ_D has at most $\left\lceil \frac{\ell_-}{2} \right\rceil$ negative roots u with $\chi'_D(u) < 0$ and at most $\left\lfloor \frac{\ell_-}{2} \right\rfloor$ negative roots $\tilde{u}$ with $\chi'_D(\tilde{u}) > 0$. These are exactly the terms in the sums above.

$\square$

4.4.2.2   Application to the deformation cochain

The relations between coefficients of λ we develop here are local in the sense that we only look at few vertices at the same time. We restrict to subcomplexes of S consisting of $m + 1$ points. For a subset $J := \{j_0, \ldots j_m\}_< \subset [N]$ and $k \in \mathbb{N}$ denote $\ell^k_J := \#\big((J \setminus \{j_0\}) \cap [k]\big)$ and

$$\mathcal{P}_J := \{\tau_+ \times \tau_- \in \mathsf{S}^2_\Delta \mid \dim(\tau_+ \times \tau_-) = m - 1, \tau_+ \cup \tau_- = J, j_0 \in \tau_+\}.$$

These are the products of simplices with vertices in J that we may insert into the deformation cochain.

Theorem 4.21 (Related coefficients of the deformation cochain). *Let f and g be general position maps of the vertex set $\langle N \rangle$ of S into $\mathbb{R}^m$ and $k \in \langle N \rangle$. Assume further that $f(i) = g(i)$ for $i \in \langle k \rangle$ and that the set $\{f(0), \ldots, f(N), g(k+1), \ldots, g(N)\}$ is in general position.*

For every subset $J \subset \langle N \rangle$ with $|J| = m + 1$ denote by $\varepsilon_g(J)$ the orientation of the simplex $g(J)$. Then the deformation cochain $\lambda_{f,g} \in \mathcal{C}^{m-1}(\mathsf{S}^2_\Delta)$ has the following properties:

$$\sum_{\tau_+ \times \tau_- \in \mathcal{P}_J} |\lambda_{f,g}(\tau_+ \times \tau_-)| \quad \leq \quad m - \ell_J^k, \tag{4.8}$$

$$-1 \quad \leq \quad \varepsilon_g(J) \sum_{\tau_+ \times \tau_- \in \mathcal{P}_J} \mathrm{sgn}(\tau_+, \tau_-) \lambda_{f,g}(\tau_+ \times \tau_-) \quad \leq \quad 0, \tag{4.9}$$

and

$$-\left\lceil \frac{m - \ell_J^k}{2} \right\rceil \quad \leq \quad \varepsilon_g(J) \, \mathrm{sgn}(\tau_+, \tau_-) \lambda_{f,g}(\tau_+ \times \tau_-) \quad \leq \quad \left\lfloor \frac{m - \ell_J^k}{2} \right\rfloor \tag{4.10}$$

for every $\tau_+ \times \tau_- \in \mathcal{P}_J$.

Proof. Fix a subset $J := \{j_0, \ldots j_m\}_< \subset \langle N \rangle$. Perform a basis transformation A_J that takes $(g(j_0), 0), \ldots, (g(j_m), 0), (f(j_0), 1)$ to $e_0, \ldots, e_{m+1}$ respectively. $\varepsilon_g(J)$ is the sign of the determinant of this basis transformation. Let $(d_1, 1), \ldots, (d_m, 1)$ be the images of $(f(j_1), 1), \ldots, (f(j_m), 1)$ and $D := (d_1, \ldots, d_m)$. Denote $j : [m] \to J$, $i \mapsto j_i$. Then $h := A_J \circ h_{f,g} \circ j$ is of the form we considered in Subsection 4.4.2.1. Moreover the first ℓ_J^k columns of D are $e_1, \ldots, e_{\ell_J^k}$. The eigenvalue 1 has at least multiplicity ℓ_J^k. Thus $m - \ell_J^k$ is a upper bound for the number of negative eigenvalues. Now

$$\lambda_{f,g}(\tau_+ \times \tau_-) = \mathcal{I}\big(h_{f,g}(\tau_+ \times [0,1]), h_{f,g}(\tau_- \times [0,1])\big)$$
$$= \varepsilon_g(J) \mathcal{I}\big(h(j^{-1}(\tau_+) \times [0,1]), h(j^{-1}(\tau_-) \times [0,1])\big)$$

and therefore

$$|\lambda_{f,g}(\tau_+ \times \tau_-)| \quad \leq \quad \#\big(h(j^{-1}(\tau_+) \times [0,1] \cap h(j^{-1}(\tau_-) \times [0,1])\big)$$

So we immediately get equation (4.8) from Corollary 4.18 and equations (4.9) and (4.10) from Corollary 4.20. □

Remark 4.22. *Condition (4.10) implies*

$$-\left\lceil \frac{m}{2} \right\rceil \quad \leq \quad \lambda_{f,g}(\tau_+ \times \tau_-) \quad \leq \quad \left\lceil \frac{m}{2} \right\rceil$$

which are the restrictions on the values of $\lambda_{f,g}$ that Novik derived (cf. [29, Theorem 3.1]).

4.5 Geometric realizability and beyond

Up to now we have looked at arbitrary general position maps. In this section we compare a map with special properties such as a geometric realization with a reference map whose intersection cocycle can be easily computed.

4.5.1 The reference map

We start by defining our reference map:

Denote by $c : \langle N \rangle \to \mathbb{R}^m$ the *cyclic map* which maps vertex i to the point $c(i) = (i, i^2, \ldots i^m)^t$ on the moment curve.

Proposition 4.23 ([35, Lemma 4.2])**.** *Let $k + \ell = m$, $k \geq \ell$, $s_0 < s_1 < \ldots < s_k$, $t_0 < t_1 < \ldots < t_\ell$. If $k = \ell$ assume further that $s_0 < t_0$. The two simplices $\sigma = \mathrm{conv}\{c(s_0), \ldots, c(s_k)\}$ and $\tau = \mathrm{conv}\{c(t_0), \ldots, c(t_\ell)\}$ of complementary dimensions intersect if and only if their dimensions differ at most by one and their vertices alternate along the curve:*

$$k = \left\lceil \frac{m}{2} \right\rceil \qquad and \qquad s_0 < t_0 < s_1 < \ldots < s_{\lfloor \frac{m}{2} \rfloor} < t_{\lfloor \frac{m}{2} \rfloor} (< s_{\lceil \frac{m}{2} \rceil})$$

In the case of intersection we have

$$\mathcal{I}(\sigma, \tau) = (-1)^{\frac{(k-1)k}{2}}.$$

Proof. For every set $\{c_0, \ldots, c_{m+1}\}$ consisting of $m + 2$ points $c_i = c(u_i)$ with $u_0 < u_1 < \ldots < u_{m+1}$ there is a unique affine dependence

$$\sum_{i=0}^{m+1} \alpha_i c_i = 0 \qquad \text{with} \qquad \sum_{i=0}^{m+1} \alpha_i = 0 \text{ and } \alpha_0 = 1.$$

We calculate the sign of the coefficients α_k.

$$\det\left(\binom{1}{c_0}, \ldots, \widehat{\binom{1}{c_k}}, \ldots, \binom{1}{c_{m+1}} \right) = -\alpha_k \det\left(\binom{1}{c_k}, \binom{1}{c_1}, \ldots, \widehat{\binom{1}{c_k}}, \ldots, \binom{1}{c_{m+1}} \right)$$

$$= (-1)^k \alpha_k \det\left(\binom{1}{c_1}, \ldots, \binom{1}{c_{m+1}} \right)$$

Since $\det\left(\binom{1}{c_0}, \ldots, \widehat{\binom{1}{c_k}}, \ldots, \binom{1}{c_{m+1}} \right)$ and $\det\left(\binom{1}{c_1}, \ldots, \binom{1}{c_{m+1}} \right)$ are both positive we get

$$(-1)^k \alpha_k > 0,$$

that is,

$$\mathrm{sgn}\ \alpha_k = \begin{cases} +1 & \text{if } k \text{ is even} \\ -1 & \text{if } k \text{ is odd.} \end{cases}$$

The proposition follows. $\square$

4.5.2   DEFORMATION COCHAINS OF GEOMETRIC REALIZATIONS

If a simplicial maps defining the deformation cochain is a simplicial *embedding*, we know, that the images of certain simplices don't intersect. The following trivial observation about the coefficients of deformation cochains is the key to bring in the combinatorics of the complex K.

Lemma 4.24. *Let $f, g : \langle N \rangle \to \mathbb{R}^m$ be general position maps.*
If $f(\sigma) \cap f(\tau) = \emptyset$ and $\dim \sigma + \dim \tau = m$ then

$$\delta\lambda_{f,g}(\sigma \times \tau) \;\; = \;\; -\varphi_g(\sigma \times \tau) \; .$$

Proof. $\varphi_f(\sigma \times \tau) = (-1)^{\dim \sigma} \mathcal{I}\big(f(\sigma), f(\tau)\big) = 0.$ $\square$

Remark 4.25. *The expression*

$$\delta\lambda(\sigma \times \tau) \;\; = \;\; \sum_{i=0}^{\dim \sigma}(-1)^i \lambda(\sigma^i \times \tau) + \sum_{j=0}^{\dim \tau}(-1)^{\dim \sigma + j}\lambda(\sigma \times \tau^j)$$

is linear in the coefficients of the deformation cochain λ. So for every pair $\sigma \times \tau$ of simplices of complementary dimensions with disjoint images we get a linear equation that is valid for the coefficients of $\lambda_{f,g}$.

This is particularly useful when we assume the existence of a geometric realization but can also be used to express geometric immersability. So we gather all information we have on the deformation cochain in our main Theorem:

Theorem 4.26 (Obstruction Polytope)**.** *If there is a geometric realization of the simplicial complex K in $\mathbb{R}^m$ then the obstruction polytope in the cochain space $\mathcal{C}^{m-1}(\mathsf{S}_\Delta^2, \mathbb{R})$ given by the following inequalities contains a point $\lambda \in \mathcal{C}^{m-1}(\mathsf{S}_\Delta^2, \mathbb{Z})$ with integer coefficients.*

1. (The symmetries of Lemma 4.10)

$$\lambda(\tau_1 \times \tau_2) = (-1)^{(\dim \tau_1 + 1)(\dim \tau_2 + 1)}\lambda(\tau_2 \times \tau_1)$$

   for all $\tau_1 \times \tau_2 \in \mathsf{S}_\Delta^2$,

2. (The deformation inequalities of Theorem 4.21) *For every subset $J \subset \langle N \rangle$*

   (a)

$$\sum_{\tau_+ \times \tau_- \in \mathcal{P}_J} |\lambda(\tau_+ \times \tau_-)| \;\; \leq \;\; m - \ell_J^m,$$

(b)
$$-1 \quad \leq \quad \sum_{\tau_+ \times \tau_- \in \mathcal{P}_J} \mathrm{sgn}(\tau_+, \tau_-)\lambda(\tau_+ \times \tau_-) \quad \leq \quad 0,$$

and for every $\tau_+ \times \tau_- \in \mathcal{P}_J$

(c)
$$-\left\lceil \frac{m - \ell_J^m}{2} \right\rceil \quad \leq \quad \mathrm{sgn}(\tau_+, \tau_-)\lambda(\tau_+ \times \tau_-) \quad \leq \quad \left\lfloor \frac{m - \ell_J^m}{2} \right\rfloor,$$

3. (The intersection and linking inequalities of Proposition 4.14)

(a) $\varphi_c(\sigma \times \tau) - 1 \quad \leq \quad \delta\lambda(\sigma \times \tau) \quad \leq \quad \varphi_c(\sigma \times \tau) + 1$
for all $\sigma \times \tau \in \mathsf{S}_\Delta^2$, $\dim \sigma + \dim \tau = m$,

(b) $\varphi_c(\sigma \times \partial\tau) - 1 \quad \leq \quad \lambda(\partial\sigma \times \partial\tau) \quad \leq \quad \varphi_c(\sigma \times \partial\tau) + 1$
for all $\sigma \times \tau \in \mathsf{S}_\Delta^2$, $\dim \sigma = m - 1$ and $\dim \tau = 2$,

4. (The equations of Lemma 4.24) *For every pair $\sigma \times \tau$ of simplices in K_Δ^2:*
$$\delta\lambda(\sigma \times \tau) \quad = \quad -\varphi_c(\sigma \times \tau)$$

Proof. If there is a geometric realization $f : \langle N \rangle \to \mathbb{R}^m$ then there also is a geometric realization $\tilde{f}$ such that the first m vertices satisfy $\tilde{f}(i) = c(i)$ for $i \in \langle m \rangle$ and such that the set $\{\tilde{f}(0), \ldots, \tilde{f}(N), c(m+1), \ldots, c(N)\}$ is in general position. The deformation cochain $\lambda_{c,\tilde{f}}$ has the desired properties as $\varepsilon_c \equiv 1$. $\qquad\square$

Remark 4.27. *The system Novik described consists of the equations 4 along with the equations 1 and the bounds from Remark 4.22 for pairs of simplices in K_Δ^2 only.*

4.6 Subsystems and experiments

Theorem 4.26 provides us with a system of linear equations and inequalities that has an integer solution if the complex K has a geometric realization. So we can attack non-realizability proofs by solving integer programming feasibility problems. However the system sizes grow rapidly with the number of vertices. There are $\mathcal{O}(n^{m+1})$ variables in the system associated to a complex with n vertices and target ambient dimension m. For Brehm's triangulated Möbius strip (and all other complexes on 9 vertices) we already get 1764 variables. The integer feasibility problems — even for complexes with few vertices — are therefore much too big to be sucessfully solved with standard integer programming software.[1] On the other hand for a non-realizability

---

[1]at the time of the research done in 2005 for the original article of 2008

proof it suffices to exhibit a subsystem of the obstruction system that has no solution.

In this section we therefore look at subsystems of the obstruction system, that only use those variables associated to simplices that belong to the complex K and certain sums of the other variables.

Subsystem 4.28. *If there is a geometric realization of the simplicial complex* K *in* $\mathbb{R}^m$ *then there is a cochain* $\lambda \in \mathcal{C}^{m-1}(\mathsf{K}_\Delta^2)$ *that satisfies the equations of Lemma 4.24 for every pair of simplices in* K_Δ^2 *and the linking inequalities* (3b) *of Proposition 4.14 that only use values of* λ *on* K_Δ^2.

The deformation inequalities of Theorem 4.21 imply the following for the variables under consideration: For every subset $J \subset \langle N \rangle$ *we have*

$$\sum_{\tau_+ \times \tau_- \in \mathcal{P}_J \cap \mathsf{K}_\Delta^2} |\lambda(\tau_+ \times \tau_-)| + |y_J| \quad \leq \quad m - \ell_J^m, \tag{4.11}$$

$$-1 \quad \leq \quad \sum_{\tau_+ \times \tau_- \in \mathcal{P}_J \cap \mathsf{K}_\Delta^2} \mathrm{sgn}(\tau_+, \tau_-)\lambda(\tau_+ \times \tau_-) + y_J \quad \leq \quad 0 \tag{4.12}$$

by introducing the new variable y_J *for 'the rest of the sum'. We still have for every* $\tau_+ \times \tau_- \in \mathsf{K}_\Delta^2$

$$-\left\lceil \frac{m - \ell_J^m}{2} \right\rceil \quad \leq \quad \mathrm{sgn}(\tau_+, \tau_-)\lambda_{f,g}(\tau_+ \times \tau_-) \quad \leq \quad \left\lfloor \frac{m - \ell_J^m}{2} \right\rfloor. \tag{4.13}$$

and the same bounds hold for y_J.

We can even do with less variables at the expense of more inequalities.

Subsystem 4.29. *If there is a geometric realization of the simplicial complex* K *in* $\mathbb{R}^m$ *then there is a cochain* $\lambda \in \mathcal{C}^{m-1}(\mathsf{K}_\Delta^2)$ *that satisfies the equations of Lemma 4.24 for every pair of simplices in* K_Δ^2 *and the linking inequalities* (3b) *of Proposition 4.14 that only use values of* λ *on* K_Δ^2. *The deformation inequalities of Theorem 4.21 imply inequalities for every subset* S *of* $\mathcal{P}_J \cap \mathsf{K}_\Delta^2$.

$$-\left\lceil \frac{m - \ell_J^m}{2} \right\rceil \quad \leq \quad \sum_{\tau_+ \times \tau_- \in S} \mathrm{sgn}(\tau_+, \tau_-)\lambda_{f,g}(\tau_+ \times \tau_-) \quad \leq \quad \left\lfloor \frac{m - \ell_J^m}{2} \right\rfloor. \tag{4.14}$$

and

$$\sum_{\tau_+ \times \tau_- \in \mathcal{P}_J \cap \mathsf{K}_\Delta^2} |\lambda(\tau_+ \times \tau_-)| \quad \leq \quad m - \ell_J^m, \tag{4.15}$$

surface	file	realizable	f-vector	var.	constr.	solv.	time
$\mathbb{R}P^2$	rp2.gap	no	(6, 15, 10)	150	1365	no	0.24 sec
$\mathcal{B}$	moebius.gap	no [11]	(9, 24, 15)	510	2262	no	46.3 sec
$\mathcal{M}_0$	bipyramid.gap	yes	(5, 9, 6)	48	500	yes	0.1 sec
$\mathcal{M}_1$	csaszar.gap	yes	(7, 21, 14)	322	2583	yes	0.78 sec
$\mathcal{M}_2$	m2_10.gap	yes [24]	(10, 36, 24)	1136	5888	yes	34.83 sec
$\mathcal{M}_3$	m3_10.gap	yes [19]	(10, 42, 28)	1490	9847	yes	143 sec
$\mathcal{M}_4$	m4_11.gap	yes [8]	(11, 51, 34)	2248	15234	yes	564 min
$\mathcal{M}_5$	m5_12.gap	?	(12, 60, 40)	3180	21840	?	
$\mathcal{M}_6$	altshuler54.gap	no [9]	(12, 66, 44)	3762	33473	?	

Table 4.1: Computational results

I wrote a GAP program to generate the systems of the above Corollaries. The resulting systems can be examined further by integer programming software. I ran several experiments using SCIP [1] to examine the resulting systems. Table 4.1 gives an overview on system sizes and solution times. $\mathcal{M}_g$ denotes an orientable surface of genus g. The triangulations under consideration have the minimum number of vertices and can be found in the file. $\mathcal{B}$ denotes the triangulated Möbius strip [11] by Brehm. The systems under consideration are those of Subsystem 4.29 expressing the inequalities involving absolute values without the use of new variables.

The smallest system showing the non-realizability of the Möbius strip only uses the parts 1, 2c, 3b and 4 of Theorem 4.26 and has 510 variables and 426 constraints. The systems for genus 5 and 6 using only these parts of Theorem 4.26 are solvable.

Bibliography

[1] T. Achterberg, *SCIP - a framework to integrate constraint and mixed integer programming*, ZIB report **04-19** (2004).

[2] M. Aigner and G. M. Ziegler, *Proofs from* THE BOOK, Springer-Verlag, Berlin Heidelberg, 1998.

[3] A. Altshuler, J. Bokowski, and P. Schuchert, *Neighborly 2-manifolds with 12 vertices*, J. Comb. Theory, Ser. A **75** (1996), 148–162, no. 1.

[4] N. Amenta and G. M. Ziegler, *Deformed products and maximal shadows of polytopes*, Contemp. Math. **223** (1999), 57–90.

[5] D. Avis and V. Chvátal, *Notes on Bland's pivoting rule*, Polyhedral Combinatorics, Math. Prog. Study, vol. 8, 1978, pp. 24–34.

[6] A. Björner, M. Las Vergnas, B. Sturmfels, N. White, and G. M. Ziegler, *Oriented matroids*, Encyclopedia of Mathematics and its Applications, vol. 46, Cambridge University Press, 1993, (Second ed. 1999).

[7] A. Bobenko, P. Schröder, J. Sullivan, and G. M. Ziegler (eds.), *Discrete differential geometry*, Oberwolfach Seminars, vol. 38, Basel, Birkhäuser, 2008.

[8] J. Bokowski and U. Brehm, *A polyhedron of genus 4 with minimal number of vertices and maximal symmetry*, Geom. Dedicata **29** (1989), 53–64.

[9] J. Bokowski and A. Guedes de Oliveira, *On the generation of oriented matroids*, Discrete Comput. Geom. **24** (2000), 197–208.

[10] K. H. Borgwardt, *The Simplex Method. A Probabilistic Analysis*, Algorithms and Combinatorics, vol. 1, Springer-Verlag, Berlin, Heidelberg, 1987.

[11] U. Brehm, *A nonpolyhedral triangulated Möbius strip*, Proc. Amer. Math. Soc. **89** (1983), 519–522.

[12] M. Fitch, MATHEMATICA *database of the Jamison–Hill slope critical configurations [20]*, personal communication, June 2008.

[13] G. K. Francis and J. R. Weeks, *Conway's ZIP proof*, Amer. Math. Monthly **May** (1999), 393–399.

[14] B. Gärtner, M. Henk, and G. M. Ziegler, *Randomized simplex algorithms on Klee–Minty cubes*, Combinatorica **18** (1998), 349–372.

[15] S. I. Gass and T. Saaty, *The computational algorithm for the parametric objective function*, Nav. Res. Logist. Q. **2** (1955), 39–45.

[16] D. Goldfarb, *Worst case complexity of the shadow vertex simplex algorithm*, Preprint, Columbia University (1983), 11 pages.

[17] J. E. Goodman and R. Pollack, *A combinatorial perspective on some problems in geometry*, Congr. Numer. **32** (1981), 383–394.

[18] M. Goresky and R. MacPherson, *Stratified Morse Theory*, Ergebnisse Series, Springer-Verlag, Berlin, 1988.

[19] S. Hougardy, F. H. Lutz, and M. Zelke, *Surface realization with the intersection edge functional*, (2006), `arXiv:math.MG/0608538`.

[20] R. E. Jamison and D. Hill, *A catalogue of sporadic slope-critical configurations*, Proceedings of the Fourteenth Southeastern Conference on Combinatorics, Graph Theory and Computing (Boca Raton, Fla. 1983), Congr. Numer., vol. 40, 1983, pp. 101–125.

[21] M. Joswig and G. M. Ziegler, *Neighborly cubical polytopes*, Discrete Comput. Geom. **24** (2000), 325–344.

[22] V. Klee and G. J. Minty, *How good is the simplex algorithm?*, Inequalities III, Proc. 3rd Symp., Los Angeles 1969 (O. Shisha, ed.), Academic Press, 1972, pp. 159–175.

[23] F. H. Lutz, *Császár's torus*, Electronic Geometry Models **No. 2001.02.069**, `http://www.eg-models.de`.

[24] _____, *Enumeration and random realization of triangulated surfaces*, in Bobenko et al. [7], pp. 235–253, `arXiv:math.CO/0506316v2`.

[25] J. Matoušek, *Using the Borsuk-Ulam Theorem*, Universitext, Springer-Verlag, Heidelberg, 2003.

[26] P. McMullen, C. Schulz, and J. Wills, *Polyhedral 2-manifolds in E^3 with unusually large genus*, Isr. J. Math. **46** (1983), 127–144.

[27] J. Milnor, *Morse theory*, Ann. Math. Stud., Princeton University Press, Princeton, New Jersey.

[28] K. G. Murty, *Computational complexity of parametric linear programming*, Math. Programming **19** (1980), 213–219.

[29] I. Novik, *A note on geometric embeddings of simplicial complexes in a euclidean space*, Discrete Comput. Geom. **23** (2000), 293–302.

[30] J. Pach, R. Pinchasi, and M. Sharir, *A tight bound for the number of different directions in three dimensions*, J. Comb. Theory, Ser. A. **108** (2004).

[31] Th. Rörig, *Polyhedral surfaces, polytopes and projections*, Ph.D. thesis, TU Berlin, Berlin, September 2008, 126 pages, `http://opus.kobv.de/tuberlin/volltexte/2009/2145/`.

[32] L. Schewe, *Satisfiability problems in discrete geometry*, Ph.D. thesis, TU Darmstadt, 2007.

[33] _____, *Nonrealizable minimal vertex triangulations of surfaces: Showing nonrealizability using oriented matroids and satisfiability solvers*, Discrete Comput. Geometry **43** (2010), 289–302.

[34] P. R. Scott, *On the sets of directions determined by n points*, Amer. Math. Monthly **77** (1970), 502–505.

[35] A. Shapiro, *Obstructions to the imbedding of a complex in a Euclidean space. I. The first obstruction*, Annals of Math. **66** (1957), 256–269, (2).

[36] W. A. Stein et al., *Sage Mathematics Software (Version 5.13)*, The Sage Development Team, 2013, `http://www.sagemath.org`.

[37] P. Ungar, *2n noncollinear points determine at least 2n directions*, J. Comb. Theory, Ser. A **33** (1982), 343–347.

[38] W. T. Wu, *A theory of imbedding, immersion and isotopy of polytopes in a euclidean space*, Science Press, Peking, 1965.

[39] G. M. Ziegler, Personal communication, 2007.

[40] _____, *Polyhedral surfaces of high genus*, in Bobenko et al. [7], pp. 191–213, `http://arXiv.org/abs/math/0412093`.

ZUSAMMENFASSUNG

In Kapitel 1 befassen wir uns mit einer Fragestellung über Punktkonfigurationen in der Ebene. Aus Ideen von Ungar [37] und Pach, Pinchasi und Sharir [30] entwickeln wir zwei Algorithmen, die für eine gegebene Punktkonfiguration Teilmengen der Verbindungsstrecken finden, die nicht parallel und zusätzlich primitiv oder nicht-vermeidend sind. Danach untersuchen wir den Katalog von Jamison und Hill [20], der alle bekannten Punktkonfigurationen enthält, die die minimale Anzahl verschiedener Steigungen definieren. Unter diesen finden wir drei Beispiele, in denen es keine Teilmenge von Verbindungsstrecken gibt, die gleichzeitig alle Richtungen repräsentieren, nicht vermeidend und primitiv sind.

In Kapitel 2 konstruieren wir eine Familie deformierter d–dimensionaler Würfel. Für jede Dimension $d \geq 4$ erhalten wir einen Würfel C_d, der einen aufsteigenden Hamiltonpfad bezüglich der letzten Koordinate x_d hat. Gleichzeitig enthält C_d die Flächen F_d auf 2^d Ecken von McMullen, Schulz and Wills [26] im 2-Skelett derart, dass F_d die Projektion auf die letzten drei Koordinaten übersteht. Dazu benutzen wir Ansätze von Ziegler [40] und Rörig [31].

Der Ausgangspunkt für Kapitel 3 ist die in [18] von Goresky und MacPherson entwickelte Stratifizierte Morse Theorie (SMT). Für polyedrische Komplexe in $\mathbb{R}^d$ zeigen wir, dass die Morsedaten nur aus der Eckenreihenfolge und den kombinatorischen Daten gewonnen werden können. Anschließend gehen wir für polyedrische Flächen im $\mathbb{R}^3$ über die reine SMT hinaus und untersuchen genauer, wie kritische Punkte aussehen können und welche Effekte sie haben.

In Kapitel 4 folgen wir einem Ansatz von Novik [29], der die klassische Hindernistheorie für stückweise lineare Einbettbarkeit nutzt, um "Hindernissysteme" für geometrische Realisierbarkeit anzugeben. Wir konstruieren zu einem gegebenen Simplizialkomplex K und $m \in \mathbb{Z}$ ein System linearer Gleichungen und Ungleichungen. Wenn K eine simpliziale Einbettung in $\mathbb{R}^m$ hat, dann hat das System eine ganzzahlige Lösung. Die Bedingungen bei Novik rühren von Schnittzahlen her. In dieser Arbeit beschreiben wir, wie wir zusätzliche Bedingungen aus Verschlingungszahlen erhalten. Dieses Kapitel ist unter dem Titel "Necessary Conditions for Geometric Realizability of Simplicial Complexes" im Tagungsband des Oberwolfach Seminars "Discrete Differential Geometry" [7] erschienen.